The relevance of the aeolian transport path for the spread of antibiotic-resistant bacteria on arable fields

Steffen Münch

Univ.-Diss.

zur Erlangung des akademischen Grades
"doctor rerum naturalium"
(Dr. rer. nat.)
in der Wissenschaftsdisziplin "Geoökologie"

eingereicht an der
Mathematisch-Naturwissenschaftlichen Fakultät
Institut für Umweltwissenschaften und Geographie/ LE Geoökologie
der Universität Potsdam
und
Leibniz-Zentrum für Agrarlandschaftsforschung (ZALF) e. V.
Programmbereich 1 „Landschaftsprozesse“

Ort und Tag der Disputation: Potsdam, den 13.12.2021

Hauptbetreuer: Prof. Dr. habil. Michael Sommer
Betreuer: Dr. Roger Funk
Gutachter: Prof. Dr. habil. Michael Sommer, Dr. Roger Funk, Prof. Dr. Ulrich Nübel

Published online on the
Publication Server of the University of Potsdam:
https://doi.org/10.25932/publishup-53608
https://nbn-resolving.org/urn:nbn:de:kobv:517-opus4-536089

Abstract

The spread of antibiotic-resistant bacteria poses a globally increasing threat to public health care. The excessive use of antibiotics in animal husbandry can develop resistances in the stables. Transmission through direct contact with animals and contamination of food has already been proven. The excrements of the animals combined with a binding material enable a further potential path of spread into the environment, if they are used as organic manure in agricultural landscapes. As most of the airborne bacteria are attached to particulate matter, the focus of the work will be the atmospheric dispersal via the dust fraction.

Field measurements on arable lands in Brandenburg, Germany and wind erosion studies in a wind tunnel were conducted to investigate the risk of a potential atmospheric dust-associated spread of antibiotic-resistant bacteria from poultry manure fertilized agricultural soils. The focus was to (i) characterize the conditions for aerosolization and (ii) qualify and quantify dust emissions during agricultural operations and wind erosion.

PM_{10} (PM, particulate matter with an aerodynamic diameter smaller than 10 µm) emission factors and bacterial fluxes for poultry manure application and incorporation have not been previously reported before. The contribution to dust emissions depends on the water content of the manure, which is affected by the manure pretreatment (fresh, composted, stored, dried), as well as by the intensity of manure spreading from the manure spreader. During poultry manure application, PM_{10} emission ranged between 0.05 kg ha^{-1} and 8.37 kg ha^{-1}. For comparison, the subsequent land preparation contributes to 0.35 – 1.15 kg ha^{-1} of PM_{10} emissions. Manure particles were still part of dust emissions but they were accounted to be less than 1% of total PM_{10} emissions due to the dilution of poultry manure in the soil after manure incorporation. Bacterial emissions of fecal origin were more relevant during manure application than during the subsequent manure incorporation, although PM_{10} emissions of manure incorporation were larger than PM_{10} emissions of manure application for the non-dried manure variants.

Wind erosion leads to preferred detachment of manure particles from sandy soils, when poultry manure has been recently incorporated. Sorting effects were determined between the low-density organic particles of manure origin and the soil particles of mineral origin close above the threshold of 7 m s^{-1}. In dependence to the wind speed, potential erosion

rates between 101 and 854 kg ha^{-1} were identified, if 6 t ha^{-1} of poultry manure were applied. Microbial investigation showed that manure bacteria got detached more easily from the soil surface during wind erosion, due to their attachment on manure particles.

Although antibiotic-resistant bacteria (ESBL-producing *E. coli*) were still found in the poultry barns, no further contamination could be detected with them in the manure, fertilized soils or in the dust generated by manure application, land preparation or wind erosion. Parallel studies of this project showed that storage of poultry manure for a few days (36 – 72 h) is sufficient to inactivate ESBL-producing *E. coli*. Further antibiotic-resistant bacteria, i.e. MRSA and VRE, were only found sporadically in the stables and not at all in the dust. Therefore, based on the results of this work, the risk of a potential infection by dust-associated antibiotic-resistant bacteria can be considered as low.

Zusammenfassung

Die Ausbreitung antibiotikaresistenter Bakterien stellt eine global zunehmende Gefahr für die öffentliche Gesundheitsfürsorge dar. Über den unsachgemäßen Einsatz von Antibiotika in der Tierhaltung können sich in den Ställen Resistenzen entwickeln. Übertragungen über den direkten Kontakt mit Tieren und der Kontaminierung von Lebensmitteln wurden bisher schon nachgewiesen. Die Exkremente der Tiere in Verbindung mit einem Bindemedium ermöglichen einen weiteren potentiellen Ausbreitungspfad in die Umwelt, wenn sie als organische Wirtschaftsdünger in Agrarlandschaften verwendet werden.

Im Rahmen dieser Arbeit wurden Feld- und Windkanalmessungen durchgeführt, um dem von den Ackerflächen ausgehenden potentiellen Risiko einer partikulären Ausbreitung antibiotikaresistenter Bakterien nachzugehen. Kern der Arbeit ist zum einen die Bedingungen zu charakterisieren, die zu Staubemissionen während der Prozesskette (Düngerausbringung mit Geflügelmist, nachfolgende Feldbearbeitungen, Winderosion) führen, zum anderen Staubemissionen dieser Prozesskette zu klassifizieren und quantifizieren.

Flächenbezogene Emissionen für PM_{10} als ein Teil des Schwebstaubs (sogenannte PM_{10} Emissionsfaktoren) wurden zum ersten Mal für die Düngerausbringung mit Geflügelmist bestimmt. Sie lagen zwischen 0,05 und 8,37 kg ha^{-1} PM_{10} und waren abhängig vom Wassergehalt des Materials, der durch die Vorbehandlungen (frisch, kompostiert, gelagert, getrocknet) der Düngervarianten bestimmt war. Im Vergleich dazu wurden für die nachfolgenden Bodenbearbeitungen zwischen 0,35 kg ha^{-1} und 1,15 kg ha^{-1} PM_{10} freigesetzt. Zwar waren Mistpartikel weiterhin Bestanteil der Staubemissionen während der Bodenbearbeitung, jedoch sank ihr Anteil durch die Verdünnung des Düngers im Boden nach der Düngereinarbeitung auf unter 1 % ab. Ähnliche Tendenzen ergaben sich bei der mikrobiellen Betrachtung der freigesetzten Bakterien während der Ausbringung und Einarbeitung des Geflügelmists. Trotz eines höheren PM_{10} Austrags während der Düngereinarbeitung, verglichen mit der Ausbringung des Düngers, waren die Bakterienemissionen während der Düngerausbringung relevanter als bei der Düngereinarbeitung.

Winderosion sorgt für eine bevorzugte Verfrachtung des Geflügelmists auf sandigen Böden, nachdem der Dünger frisch eingearbeitet wurde. Da vor allem organische Bestandteile im Boden durch ihre geringe Dichte von der Auswehung betroffen sind, führt Winderosion auch bei mit Geflügelmist gedüngten Böden bereits kurz nach Erreichen der Schwellenwindgeschwindigkeit von 7 m s^{-1} zu einer Entmischung der eingebrachten organischen Mistpartikel und der mineralischen Bestandteile des Bodens. Diese Effekte treten vor allem dann auf, wenn in trockenen Böden der Gefügezustand zwischen mineralischen und organischen Partikeln kaum oder nicht vorhanden ist. In Abhängigkeit der Windgeschwindigkeit konnten potentielle Austräge zwischen 101 und 854 kg ha^{-1} bei einer eingebrachten Düngermenge von 6 t ha^{-1} bestimmt werden. Der bevorzugte Austrag von Mistpartikeln bedingt auch einen bevorzugten Austrag von Bakterien fäkalen Ursprungs, da diese nach der Einarbeitung an den Mistpartikeln mit geringerer Dichte anhaften.

Obwohl in den Geflügelställen antibiotikaresistente Bakterien in Form von ESBL bildenden *Escherichia Coli* (*E. coli*) in hohen Keimzahlen gefunden wurden, konnten keine weiteren Kontaminationen mit resistenten *E.coli* im Mist, in gedüngten Böden oder im Staub nachgewiesen werden. Parallelstudien aus dem Projekt zeigten, dass eine mehrtägige Lagerung von Hühnerstreu ausreichend ist (36 – 72 h), die Mehrzahl resistenter *E.coli* zu reduzieren, sodass sie sich nach der Düngerausbringung nicht mehr über Agrarflächen ausbreiten konnten. Weitere antibiotikaresistente Bakterien (MRSA, VRE) wurden nur vereinzelt in den Ställen und überhaupt nicht im Staub nachgewiesen. Aus unseren Versuchen kann daher das Risiko einer möglichen Infektion durch staubassoziierte antibiotikaresistente Bakterien als gering eingeschätzt werden.

Contents

List of figures

List of tables

List of supplemented figures

1 Introduction

1.1 Background

1.1.1 Aeolian removal by wind erosion

Soil erosion by wind is a natural process of aeolian removal and transportation of soil material (Shao, 2008). It is influenced by soil erodibility, climate properties, vegetation coverage and anthropogenic activities (e.g. intensive crop management) (Borrelli et al., 2015; Skidmore, 1986).

If the wind speed exceeds a specific threshold velocity (u_t), soil particles detach from the soil surface, depending on their particle diameter and specific density (Bagnold, 1941). The transport of particles results in a size-dependent segregation and is divided in three grain size-dependent modes (Fig. 1.1): “Saltation” is the principal transport mode for initiating wind erosion and is indicated by a leaping movement of soil particles and aggregates across the soil surface, typical between 70 µm and 500 µm of diameter. Pushed by the contact of particles in the saltation mode, coarser particles or aggregates with a diameter greater than 500 µm begin to “creep” over the surface, as they are too heavy to be lifted in the air. Collisions in the saltation mode also result in the abrasion of aggregates and thus in the entrainment of fine soil particles or aggregates (< 70 µm). Driven by atmospheric turbulences, fine particles get into “suspension” and transported up to thousands of kilometers before being deposited. Particles in the suspension mode have an impact on carbon cycle, solar radiation and cloud formation as well as on environmental and living health (air pollution, decreasing visibility, transport of fertilizers, herbicides and pesticides) (Borrelli et al., 2015; Buschiazzo and Funk, 2015; Riksen and Goossens, 2004; Shao et al., 2011; Steinke et al., 2016). In particular, particulate matter (PM) with a particle diameter smaller than 10 µm (PM_{10}), as a part of soil loss by wind erosion, contributes to the long-distance transport of suspended particles (Birmili et al., 2008; Katra, 2020; Prospero, 1999; Sterk and Goossens, 2007).

The wind erodibility of soils is determined by the texture and organic matter, which affect the size distribution and stability of soil aggregates (Tatarko, 2001). Especially, soils with a single grain structure (sandy soils) are susceptible to wind erosion, as their stability of soil aggregates is low. Soil organic matter (SOM) is concentrated in the soil top layer and

is characterized by a lower density compared to mineral particles. Due to the lower density, sorting effects between mineral and organic particles are particularly observable, shortly after the threshold velocity is exceeded. Therefore, SOM is particularly vulnerable to wind erosion. As the finest particles often contain SOM (Iturri et al., 2017), the loss of finest particles is connected with an irretrievable loss of soil fertility at the eroded side and lead to gradual soil degradation without visible effects of soil removal.

Soil degradation due to wind erosion is not only an issue for arid or semi-arid regions but also a seasonable phenomenon in mid-latitudes and temperate climate areas (e.g. Central Europe) (Borrelli et al., 2014; Sterk and Goossens, 2007; Wiggs, 2006) (chapter 1.1.3). It is temporary terminated to the spring months and limited to the acreage of summer crops (e.g. maize), as the preparation for summer crops leads to bare soil surfaces at the time of high wind erosion severe (Goossens and Riksen, 2004).

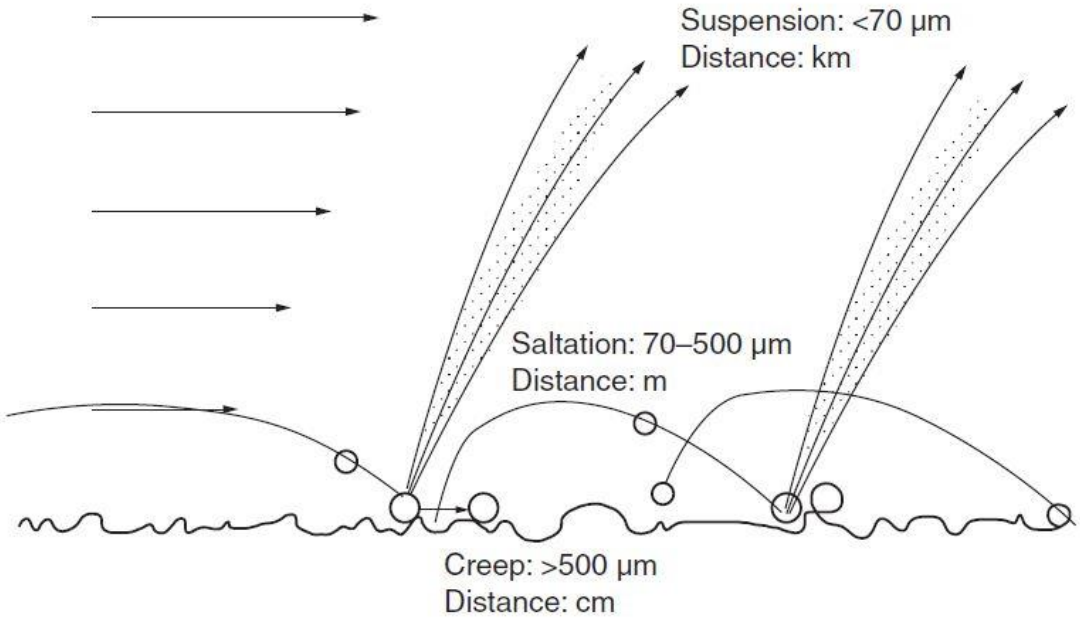

Fig. 1.1. Grain-size and transport distance depended transport modes of wind erosion (Buschiazzo and Funk, 2015).

1.1.2 Dust emissions by agricultural operations

Land preparation practices are not only a driver for wind erosion and associated dust emissions due to the reduction of soil structure, but also a cause for dust entrainment to the atmosphere. Dust emissions by land preparation affect all soils, including these which are not considered to be erodible for wind erosion (e.g. loamy soils). The most determining factor for dust emissions is the soil water content (SWC). Depending on soil texture and SOM, a decrease in SWC is responsible for increasing dust emissions (Aimar

et al., 2012; Funk et al., 2008; Hoffmann and Funk, 2015). Further, dust emissions depend on atmospheric conditions, i.e. air humidity and atmospheric turbulence (Avecilla et al., 2017), and the mechanical intensity of agricultural operations (Clausnitzer and Singer, 1996). As agricultural operations are significant sources of PM_{10}, area-related PM_{10} emission factors were used to allow accurate quantifications and comparisons of these dust sources (e.g. Holmén et al., 2001). PM_{10} emission factors were reported for different land preparation techniques (plowing/disking, harrowing and land planning/floating), ranging between 12.1 and 2322 mg m^{-2} (0.121 and 23.22 kg ha^{-1}) (Maffia et al., 2020). Dust particles from harvesting are characterized by finer and more organic particles compared to land preparation practices. Harvesting techniques are responsible for PM_{10} emissions between 9.5 and 1110 mg m^{-2} (0.095 kg ha^{-1} and 11.1 kg ha^{-1}). Sowing causes for dust emissions mainly from the soil but in small proportions also from the seeds (Maffia et al., 2020). Comparing the agricultural operations, land preparation (tillage) has the strongest impact on PM_{10} dust emissions, as land preparation consists of more passages than the other operations (Fig. 1.2).

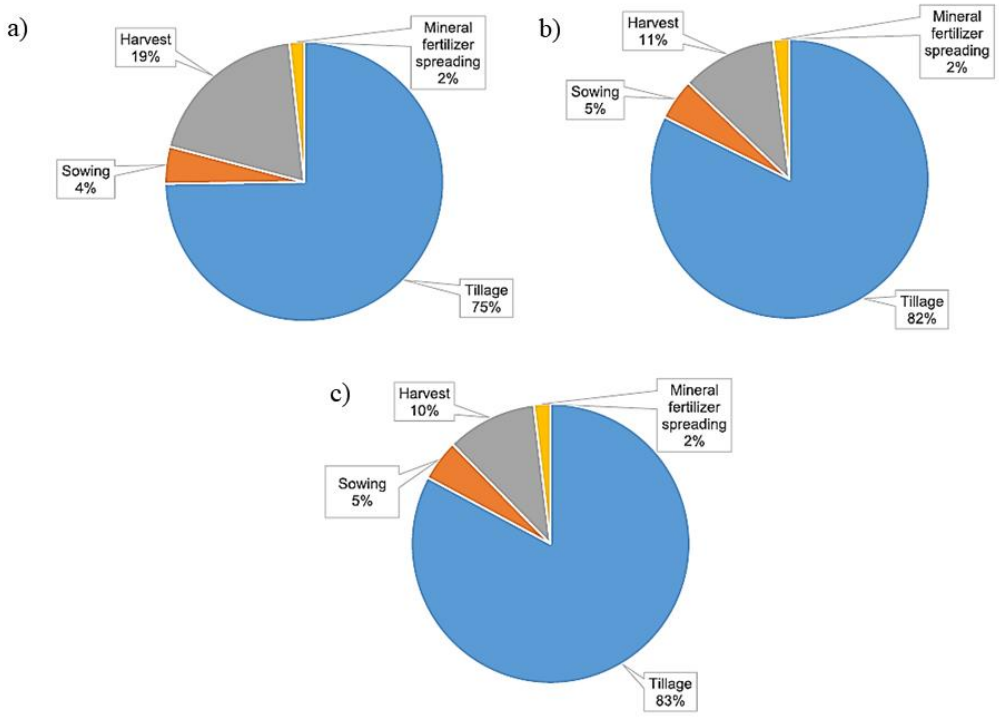

Fig. 1.2. Summary of the contribution of tillage practices, harvesting, sowing and fertilizer spreading to the total PM_{10} emitted from the cropping operations of a) wheat, b) maize and c) cotton. The summary includes studies of agriculture PM_{10} emission factors worldwide (Maffia et al., 2020).

1.1.3 Wind erosion and dust emissions in Germany

In Germany, wind erosion affects the arable lands of the North German Lowlands (Steininger and Wurbs, 2017). Highly susceptible regions were found in the Federal States of Mecklenburg-Western Pomerania, Lower Saxony, Schleswig-Holstein and parts of Brandenburg (Borrelli et al., 2014; Frielinghaus and Schmidt, 1993). The increased risk of wind erosion results from the predominant coverage of erodible sandy or loamy sand soils of glacial origin in combination with frequent high wind speeds in these areas (Steininger and Wurbs, 2017). Field studies in Brandenburg showed that single wind erosion events of about a couple of hours can cause for soil losses up to 60 t ha^{-1} (Funk, 1995).

In the spring months, wind erosion occurs frequently, because climatic conditions (increased frequency of high wind speeds and drier periods) and susceptible soil surfaces (bare arable soils with a single grain structure), due to the seedbed preparation of summer crops, coincide in this time (Funk, 2004). Meanwhile, maize has become the main summer crop and occupies the second largest acreage in Germany. This development is to be assessed as critical, as the acreage of maize occurs frequently on sandy soils (Steininger and Wurbs, 2017) and contributes to a limited soil protection against wind erosion due to a comparatively late seedbed preparation in spring. Thus, soil susceptibility to wind erosion is increased on arable lands with maize cultivation.

Dust activity on arable lands correlates with the preparation of the seedbed and lasts from March to May and from October to December (Goossens, 2004). Land preparation generates dust emissions on fine textured soils as well as on sandy soils (Funk et al., 2008; Öttl and Funk, 2007). It was shown in Lower Saxony that dust production due to land preparation can be even 4 - 6 times higher per year than dust production due to wind erosion (Goossens, 2004; Goossens et al., 2001).

1.1.4 Antibiotic resistance

Antibiotic substances are still highly effective for the treatment of bacterial infections but it became apparent that bacteria have developed resistances to antibiotics with increasing prevalence in the last decades, which limits therapeutic options (Zaman et al., 2017). Overused antibiotic consumption is an important cause of antibiotic resistance, which has become a major concern for human and animal health worldwide (Bell et al., 2014; Bush et al., 2011). In Germany and other European countries, the prevalence of methicillin-

resistant *Staphylococcus aureus* (MRSA) and extended-spectrum beta-lactamase (ESBL)-producing *Escherichia coli (E. coli*) has increased in recent years and is of great concern, regarding public health (Idelevich et al., 2016). Antibiotic-resistant bacteria (ARB) are transmitted nosocomial and outside of hospital facilities (Idelevich et al., 2016). Transmission pathways from livestock to human include the known transmission via the food chain or contact with farm animals (Kola et al., 2012; Sharp et al., 2014).

ARB were also found in abundant amounts in feces of pigs and chicken (Friese et al., 2013), which are components of farmyard manure. The use of manure on agricultural fields is a common and effective practice to maintain or improve nutrient and organic matter content in soil, but there is only scarce knowledge of continuous manure application on microbial impacts (Tyrrell et al., 2019). Microorganisms are known to be carried in dust over long distances and long periods of time (Acosta-Martínez et al., 2015). Thus, the fertilization with organic fertilizers (e.g. farmyard manure) and subsequent land preparation (chapter 1.1.2) of agricultural fields may represent a further transmission path to the environment via the dust fraction. Especially, solid manure (e.g. poultry manure) is characterized by a fine crumbled structure and a low water content and therefore susceptible to release those particles, which may carry ARB in the atmosphere. To date, studies about the dust-associated spread and atmospheric dispersal of ARB during agricultural operations are still lacking. Since ARB have been still detected in fertilized agricultural soils up to one year after fertilization (Hartmann et al., 2012; Xie et al., 2018), the detachment of soil or manure particles from arable lands due to wind erosion (chapter 1.1.1) could be also a source of ARB spread to the environment.

1.2 Material and methods

Measurements and experiments were conducted within the "Senatsausschuss Wettbewerb" (SAW-) project **S**pread **o**f **a**ntibiotic **r**esistance **i**n an **a**grarian **l**andscape (SOARiAL), funded by the Leibniz Association. It is an interdisciplinary project, combining the expertise of microbial live science and environmental science. The measurements were divided into field and wind tunnel studies to follow a typical process chain, where emissions of dust and ARB may occur (Fig. 1.3).

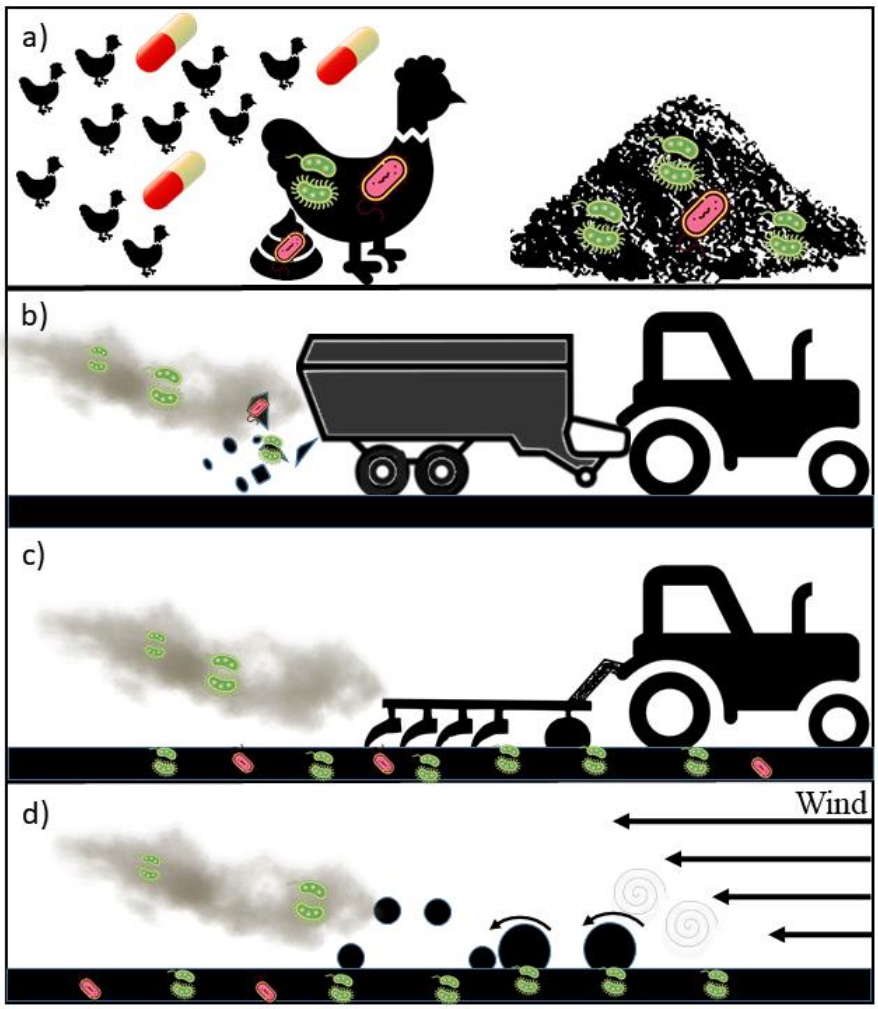

Fig. 1.3. Following the process chain: a) contaminated feces in the poultry barns and the appropriate manure, b) poultry manure application, c) incorporation of manure and further agricultural operations and d) wind erosion.

Feces, manure, soil and air samples were taken to analyze them microbiologically for *Escherichia coli* (*E. coli*), extended-spectrum beta-lactamase (ESBL)-producing *E. coli*, Enterococci spp. (indicator of fecal contamination), *Enterococcous faecium*, vancomycin-resistant enterococci (VRE), and methicillin-resistant Staphylococcus aureus (MRSA).

Field studies were conducted on arable lands in Brandenburg, Germany (Fig. 1.4), tracking the process chain of agricultural operations by dust monitoring (chapter 2 & 3). Wind tunnel studies were performed with sandy soils from five sites in Brandenburg and Mecklenburg-Western Pomerania (chapter 3 & 4) (Fig. 1.4) to simulate wind erosion of fertilized soils under controlled conditions.

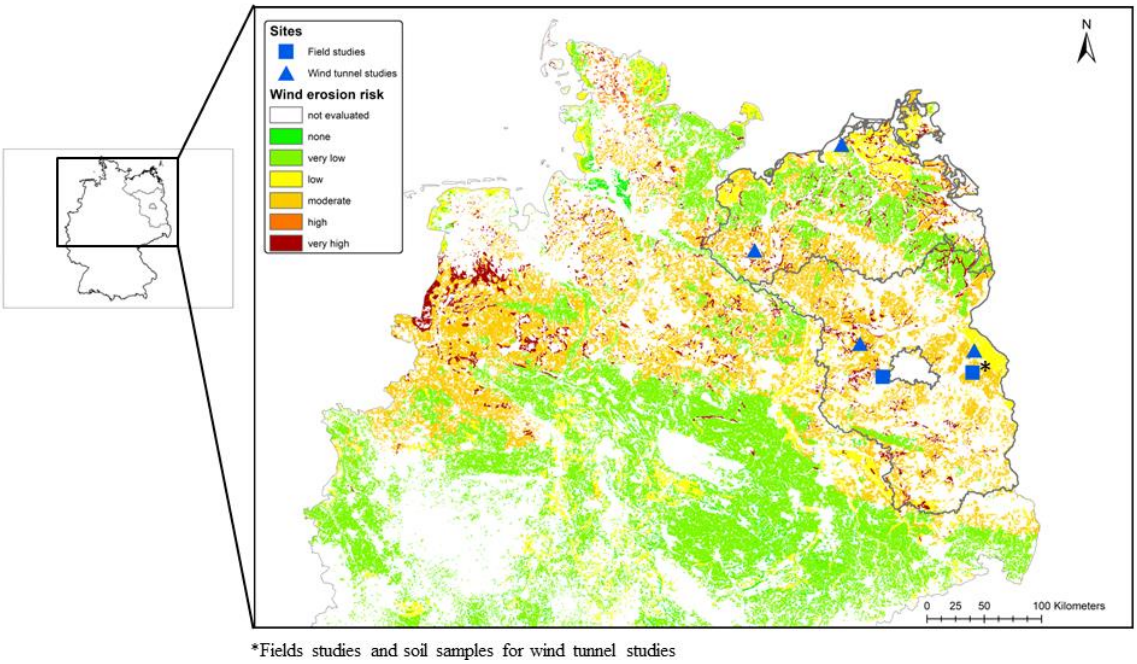

Fig. 1.4. Map of the potential wind erosion in the study region. Symbols indicate the sites.

1.2.1 Field experiments

A part of the field experiments was carried out on a maize-cultivated field in Potsdam (4 plots, 1.8 ha per plot, 52°25′48″ N, 13°01′25″ E). Field plots were applied with the respective pretreated manure (fresh, stored, composted and dried). The treatment conditions are described in chapter 2.2.1.2. The field experiments were repeated on a fallow land in Müncheberg (2.1 ha, 52°28′36″ N, 14°10′37″ E) but here the manure was only stored in a pile overnight.

The arable lands are composed of loamy sand (Potsdam) and sandy loam (Müncheberg). The average temperature is 9.3 °C and 9 °C, respectively, the annual precipitation is 586 mm and 563 mm, respectively. The climate is warmer and dryer than the German average (T = 8.8 °C, 831 mm, 1981 – 2010) and is classified as “temperate continental” (DWD, 2021). Dust emissions were monitored with mobile dust monitors and aerosol collectors for microbiological and molecular analyses downwind during the agricultural operations (Fig. 1.5) (chapter 2 & 3).

Fig. 1.5. Monitoring dust emissions downwind during a) manure application (Photo: © O. Biniasch) and b) land preparation (Photo: © R. Funk).

1.2.2 Wind tunnel studies

Wind erosion experiments were performed in a stationary wind tunnel (Fig. 1.6), which is located on the campus of the Leibniz Centre of Agricultural Landscape Research (ZALF). The wind tunnel (open-circuit push type system) is a suitable tool to reproduce the basic processes of wind erosion. Wind speeds can be adapted quickly and measurements are independent from external conditions. The working section of the wind tunnel was filled with soil samples from the test field in Müncheberg (chapter 3) and from four further sites in Brandenburg and Mecklenburg-Western Pomerania (chapter 4). All soil samples, used for wind tunnel studies, were susceptible to wind erosion. Dust emissions were also monitored with a dust monitor and an aerosol collector for microbial analyses in the chamber behind the working section (suspension chamber). In addition, the amount and composition of the wind-eroded sediment material were investigated.

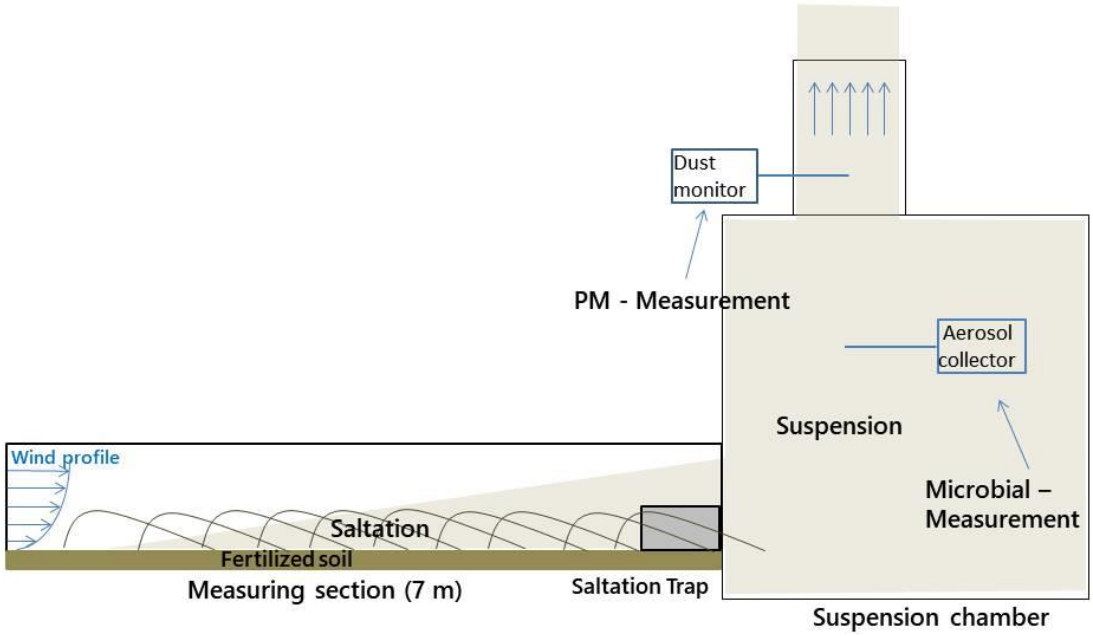

Fig. 1.6. Set-up for wind erosion experiments in the wind tunnel (modified after Funk et al., (2019)).

1.3 Motivation and research questions

1.3.1 Motivation

The overall aim of the project was to identify and quantify the risk of a possible spread of ARB, using contaminated farmyard manure on arable lands. To date, a few studies have been conducted on dust concentrations and bioaerosols from livestock production (Aarnink and Ellen, 2007; Seedorf, 2004; Takai et al., 1998). However, the transmission path via the air and associated dust emissions of fertilized soils (including the application of manure) are unexplored so far (Huijbers et al., 2015; Maffia et al., 2020; Sharratt and Auvermann, 2014). To address these gaps, the work concentrates on all processes on arable lands, where dust emissions and a possible dust-associated spread of ARB may occur: manure application with different pretreatments of poultry manure, land preparation (including the incorporation of poultry manure), sowing and wind erosion. For this, field and wind tunnel experiments were conducted to quantify and qualify the emitted dust and wind-eroded sediments regarding particle size, organic composition and bacterial concentrations.

1.3.2 Research questions

The main research questions (RQ) were:

(RQ 1): To what extent poultry manure application contributes to PM_{10} emissions, compared to land preparation, and how do the pretreatments of manure influence PM_{10} emissions?

(RQ 2): Does the different pretreatments of poultry manure have an effect on the bacterial spread during the application of manure?

(RQ 3): To which extent ARB are released from poultry manure fertilized soils and what are the differences between application and incorporation of manure?

(RQ 4): Is it possible to trace back fecal contamination to its source?

(RQ 5): What are the effects on soil properties after poultry manure incorporation at short-term?

(RQ 6): How does the incorporated poultry manure affect the wind-eroded sediment and how much is lost due to wind erosion?

1.4 Structure of the work

Field measurements were made within a typical agricultural process chain, starting with the dust emissions of poultry manure application with different pretreatments (RQ 1) and the influence of pretreatments on bacterial spread during manure application (RQ 2). The measuring instruments and results of that are described in chapter 2 (Paper: Münch et al., 2020).

The extent of a possible spread of ARB is answered in chapter 2 and 3 (Paper: Thiel et al., 2020) (RQ 3). In particular, bacterial concentrations and fluxes between application and incorporation of manure are compared to each other and with dust emissions. Further, it was shown, whether it is possible to trace back fecal contamination (RQ 4).

Chapter 4 (Paper: Münch et al., 2021, submitted) examines the soil composition (RQ 5) and the susceptibility to wind erosion of poultry manure fertilized soils (RQ 6). In addition, the spread of bacteria due to wind erosion from chapter 3 is discussed in RQ 6. The wind erosion experiments in chapter 3 and 4 were conducted in the wind tunnel under controlled conditions.

1.5 Publication list

First author:

Münch, S., Papke, N., Thiel, N., Nübel, U., Siller, P., Roesler, U., Biniasch, O., Funk, R., Amon, T., 2020. Effects of farmyard manure application on dust emissions from arable soils. Atmospheric Pollut. Res. 11, 1610–1624. https://doi.org/10.1016/j.apr.2020.06.007

Thiel, N*., **Münch, S**.*, Behrens, W., Junker, V., Faust, M., Biniasch, O., Kabelitz, T., Siller, P., Boedeker, C., Schumann, P., Roesler, U., Amon, T., Schepanski, K., Funk, R., Nübel, U., 2020. Airborne bacterial emission fluxes from manure-fertilized agricultural soil. Microb. Biotechnol. 13, 1631–1647. https://doi.org/10.1111/1751-7915.13632

*equal contribution

Münch, S., Papke, N., Leue, M., Faust, M., Schepanski, K., Siller, P., Roesler, U., Nübel, U., Kabelitz, T., Amon, T., Funk, R., 2021. Differences in the sediment composition of wind eroded sandy soils before and after fertilization with poultry manure. Soil & Tillage Res. (Submitted)

Second author:

Faust, M., Wolke, R., **Münch, S**., Funk, R., Schepanski, K., 2021. A new Lagrangian in-time particle simulation module (Itpas v1) for atmospheric particle dispersion. Geosci. Model Dev. 14, 2205–2220. https://doi.org/10.5194/gmd-14-2205-2021

Frentrup, M., Thiel, N., Junker, V., Behrens, W., **Münch, S**., Siller, P., Kabelitz, T., Faust, M., Indra, A., Baumgartner, S., Schepanski, K., Amon, T., Roesler, U., Funk, R., Nübel, U., 2021. Agricultural fertilization with poultry manure results in persistent environmental contamination with the pathogen Clostridioides difficile. Environ. Microbiol. (In Press) https://doi.org/10.1111/1462-2920.15601

Kabelitz, T., Ammon, C., Funk, R., **Münch, S**., Biniasch, O., Nübel, U., Thiel, N., Rösler, U., Siller, P., Amon, B., Aarnink, A.J.A., Amon, T., 2020. Functional relationship of particulate matter (PM) emissions, animal species, and moisture content during manure application. Environ. Int. 143, 105577. https://doi.org/10.1016/j.envint.2020.105577

Kabelitz, T., Biniasch, O., Ammon, C., Nübel, U., Thiel, N., Janke, D., Swaminathan, S., Funk, R., **Münch, S**., Rösler, U., Siller, P., Amon, B., Aarnink, A.J.A., Amon, T., 2021. Particulate matter emissions during field application of poultry manure - The influence of moisture content and treatment. Sci. Total Environ. 146652. https://doi.org/10.1016/j.scitotenv.2021.146652

Siller, P., Daehre, K., Rosen, K., **Münch, S**., Bartel, A., Funk, R., Nübel, U., Amon, T., Roesler, U., 2021. Low airborne tenacity and spread of ESBL-/AmpC-producing Escherichia coli from fertilized soil by wind erosion. Environ. Microbiol. n/a (In Press). https://doi.org/10.1111/1462-2920.15437

2 Effects of farmyard manure application on dust emissions from arable soils

Published in:

Münch, S., Papke, N., Thiel, N., Nübel, U., Siller, P., Roesler, U., Biniasch, O., Funk, R., Amon, T., 2020. Effects of farmyard manure application on dust emissions from arable soils. Atmospheric Pollut. Res. 11, 1610–1624. https://doi.org/10.1016/j.apr.2020.06.007

Abstract

Particulate matter (PM), emitted during agricultural activities, could be a source for the atmospheric dispersal of pathogenic or antibiotic resistant bacteria when agricultural fields are fertilized with contaminated manure. The use of contaminated bedding material from chicken breeding as farmyard manure can initiate a releasing process for resistant bacteria into the environment. In this study, we focus on the physical processes of the release, regarding application and manure mixtures. The addition of several tons per hectare of organic manure to the topsoil has effects on the soil composition and should effect the dust emissions, if the same sorting effects are assumed such as for other organic particles. Based on dust measurements within an agricultural process chain from manure application, soil preparation to maize seeding, dust emissions were measured and PM_{10} emission factors (PM_{10} EFs) were derived using a standard dispersion model. The PM_{10} emissions during manure application ranged between 0.05 and 8.37 kg/ha, depending on the moisture content due to different pretreatments of the manure. In the subsequent tillage operations, a share of 0.39 – 0.59% of manure in the total PM_{10} could be determined. Our investigations show that particles in the PM_{10} fraction of manure origin are released within the entire process chain. These particles are small and light enough to be transported over long distances and be a potential risk for antibiotic resistant bacteria dispersal at remote places as human settlements, when they will deposit there.

2.1 Introduction

The increasing prevalence of antibiotic resistance among human pathogenic bacteria is a major global threat. More than 50% of total antibiotic consumption in Europe is administered to livestock (Meyer et al., 2013). With the use of animal manure as fertilizer, antibiotic resistant bacteria are transferred to a completely different ecosystem and are in the following subject to technological or natural releasing processes of that new

environment. Antibiotic resistant bacteria in soils were detected up to one year after manure application by Friese et al. (2013) and Hartmann et al. (2012). The prevalence of antibiotic resistant bacteria genes was already detected in the aquatic environment along rivers. Stange et al. (2016) found that surface water plays an important role as reservoirs for antibiotic resistance bacteria along the River Rhine. Proia et al. (2018) showed an increased influence of waste water on increased concentration of antibiotic resistant bacteria.

A second potential pathway is the atmospheric dispersal via dust particles from agricultural soils supplied with contaminated manure. Dust particles can be a carrier for microorganisms, including pathogenic bacteria (Acosta-Martínez et al., 2015; Burrows et al., 2009b; Despres et al., 2012). These dust particles first need a releasing process, before they are transported through the atmosphere. One releasing process is the movement of soil particles by wind erosion. After the application of manure and incorporation by soil tillage, its organic matter (OM) is concentrated in the top soil as an unconsolidated mixture, which is highly susceptible to wind erosion. Because of its lower density, OM will be preferentially removed by wind erosion (Blanco-Canqui et al., 2006; Nerger et al., 2017; Rühlmann et al., 2006). As wind erosion is not only a transporting process, but also an efficient sorting mechanism between mineral and organic compounds, it leads to disproportional higher losses of OM from the eroding site. Enrichment ratios of the OM in the eroded material between 2 and 17 have been documented (Iturri et al., 2017; Nerger et al., 2017).

This transporting and sorting process results in two transport modes: Saltation and suspension. A part of the suspension load includes the particulate matter fraction < 10 µm (PM_{10}: aerodynamic diameter d_p < 10 µm). This suspension load can lead to pollution of adjacent fields and remote areas. Due to their small size, suspended particles of PM_{10} are a growing public concern responsible for severe health impacts (Davidson et al., 2005; Kappos et al., 2004).

Particles of about 2.5 µm and smaller ($PM_{2.5}$: aerodynamic diameter d_p < 2.5 µm) can penetrate deep into the respiratory tract and have a negative impact on the lung function (Zhang et al., 2015). By using the ECHAM5/MESSy atmospheric chemistry model, it was found that $PM_{2.5}$ emissions from agricultural sources are even responsible for premature mortality in Central Europe (Lelieveld et al., 2015). However, this study

pointed out that agricultural emissions of this particle class are mainly induced by secondary particle nucleation of ammonia emissions associated with the use of fertilizers and livestock farming.

Dust in the PM_{10} fraction represents the most valuable part of agricultural soils, e.g. fine silt, clay and partly OM. Iturri et al. (2017) found out that the PM_{10} fraction is more enriched with OM, when it was wind eroded from sandy compared to fine textured soils. Hence, sandy soils are highly susceptible for the export of OM (including manure) to the atmosphere. Dust particles with a higher OM content are also beneficial for bacteria. They result in an enhanced survival rate of bacteria carried by OM-enriched dust (Acosta-Martínez et al., 2015). As bacteria have an enhanced survival rate in OM-enriched dust, they can travel over long distances. The long-distance transport of large quantities of soil-derived dust from arid regions in Africa and Asia and its dust-associated microbial load upon deposition has been also well reported (Griffin et al., 2002; Kellogg and Griffin, 2006; Maki et al., 2019) Birmili et al., (2008) investigated wind-driven, atmospheric long-distance transport of eroded soil material from agricultural land over Europe. As a proof of that, a dust plume arrived Central-Europe, which have its origin in Southern Eurasia. Hence, there is a potential risk that the soil dust with microbial load can affect rural communities or urban areas (Jahne et al., 2015), but also neighboring or distant ecosystems, such as rivers or oceans (Hoffmann and Funk, 2015; Lal, 2003).

The risk for dust emissions due to wind erosion is limited to a specific period, when soils are more susceptible to wind erosion by bare, dry or freshly harrowed surfaces. In combination with drought, wind erosion increases with stronger winds and lower relative humidity (Avecilla et al., 2017). Borrelli et al. (2014), Frielinghaus and Schmidt (1993) and Steininger and Wurbs (2017) showed that the risk of wind erosion is enhanced in the northern part of Germany due to dominating sandy soils and drier conditions, compared to other regions in Germany. Summer cereals, root crops, legume (mainly peas) and maize (Zea mays L), which amount to 34% of total agricultural land in North German Lowlands, are more affected by wind erosion than other crops (Statistisches Bundesamt, 2017). Especially, the acreage of maize has doubled in recent years due to the increasing production of biogas.

Agricultural tillage operations are also an important source of particulate matter emissions to the atmosphere (Funk et al., 2008; Hinz, 2007; Lee et al., 2004; Schenker M,

2000). In contrast to wind erosion, all soils are affected several times a year. Goossens et al. (2001) and Goossens (2004) reported that dust production due to tillage can be even 6 times higher than by wind erosion. Compared to wind erosion, dust emissions produced by agricultural operations also occur in sub humid landscapes (Baker et al., 2005; Sharratt et al., 2010). Higher shares of clay and silt increase PM_{10} emissions by agricultural operations. In contrast, greater amounts of organic matter decline the dust emissions by aggregation of fine particulates (Aimar et al., 2012; Carvacho et al., 2004). Soil moisture is one of the important factors that limit the dust emissions from agricultural operations. The influence of soil moisture is quantified in numerous studies (Bolte et al., 2011; Chen et al., 1996; Funk et al., 2008). The threshold of the soil water content (SWC) varied from 2 to 5 mass percent for sandy soils to 25 – 40 mass percent for organic soils (Funk et al., 2008). On the one hand, a higher ratio of OM decreases the dust emissions, while on the other hand, soils with a higher ratio of OM can emit dust at higher moisture levels than soils with less OM.

To estimate the real dust output of agricultural operations, emission factors (EF) [kg/ha] were identified in several studies for different agricultural techniques (Cassel et al., 2003; Chen et al., 2017; Funk et al., 2008; Holmén et al., 2001; Öttl and Funk, 2007). They are very variable and depend on the soil texture, moisture content and tillage intensity (active or passive tools). Same tillage operations on the same soil can result in 10 times higher emissions in summer compared to spring because of the lack of soil moisture. For a SWC < 10 mass percent, Chen et al. (2017) found out that averaged PM_{10} EFs for field tilling were about 2 kg/ha and for planting 0.2 kg/ha. Under drier soil conditions (i.e. < 3 mass percent), PM_{10} EFs can exceed 10 kg/ha as for disking, plowing, land planting (Cassel et al., 2003; Öttl and Funk, 2007) A successful measure to reduce dust emissions is conservation tillage, which results in emissions of 52–93% compared to conventional tillage (Madden et al., 2008). However, these methods are not affordable for every farmer.

There is a lack of information with regard to dust emissions during and after manure applications on arable fields. Since now, no emission factors are reported regarding manure application (Maffia et al., 2020). So far, no investigations of dust emissions were made from application of manure and subsequent typical tillage operations.

The aim of this study is to quantify and qualify particulate matter emissions related to agricultural operations during and after manure application. The focus is on the organic fertilizer components. We investigate the physical basics and compare the dust release and bioaerosol emissions of different pretreated manure (stored, fresh, dried and composted) as well as its contribution to dust emissions after application and mixture with soils.

2.2 Methods

2.2.1 Field experiments

2.2.1.1 Field site description

Dust emissions, produced by agricultural activities were determined from two agricultural fields in Brandenburg, Germany during spring/early summer 2017. The fields are located in the Northeast German Lowlands at Potsdam-Bornim (PS) (N52°25′48, E13°1′25) and Müncheberg-Friedrichshof (MBG) (N52°28′36, E14°10′37), west and east of Berlin, respectively (Fig. 2.1).

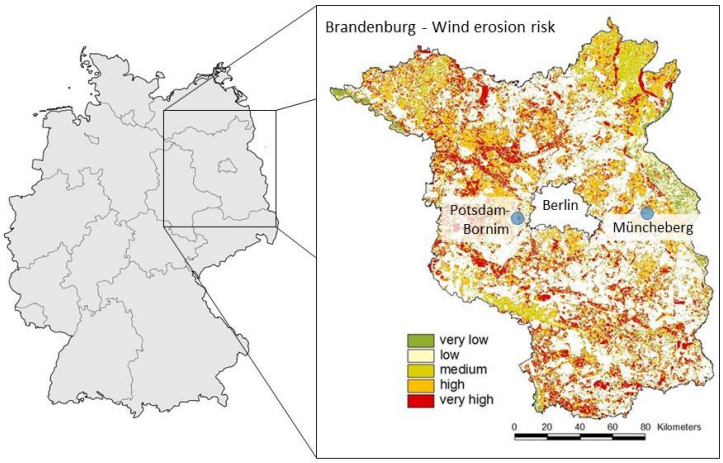

Fig. 2.1. Map of the potential wind erosion risk in the study region. Points indicate the measuring sites at Potsdam and Müncheberg.

Both plots are in the transition zone from oceanic to continental climate. It can be classified as temperate oceanic (Köppen-Geiger Climate Classification) and is often influenced by winds from western directions. The annual average temperature is around

9 °C and the annual precipitation is 550 mm with precipitation deficits from April to September (MLUL, 2016).

Soil and manure samples were taken to characterize the field properties. Grain size distributions were measured by wet sieving and sedimentation method (DIN ISO 11277, 2002). Table 2.1 shows the particle size composition of the two soils from the test fields. To determine the water content, the gravimetric water content method was used. For this, the mass of the samples was weighed before and after the samples were dried in an oven at 105 °C for 24 h.

Table 2.1 Soil texture of the two test fields (MBG = Müncheberg-Friedrichshof; PS =Potsdam-Bornim).

Fraction	Diameter [µm]	MBG share [%]	PS share [%]
Coarse sand	2000 – 630	6	3
Middle sand	630 – 200	27	30
Fine sand	200 – 63	36	50
Coarse silt	63 – 20	14	9
Middle silt	20 – 6	8	3
Fine silt	6 – 2	3	1
Clay	< 2	6	4
Soil texture (WRB)[1]		Sandy loam	Loamy sand
Soil type		Luvisol	Arenosol

2.2.1.2 Experimental setup

Dust measurements were made within a typical process chain for growing maize: application of manure, incorporation of manure, incorporation of mineral nitrogen fertilizer and seeding maize. The first experiment started on March 27, 2017 on the test field near Potsdam-Bornim (PS). On this day, we measured dust concentrations during a simulated organic fertilizer application, which was realized by a quasi-stationary spreading of different stored farmyard manures (Fig. 2.2a). Measurements were carried out with a constant distance to the dust source while the spreading unit (tractor – manure spreader) operated stationary during unloading. The solid manure was from poultry production of a chicken farm in four states: Fresh manure (2.5 weeks old), stored manure (5–6 weeks old), composted manure (same storing time as the stored manure, but

[1] (FAO, 2014)

repeatedly mixed with an excavator once per week) and dried manure (same origin as fresh manure, but heated up 48 h with a hot air dryer before application). The fresh, stored and composted treatments were stored outside in an open silo. At all farms, poultry chickens were kept under conventional conditions with wood pellets as bedding material.

For application a Bergmann manure spreader TSW 6240 S was used (height of spreading: 1 m, width of spreading: 6 m). The released dust was always measured with two Environmental Dust Monitors (EDM 164, GRIMM-Aerosol Technique, hereinafter EDM) at two heights (1.50 m and 3.80 m). The particle number concentration [L^{-1}] was counted in 31 size channels between 0.25 µm and 32 µm every 6 s. The particle counts were then converted automatically in particulate matter classes (PM_{10}, $PM_{2.5}$ and PM_1 [µg m^{-3}]). Simultaneously, temperature, relative humidity, wind speed, and wind direction were registered. The stationary measuring set-up remained at the same point in the field downwind for each type of fertilizer in order to ensure the same basic conditions for spreading the different types of the fertilizer.

The stationary application of manure occurred as far as possible under homogenous flow conditions. The flow was considered to be homogeneous if deviations from the mean wind direction were less than + - 22.5° around the main wind direction and the wind speed was less than 1 m/s. If major deviations occurred, the data from the dust concentration measurements were not included in the evaluation. Table 2.2 shows how often the wind direction was optimal to cross the points of application and instrument on a line and predominant wind speeds during all manure applications. The predominant wind directions were NW/W and W/SW, respectively. In 70 – 85% of all measuring intervals, the wind direction was optimal that the dust emissions hit the measuring device Table 2.2. The wind speed ranged between 0.5 and 3.6 m/s at which the period of the dried manure application showed the highest percentage share of wind speeds under 1 m/s. Fig. 2.2a exemplarily shows the measured PM_{10} concentrations with associated wind speed and wind direction during the stationary application of the dried manure with a constant distance to the dust source. During the application, the measured concentration of PM_{10} was on a quite constant level, when the wind direction was optimal to cross the points of application and measurement on a line. The low concentration was caused by variable wind directions and almost windless conditions (cyan-blue bar in Fig. 2.2a). Hence, the emitted dust cloud from the manure spreader did not reach the inlets of the EDM. These sections will be excluded from further consideration.

Table 2.2 Meteorological conditions (wind directions, wind speed range and calm conditions) and usable data during stationary manure application.

Manure pretreatment	Wind direction [°]	Wind speed range [m/s]	Calm conditions (< 1 m/s) [%]	Usable data [%]
Dried	NW/W (70%)	0.5 – 2.4	17.1	70
Fresh	W/SW (85%)	0.8 – 2	7	83
Composted	NW/W (80%)	1.5 – 3.6	0	80
Stored	W/SW (80%)	0.9 – 2.6	3.5	79

One day later, the manure from the same origin was applied on four rectangular blocks on the test field, one type of manure per block. Each block had a size of 1.8 ha. After application of manure, we measured the dust concentration on each block, which was generated by tillage, using a disk harrow Lemken Rubin 9 (working depth: 10 cm, working width: 6 m) for the incorporation of manure. The dust measurement took place 50 m downwind from the end of each block. For this and the following agricultural operations, dust was not measured continuously, but as peak value at each passage of the tractor (Fig. 2.2b)[2].

On April 7, dust measurements were conducted in the same way for the incorporation of nitrogen fertilizer at the same blocks as described before (Lemken Karat cultivator, working depth: 15 cm, working width: 6 m). Dust measurements were repeated on April 13 for the last operation of the process chain. Seedbed preparation and seeding were conducted with a rotary harrow air seeder-combination with a working width of 6 m.

During manure application and incorporation, dust measurements were accompanied by taking air samples for microbiological analysis additionally, using all-glass impingers 30 (AGI-30; Neubert Glas GbR, Geschwenda, Germany, VDI Norm 4252–3) in different distances to the emission source. During the application, air samples were taken simultaneously at a distance of 20 m, 50 m and 100 m downwind from the manure spreader for each type of pretreated manure. During manure incorporation, air samples were taken at a distance of 50 m and 100 m downwind from the field edge. One sample

[2] The realization of the experiment can be observed with Google Earth. Please use the time slider to view the correct historical imagery of 03/28/2017.

was taken per treatment and distance on both days. The impingers were filled with 30 ml of phosphate buffered saline (PBS; Oxoid, Wesel, Germany). Vacuum pumps with a flow rate of 9.5 – 11.75 l/min were connected to the AGI-30 impingers. The airflow was verified using a rotameter. Air samples were taken for a time span of 10 min. The impingers were stored in polystyrene containers with cool packs before and after air sampling and further processed in laboratory on the same day.

The experiments were repeated on the second test field with an area of 2.1 ha near MBG on May 31. We started measuring downwind the dust concentration of manure spreading. For application, a manure spreader Strautmann BE4 with a horizontal 2-beater spreading unit (spreading height: 1 m, spreading width: 3 m) was used. In contrast to the experiments in PS, only fresh manure, removed the day before, was used. Again, the bedding material was wood pellets. After application, the manure was incorporated with the cultivator Lemken Smaragd 9 (working depth: 8 cm; working width: 3 m) and released dust was measured in the same way, using the two EDMs. In contrast to the previous experiments in PS, the direction of the spreader and the cultivator was perpendicular to wind direction (Fig. 2.2c). In this experiment, the measured PM_{10} concentration from the incorporation of manure with a passing dust cloud decreased with increasing distance to the dust source because of increasing dispersion of dust.

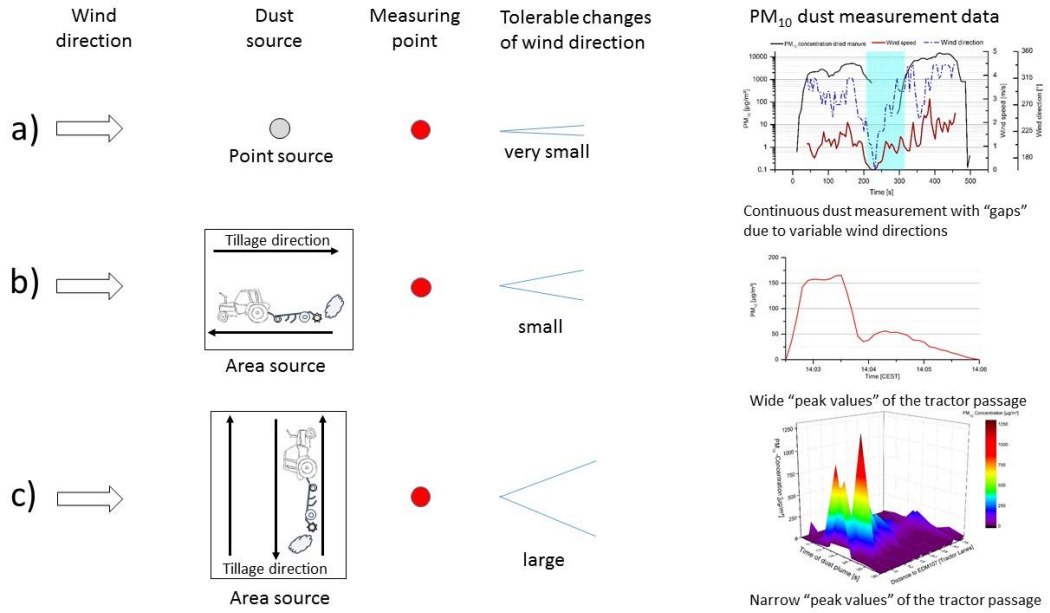

Fig. 2.2. Three different possible ways to monitor dust emissions from agricultural management activities, and corresponding tolerable changes of wind direction, depending on the dust source (stationary (a)/mobile dust source (b, c)). The induced PM_{10} emission of a stationary dust source and of two types of a mobile dust source (parallel and perpendicular to wind direction) and its impact on usable data for further consideration are shown on the right-hand side. The cyan-blue bar in a) represents the period, where the dust cloud did not reach the inlet of the EDM.

2.2.1.3 Dust suspension

The indication of particle motion (deposition or suspension) depends on the current meteorological conditions and can be determined by calculating the ratio of surface friction velocity u_* and the particle terminal velocity V_s of each particle size class for mineral or organic origin. U_* is used as a measure for vertical turbulent dispersion and is valid for neutral conditions. It can be determined using the equation:

$$u_* = \kappa \frac{v_{z_1} - v_{z_2}}{ln\frac{z_1}{z_2}} \quad \text{Eq. 2.1}$$

where κ is the *von Kármán-constant* (0.4) and v_{z1} and v_{z2} are the wind speeds at the height z_1 and z_2. The wind speed was constantly measured with two anemometers at 2.80 and 0.80 m height, respectively. The anemometers were fixed to two vertical bars, either attached to the weather housing or anchored in the ground (Fig. 2.3).

Hagen et al. (2007) and Hoffmann et al. (2008) used an empirical equation, which was estimated from data given by Royco Instruments (1974) and in good agreement with a line-source diffusion deposition model, to calculate the particle terminal velocity V_s of the considered particle sizes:

$$V_s = \exp(-9.261 + 1.85\ln(S))(\rho/2) \quad \text{Eq. 2.2}$$

where S [µm] is the particle diameter and ρ is the particle density, which was estimated to be 2.65 Mg/m^3 for mineral particles and 0.8 Mg/m^3 for OM particles (manure and SOM).

Upward turbulent dispersion dominates over gravitational settling for particles, when $V_s/u_* < 1$. Particles remain in suspension and can affect at least adjacent landscapes. Otherwise, the gravitation of a particle predominates, i.e. $V_s/u_* > 1$ and particles will settle down (Shao, 2008).

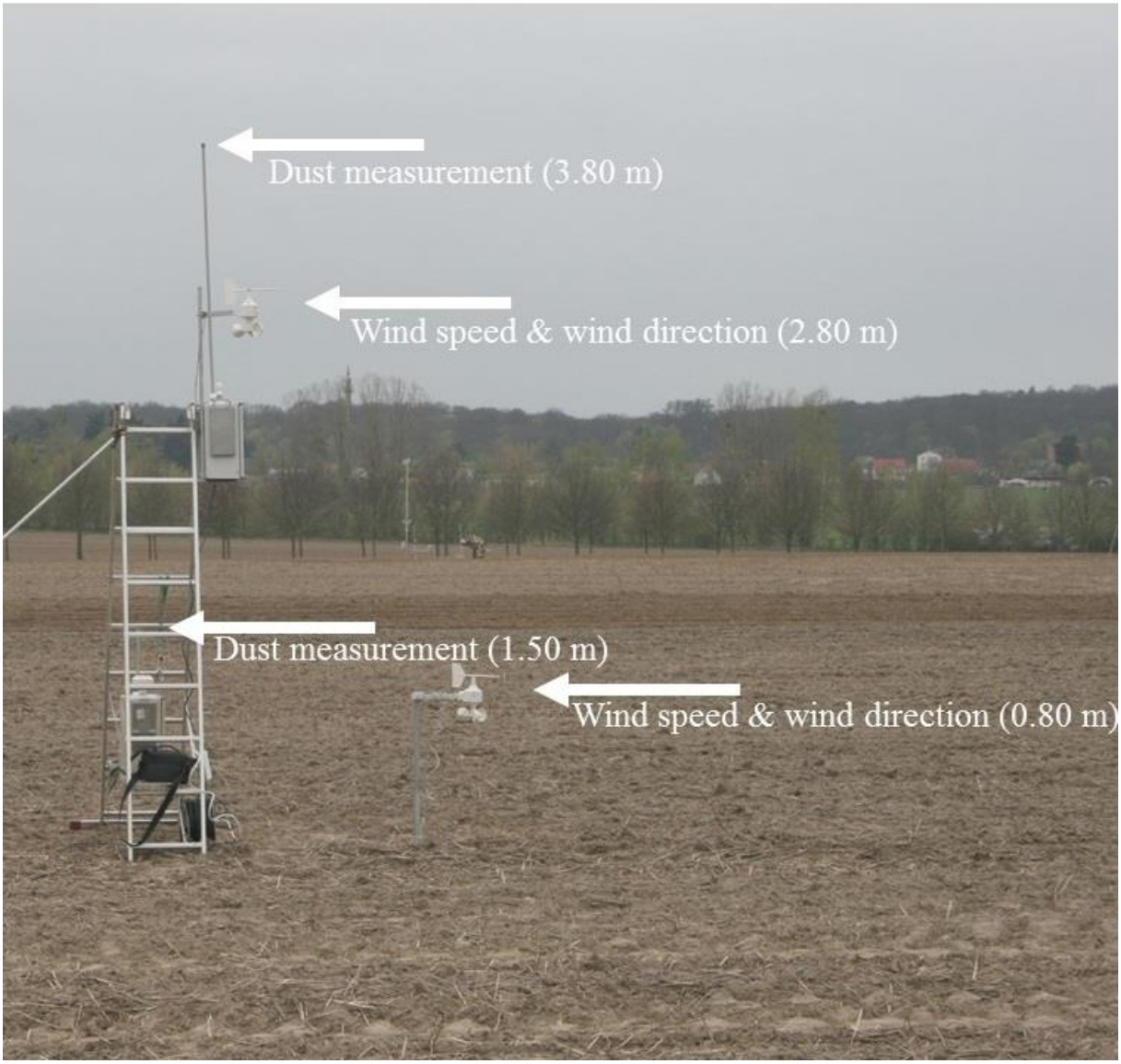

Fig. 2.3. Set-up for measuring dust concentration with two EDMs 164 during manure application and tillage operations.

2.2.2 Emission factors (EFs) and PM_{10} fraction of manure origin.

To estimate, how much dust, either manure or soil dust, is released due to agricultural management, we calculated PM_{10} EFs from the measured PM_{10} concentration using the Gaussian dispersion model of the German standard "TA Luft". It is described by the following equation (Seinfeld and Pandis, 2006; TA Luft, 1986; Weber, 1976):

$$c\,(x,y,z) = \frac{Q}{2\pi\sigma_y\sigma_z u_h}\exp\left(\frac{-y^2}{a_{1,2}}\right)\left(\exp\left(\frac{-(z-h)^2}{a_{1,2}}\right) + \exp\left(\frac{-(z+h)^2}{a_{1,2}}\right)\right)\exp\left[-\sqrt{\frac{2}{\pi}\frac{V_{di}}{u_h}\int_0^x \frac{1}{\sigma_z(\xi)}\exp\left(-\frac{h^2}{a_{1,2}(\xi)}\right)d\xi}\right] \quad \text{Eq. 2.3}$$

where c [µg/m³] is the dust concentration (e.g. PM_{10}) at a given position, measured by EDM, Q [µg/s] is the source term (e.g. manure spreader), x [m] is the downwind, y [m] is

the crosswind (= 0 because of the focus on the dust peaks), z [m] is the vertical distance, V_{di} [m/s] is the deposition rate of particles (V_{di} ($PM_{2.5}$) = 0.001 m/s; V_{di} (PM_{10}) = 0.07 m/s), u_h [m/s] is the wind speed at the height h [m]. The parameter a differs between the calculations from tillage ($a_1 = \sigma_z^2$) and manure application ($a_2 = 2\sigma_z^2$) activities because dust from tillage is emitted just above the ground, so the dust plume from tillage develops only upward. Therefore, the vertical dispersion parameter for tillage operation will be reduced to σ_z^2 instead of $2\sigma_z^2$. Generally, the two parameters σ_y and σ_z describe the horizontal and vertical dispersion of the dust. The dispersion is defined by stability parameters. The stability parameters are based on the wind speed, cloud cover, time of the day and season.

Eq. 2.3 can be solved for the source term Q to get the EF of PM_{10} in the unit of [kg/s]:

$$Q = \frac{2\pi\sigma_y\sigma_z u C}{\exp\left(\frac{-y^2}{2\sigma_y^2}\right)\left(\exp\left(\frac{-(z-h)^2}{2\sigma_z^2}\right)+\exp\left(\frac{-(z+h)^2}{2\sigma_z^2}\right)\right)\exp\left[-\sqrt{\frac{2V_{di}}{\pi u_h}}\int_0^x \frac{1}{\sigma_z(\xi)}\exp\left(-\frac{h^2}{2\sigma_z^2(\xi)}\right)d\xi\right]} \quad \text{Eq. 2.4}$$

With the knowledge of the process time t [s] and by division through the surface area of the field A [ha], the dust release per hectare EF [kg/ha] can be calculated by:

$$EF = \frac{Q \cdot t}{A} \quad \text{Eq. 2.5}$$

With this formula, we can estimate the PM_{10} related EF of agricultural activities from the concentration measurements, either from manure application or from tillage.

From the manure to soil mass ratio per area in a specific volume depending on the tillage depth and total PM_{10} emission, it is possible to estimate the PM_{10} fraction of manure EF_{manure} from total PM_{10} emissions.

It can be calculated as followed:

$$EF_{manure} = \frac{AR_{manure}}{A \cdot d_{tillage} \cdot \rho_{soil}} EF_{total} \quad \text{Eq. 2.6}$$

where AR_{manure} [kg/m^2] is the application rate of manure, A [m^2] is the surface area, $d_{tillage}$ [m] is the tillage depth, ρ_{soil} is the bulk soil density (1400 kg/m³) and EF_{total} [kg/ha] is the calculated EF of the tillage operation.

2.2.2.1 Microbiological analyses

The air samples taken in the first field trial were microbiologically analyzed for *Escherichia coli* (*E. coli*), extended-spectrum beta-lactamase (ESBL)-producing *E. coli* and the total viable bacteria count. Quantitative analysis was performed by directly streaking 100 µL of the mixed samples in triplicates on specific agar plates after serial dilution. For the quantification of *E. coli*, MacConkey agar No. 3 was used. To quantify ESBL-producing *E. coli*, 1 mg/l Cefotaxime (AppliChem, Darmstadt, Germany) was added to the MacConkey agar plates, as suggested by the EFSA Panel on Biological Hazards (BIOHAZ) (2011). For the determination of the total viable bacteria count, blood base agar (Blood agar Base No. 2, Oxoid, Wesel, Germany) was used.

For the qualitative analysis of *E. coli* and ESBL-producing *E. coli*, the air samples were incubated for 24 h at 37 °C after a 1:10 dilution with Luria/Miller-broth (Roth, Karlsruhe, Germany) in Erlenmeyer flasks. Subsequently, 10 µL of each sample were streaked on MacConkey agar plates with and without the addition of Cefotaxime with an inoculation loop and analyzed after another incubation period of 24 h at 37 °C.

2.2.3 Laboratory experiments

2.2.3.1 Particulate properties of manure mixtures with soil samples

The incorporation of organic manure should have effects on physical properties of a soil immediately. The question was in our case in what way the PM emissions are affected. A subsequent analysis of the applied amounts to a field after application and incorporation from taking soil samples afterwards is difficult, so we complemented our investigations with laboratory experiments under controlled conditions. Samples of the soil from the test sites (MBG, PS) and the solid manure were air-dried and dry sieved through a 2 mm mesh sieve (DIN 66118, 2016; DIN ISO 11277, 2002). The soils were mixed with different quantities of manure always equivalent to an incorporation depth of 15 cm. We tested commonly used amounts for fertilizing agricultural fields with 3 t/ha, 6 t/ha, 12 t/ha plus one extreme rate of 90 t/ha to illustrate the physical influence of manure adding to soil. In practice, the applied amount depends on the containing nutrients but this was not part of our investigations. Taking the soil type specific soil density of 1400 kg/m^3 (Renger et al., 2008), it was possible to calculate the soil/manure mass ratio for a depth of 15 cm. For laboratory investigations, we referred the amount of manure to a soil sample of 150 g. Particle size distributions of the soils and the soils with incorporated manure were

determined using the Malvern Mastersizer 3000 laser diffractometer (Malvern Instrument, Malvern, England). The measurements were conducted using the automated dry powder dispersion unit (Aero S). The dispersion was achieved by accelerating dry particles through a venturi nozzle using compressed air. The pressure range was from 0 to 400 kPa resulting in an increasing dispersion of the material caused by shear stress and collisions. In this way, different stresses on the particles or aggregates can be simulated, comparable with the situations during tillage or wind erosion. Each sample was investigated with the same setting of dry dispersion to achieve the size distribution: Particle type: non-spherical, refractive (1.543) and absorption (0.01) index of Quartz, background-measuring time of 10 s, measuring time of 5 s, number of measurements 3, creating an average and obscuration range of 1 – 10% (recommended).

Here we used the volume size distribution as obtained from the Mastersizer measurements (Mastersizer 3000 user manual (English), 2015). The volume based size distribution of particles is the probability density obtained using the total volume V_i. The total volume of all particles V_i with a given radius assuming a spherical shape is determined by:

$$V_i = \frac{4}{3}\pi r_i^3 n_i \qquad \text{Eq. 2.7}$$

where r_i is the radius of the particle i and n_i is the number of particles of radius r_i.

2.3 Results and discussion

2.3.1 Field Experiment

2.3.1.1 Meteorological situation and dust deposition

Using Eq. 2.1 and Eq. 2.2, we can estimate the threshold for each measurement, whether particles will settle down by gravitation or remain in suspension and can affect neighboring areas or are transported over longer distances. V_s was 0.009 m/s for the mineral particles of a diameter of 10 µm and 0.003 m/s for organic particles of the same size. All particles smaller in diameter and thus part of the PM_{10} fraction are included by lower V_s. Fig. 2.4 shows that during all agricultural activities, the vertical component of the wind was greater than the settling velocity V_s. In this case, particles of PM_{10} remain in

suspension until they were trapped by local vegetation, washed out by precipitation or when the wind speed drops.

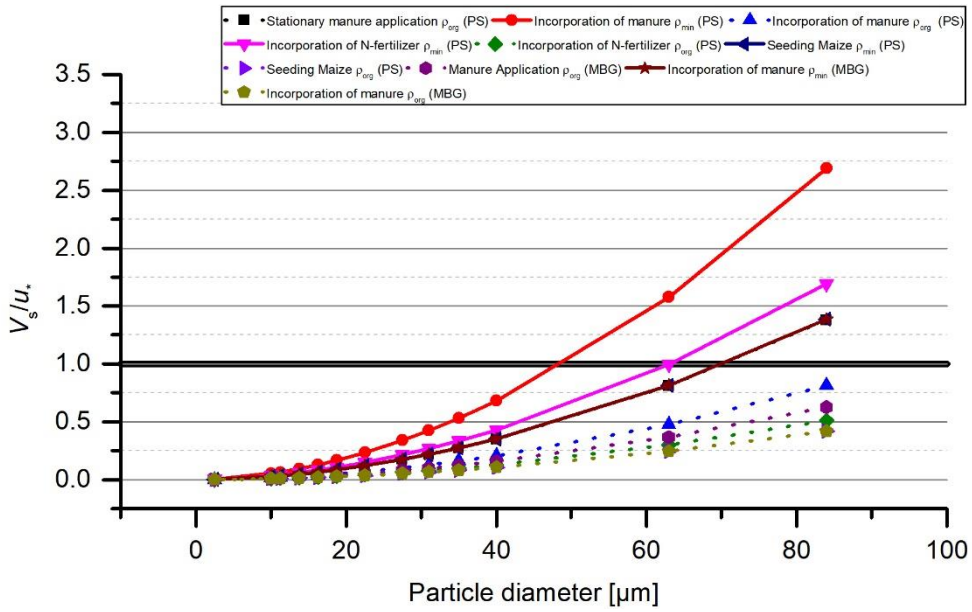

Fig. 2.4. Relationship between the particle diameter and the ratio of particle terminal velocity V_s and surface friction velocity u_*, indicating the mode of particle motion during all agricultural operations. $V_s/u_* < 1$ indicates particle suspension, $V_s/u_* > 1$ indicates particle deposition. Dotted curves represent the ratio of organic particles.

The lowest frictions velocities were measured during low wind speed conditions with low differences in wind speed at both heights at the beginning of the study (e.g. stationary manure application on March 27[3]) (Table 2.3). Even here, only coarser organic particles with a diameter above 70 µm could settle down. In contrast, mineral particles settled down at diameters larger than 47 µm. For the incorporation of manure, which was one day later, surface friction velocity was also high enough that particles sizes of the PM_{10} fraction remain in suspension. In this case, the threshold value was for mineral particles 50 µm, which were too heavy to stay in suspension.

[3] For the experiment of manure application, organic particles were only considered.

Table 2.3 Observed meteorological conditions and Klug/Manier dispersion categories during the experiment at 2.8 m height.

	Wind speed [m s^{-1}]	Wind direction	Dispersion category	Relative humidity [%]	Air temperature [°C]	u_* [m s^{-1}]	Vertical direction of transport flux (d_p < 10 µm)
Application of manure (March 27)	1.8	W	IV	26.7	21.8	0.10 ± 0.03	$V_s/u_* < 1$
Incorporation of manure (March 28)	2.7	SW/W	III/2 & IV	23.7	25.2	0.17 ± 0.14	$V_s/u_* < 1$
Incorporation of nitrogen fertilizer (April 7)	4.9	W	III/1 & III/2	84.5	10.8	0.27 ± 0.08	$V_s/u_* < 1$
Seeding of maize (April 13)	5.5	SW/W/NW	III/2	60.6	12.2	0.33 ± 0.06	$V_s/u_* < 1$
Application of manure (May 31)	5.7	W/NW	III/1 & III/2	59.4	22.4	0.22 ± 0.02	$V_s/u_* < 1$
Incorporation of manure (May 31)	6.6	W/NW	III/1	45.6	22.8	0.33 ± 0.08	$V_s/u_* < 1$

2.3.1.2 Particle emissions and EFs from manure application

The average particle number concentration [L^{-1}] and the particle mass concentration [$\mu g\ m^{-3}$] are shown in Fig. 2.5. There are distinct differences caused by the different pretreatments of the manure. Over the whole measuring range of the EDM, the number and mass concentrations of the dried manure dust were at least 10 times higher than the concentrations of the other manure states with higher water contents (Fig. 2.5). As shown in Fig. 2.4, the meteorological conditions were sufficient to keep all particles smaller than 70 µm in suspension, so all measured particles in the size classes of the EDM (0.25 – 32 µm) can be regarded to become part of the suspension load. As the composted and stored material had the highest water content of all pretreatments, higher aggregation and binding of finer particles with larger ones is more probable and smaller amounts of PM_{10} can be released. Therefore, the process of coagulation of aerosols could also become important, when the water content is greater (Aloyan et al., 1997).

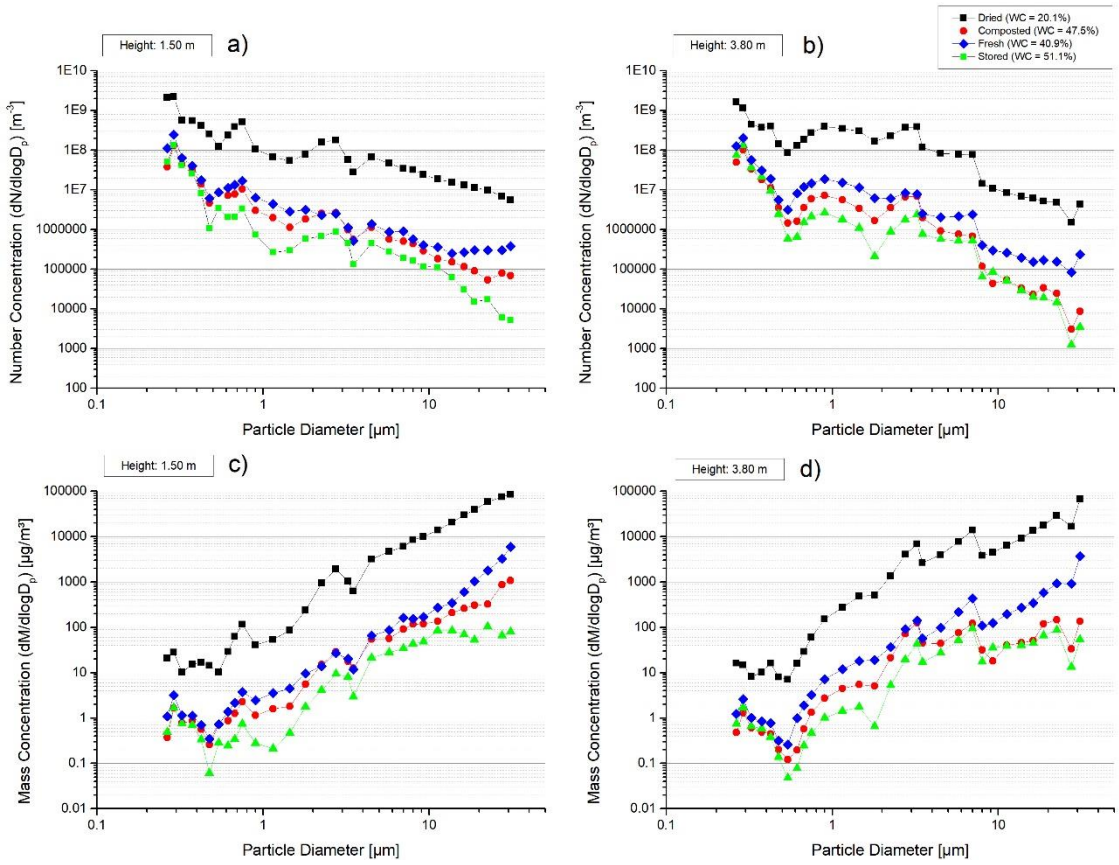

Fig. 2.5. Average number of particles (a, b) and their total mass (c, d) during stationary manure application at various water contents (mass per cent) in PS. The masses were calculated using the idealized estimation of a sphere particle shape and a density of ρ = 1000 kg/m³. Note the logarithmic scale at the y-axes.

Comparing number and mass concentration over the whole measuring range showed an oppositional trend. While the number concentration typically decreased with increasing

diameters, the mass concentration increased with size. The particle number share between 10 and 32 µm at 1.50 m height was only 0.96% (e.g., dried manure), but their mass share was 89.6%. It shows the general dilemma of PM measurements, that only a small number of larger particles determine nearly the complete mass of regarded class (Fig. 2.6). The median diameter illustrates the trend of different particle sizes for number and mass distribution. In summary, it can be shown that the pretreatment of manure has an influence on the quantity of particles of all diameters. Less particle concentrations (mass and number) were measured during the application of composted and stored material and higher particle concentrations during the application of dried manure.

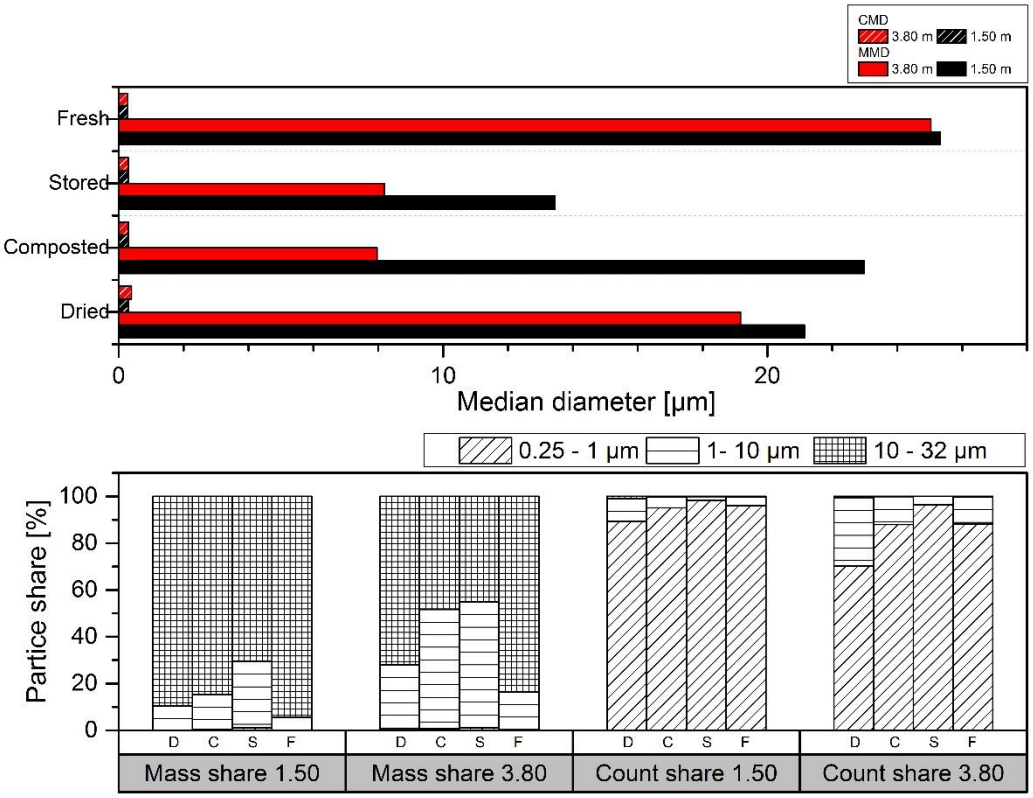

Fig. 2.6. Median diameter [µm] of number concentration (shaded) and mass concentration (non-shaded) and percentage share of three particle size classes [µm] from all poultry manure treatments during stationary manure application in PS. The values of 1.50 and 3.80 represent the height [m] of both instruments.

EFs for PM_{10} from the stationary application of manure were obtained, using the Gaussian dispersion model (Eq. 2.4). With the knowledge of the size of the plots and the estimated duration of a movable manure application (38 min), we transferred the emissions from the stationary application to a typical movable application form to make the results comparable with the EFs of the subsequent tillage activities.

The EFs and the water content of all used manure variants are given in Table 2.4. The water content varied between 20 mass percent for dried to more than 50 mass percent of the fresh manure. Despite the relatively high gravimetric water content (20–50 mass percent) of manure, its application led always to dust emissions. These dust releases agrees with investigations about dust emissions of highly organic soils or the water content of air dried organic materials (grains, hay etc.) in general, which ranged between water contents of 15 – 25 mass percent (Funk et al., 2008).

The PM_{10} EFs were also highly variable and differed by a factor of 100. It was apparent in the study that the emission of PM_{10} depended on the water content of the manure. Between a water content of 20 mass percent and 28 mass percent, the PM_{10} emissions decreased exponentially. Above a water content of 30 mass percent, the dust emission remained on a low level. Similar trends in the emission behavior of manure were found at the same water content range in wind tunnel studies (Kabelitz et al., 2020). Beside the water content of manure, dust emissions also depended on the power of the manure spreader and the application rate per unit time. The manure spreader, used in PS (Bergmann TSW 6240 S; power requirement: 118–221 kW), spread the manure out with high energy up to 6 m width, which resulted in higher emissions than the manure spreader in MBG (Strautmann BE4, power requirement: 20 kW), which spread the manure out just for the width of the track of about 3 m with much lower energy.

The $PM_{2.5}/PM_{10}$ ratio ranged between 0.09 and 0.13 with no correlation to the manure water content. Compared to previous studies of measuring dust from agricultural activities ($PM_{2.5}/PM_{10}$: 0.1–0.5) (CARB, 2003; Chen et al., 2017; Countess, 1999; Cowherd, 2006; Cowherd et al., 2010), the values from manure application were lower, which indicates a coarser dust composition. Dust emissions experiments in a wind tunnel with highly carbonized substrates of open-cast lignite mines showed similar shares of $PM_{2.5}$ on PM_{10} (0.094) (Funk et al., 2019).

Table 2.4 Emission factors (EF) for PM_{10}, $PM_{2.5}/PM_{10}$ ratio and water content (WC) for different pretreatments of manure during application. "Recently collected" means that the manure was directly applied on the test field with no storing time.

Manure pretreatment	PM_{10} [kg/ha]	$PM_{2.5}/PM_{10}$	WC (mass percent)
PS			
Dried	8.37 ± 2.38	0.08	20.1
Composted	0.15 ± 0.07	0.13	47.5
Stored	0.05 ± 0.02	0.12	40.9
Fresh	0.15 ± 0.02	0.09	51.1
MBG			
Recently collected	0.18 ± 0.12	0.13	28.7

2.3.1.3 Dust emissions from tillage

After manure was applied on the fields, the process chain was continued with subsequent tillage operations producing dust: Immediate incorporation of the animal manure (disc harrow), incorporation of mineral nitrogen (cultivator), and seeding maize (seed combination with a rotary harrow) in PS, and immediate incorporation of manure on the test field in MBG (chisel plough). The EFs were also derived by using the Gaussian Model, by taking the peak values of every passage of the tractor, the distance of the tractor (i.e. dust source) and the atmospheric dispersion and stability parameters.

Table 2.5 summarizes the calculated PM_{10} EFs for the different tillage operations. These factors ranged between 0.35 and 1.15 kg/ha. Compared to previous field studies, where EFs of PM_{10} were calculated, the values of PM_{10} EF were of similar magnitude (Cassel et al., 2003; Chen et al., 2017). The $PM_{2.5}/PM_{10}$ ratios for the tillage operations were highly variable. The values ranged between 0.09 and 0.57 with the highest value at the lowest SWC of 1.9 mass percent. The large range in the PM-ratios results from different SWCs. It leads to more fine dust of drier soils and resulted in a finer dust composition and thus in a higher $PM_{2.5}/PM_{10}$ ratio. A low SWC led to an easier destruction of aggregates in the coarse fraction (2.5 – 10 µm) during tillage, which resulted in a higher share of $PM_{2.5}$ in the airborne dust. During the seeding of maize, no dust was measured for the whole experiment and therefore, no EF could be derived. The seeding of maize was preceded by two rainy days. The highest measured SWC (12.2 mass percent) illustrated the absence of dust emissions.

The highest PM_{10} emissions occurred during the incorporation of manure on the second test field in MBG. Here, the soil was finer textured than in PS and the SWC was 8.8%. In addition, higher wind velocities were also measured during the experiments in MBG,

which favored the surface drying and led to a straight flow of the emitted dust to the EDM with only small horizontal dispersion.

Table 2.5 Emission factors (EF) for PM_{10}, $PM_{2.5}/PM_{10}$ ratio and soil water content (SWC) during the different tillage operations.

Tillage operation	PM_{10} [kg/ha]	$PM_{2.5}/PM_{10}$	SWC (mass percent)
PS			
Incorporation of manure (March 28)	0.64 ± 0.40	0.08	9.6 ± 1.2
Incorporation of nitrogen fertilizer (April 7)	0.35 ± 0.24	0.56	1.9 ± 0.43
Seeding maize (April 13)	No emissions	/	12.2 ± 1.2
MBG			
Incorporation of manure (May 31)	1.15 ± 0.59	0.11	8.8 ± 0.96

Different dispersion of organic and mineral particles short after emissions can also derived from the field experiment in MBG for spreading of manure and the subsequent incorporation by a cultivator (Fig. 2.7). During the application of manure (top panel), the measured PM_{10} peaks were greater at 3.80 m than at 1.50 m. In contrast, the PM_{10} peaks from the immediate incorporation of manure (bottom panel) were lower at the height of 3.80 m than at 1.50 m. This can be explained as follows: As organic matter has a lower density than mineral soil particles, OM dust reaches greater heights. Dust released by tillage consists mainly of mineral components with different aerodynamic properties caused by higher density and compact shapes.

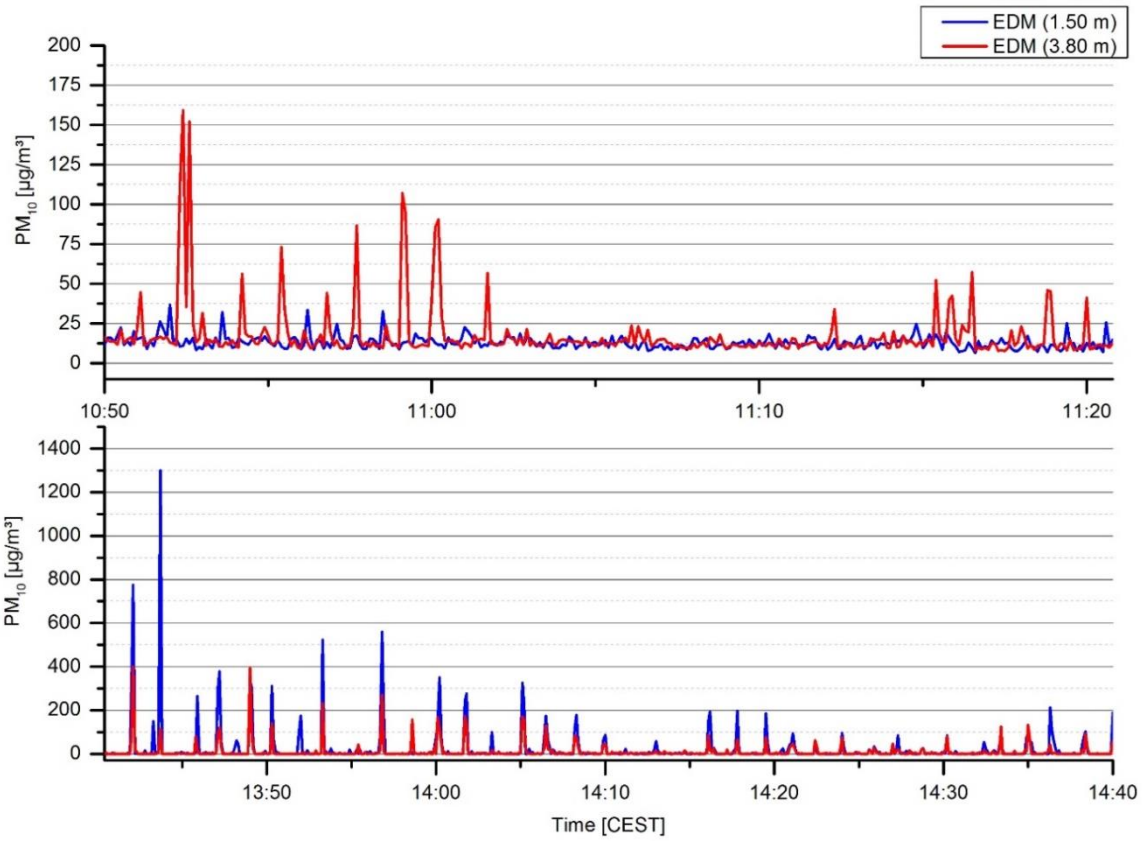

Fig. 2.7. PM_{10} concentration for the application of manure (top) and the subsequent incorporation of manure (bottom), measured at two heights (1.50 m; 3.80 m) from the same location in MBG. Please note the different resolution of both y-axes.

As organic particles can be easier released and transported over longer distances, they can affect more distant regions than mineral particles. Studies, showing the enrichment of OM in the released dust, support these findings (Buschiazzo and Funk, 2015; Iturri et al., 2017). Dispersion modelling is a common and accepted technique to calculate EF for agricultural field operations (Maffia et al., 2020). Dispersion models are often used inversely to predict the EF of a dust source, measuring the dust concentrations downwind (Faulkner et al., 2011). One of the dispersion models is the Gaussian plume model, which has been used for the determination of dust emissions from agricultural operations in this study. It is a simple computationally efficient model with a minimum of input parameters and provides good results comparable to the Lagrangian dispersion model (Öttl et al., 2001). Nevertheless, the measurement of the required input parameters (e.g. meteorological data) is subject to uncertainties. The calculation of u_*, which is a parameter for the vertical dispersion of dust, only provides a rough estimation of the turbulent velocities derived from two horizontal wind velocity measurements in two heights. A further point of uncertainty is the measured dust concentration, which is also a

crucial input parameter for the model. The measured concentration depends on the accuracy of the measuring instrument and the operation limitations for the EDM (1 … 100,000 µg/m³; $2 \cdot 10^6$ Particles L^{-1}). In general, the EDM measures particle concentrations until a particle diameter of 32 µm, whereas high sampling efficiency was determined until 20 µm (Grimm and Eatough, 2009). High particulate matter and number particle concentrations above 20 µm can be only measured close nearby the dust source. However, our set-up guaranteed high sampling efficiency as our instruments were not located close to the dust source, so exceedances in concentrations and particles diameters are prevented. The sampling head of the EDM, provided by the manufacturer, is useable for a wide range of wind speeds. However, the inlet has some sensitivity to the wind speed, whereas the sampling efficiency decrease at wind speeds above 8 m/s (Grimm and Eatough, 2009). Our experiments ensured high sampling efficiency as the measurements were conducted at weak wind speeds (Table 2.2). Direct differences of 10% were determined by comparison of EDM measurements during a synchronous test run. These differences are acceptable because they are within the tolerated measurement uncertainty of 25% for PM_{10} concentrations (SenUVK, 2018). Furthermore, variable concentrations may result from different measurement devices with different particle measurement techniques.

Agricultural activities have a variety of dust sources, either stationary or mobile. Dust measurements from stationary sources allow only small variances in wind direction, otherwise the emitted dust plumes pass the point of the instrument inlet several meters away. Therefore, such stationary experiments can be only done, when the wind is coming from a constant direction. Dust measurements from mobile sources allow larger fluctuations in wind direction (but still downwind). In contrast to stationary dust measurements, the dust cloud is only caught temporarily, but then optimally. Furthermore, different distances between the measuring instrument and the dust source have to be taken in account. These parameters, such as the distance, are included in Eq. (4) so that an EF can be calculated from each distance.

2.3.1.4 Calculation of PM_{10} fraction of manure in the topsoil

The release of manure particles from the soil continues during the subsequent agricultural operations after manure was applied on the field. It starts immediately with the incorporation of manure and carries on until the manure is decomposed. Based on the applied amount of manure per area and the appropriate soil volume, determined by the

incorporation depth, it is possible to calculate the theoretical fraction of PM_{10} emissions from manure to the total PM_{10} emissions during tillage operations. For this, we assume that the soil and manure are uniformly mixed together, is not decomposed and having the SWC in Table 2.5. The mass ratio of the incorporated manure and the soil is given in Table 2.6.

Table 2.6 Parameters for calculating the theoretical PM_{10} fraction of manure to total PM_{10} emissions during the tillage activities.

Tillage operation	Amount of Manure [t/ha]	Tillage depth (cm)	Manure to soil ratio
PS			
Incorporation of manure (March 28)	8.3	10	0.0059
Incorporation of nitrogen fertilizer (April 7)		15	0.0039
MBG			
Incorporation of manure (May 31)	5.7	8	0.0051

Fig. 2.8 shows the total PM_{10} release and the theoretical calculated fraction from manure, which is more than two orders smaller than for the total PM_{10} release. The estimated PM_{10} fraction of manure origin ranged between 1.4 ± 0.9 g/ha and 5.9 ± 2.3 g/ha. According to the manure-mixing ratio, PM_{10} from manure during tillage contributed to about 0.39% and 0.59% of the total PM_{10} release.

The probable release of manure particles from the soil also continues after its incorporation if soils are affected by wind erosion. The reason is that the incorporated manure consists more or less completely of organic matter. This mixture of organic and mineral particles in sandy soils is still very susceptible to wind erosion, because mineral and organic components will not form aggregations immediately and present a loose mixture of particles side by side for a certain time (Iturri et al., 2017). Consequently, the manure particles will be affected by the same sorting processes as the particulate SOM.

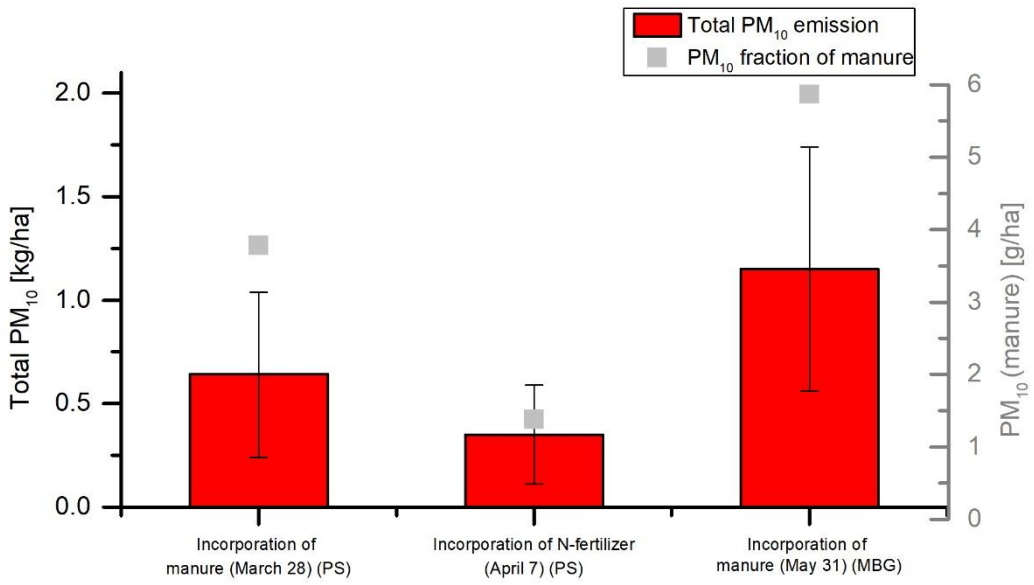

Fig. 2.8. EFs for total PM_{10} [kg/ha] (left) and the calculated PM_{10} [g/ha] fraction of manure (right).

2.3.1.5 Bioaerosol emissions from the application and incorporation of manure

Air sampling with subsequent microbiological analysis was carried out for the field trial in Potsdam-Bornim, to assess the influence of manure pretreatment on bioaerosol emissions during agricultural operations.

Neither ESBL-producing nor non-resistant *E. coli* were detected in all air samples taken during manure application and incorporation. ESBL-producing *E. coli* have been detected in exhaust air samples of chicken stables (Laube et al., 2014), but Gram-negative bacteria account for only a small amount of 0.02 – 5.2% of total viable bacteria in animal houses (Zucker et al., 2000). This leads to the assumption, that the vast majority of bacteria aerosolized from poultry manure in the field trials are Gram-positive bacteria or spore forming aerobic bacteria. Additionally, it was recently shown by Siller et al. (2020) that the majority of *E. coli* and ESBL-producing *E. coli* are inactivated in stored poultry manure after a storage period of five days. The inactivation of these bacteria starts directly when the manure is removed from the chicken stables, which might explain why no *E. coli* or ESBL-producing *E. coli* were detected in the air samples taken in the field trial.

The total viable bacteria count detected in the air samples during manure application and incorporation is depicted in Fig. 2.9. The highest total viable bacteria count per m^3 air was detected for the dried manure, followed by fresh manure. The total viable count detected for composted manure was over ten times lower compared to fresh or dried manure. The

lowest total viable bacteria count was detected for the stored manure, for which we also observed the lowest dust emission. The highest number of viable bacteria detected was 8.2 Log_{10} cfu/m^3 (colony-forming units per m^3) of air in the sample taken during the application of dried manure in 20 m distance. This number is approximately 5 million times higher than the amount of viable bacteria we detected in the sample taken on the field before the start of the manure application (1.49 Log_{10} cfu/m^3). The finding that the highest total viable bacteria count was detected during the application of dried manure was surprising at first (Fig. 2.9). We expected that the pretreatment over two days with hot air would have inactivated a large proportion of the bacteria in the dried manure.

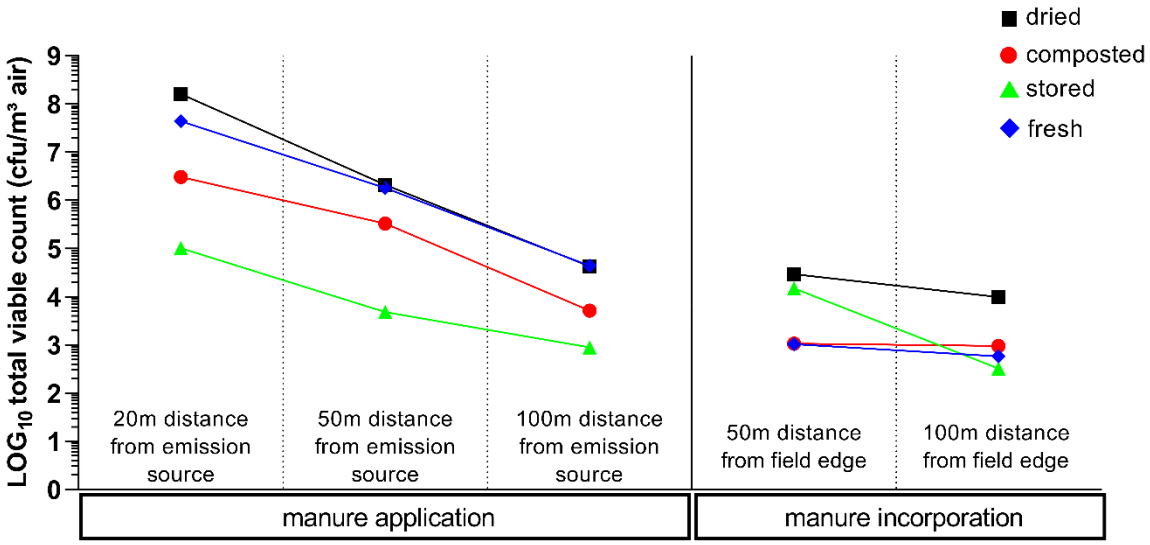

Fig. 2.9 Total viable bacterial count detected per m^3 of air during manure application and incorporation in different distances from the emission source depending on manure pretreatment in PS.

To be better able to compare between the bacteria counts and dust concentration, the bacteria counts were put in relation to the summed PM_{10} concentration. From this, a ratio between the two values can be formed for each application experiment. Taken the ratio into account, it resulted in a distinct lower cfu per µg PM_{10} during the application of dried manure compared to e.g. fresh manure (Fig. 2.10). Therefore, it can be assumed that a large proportion of the bacteria was inactivated during the pretreatment of manure with hot air.

However, taking the results of the dust emission from manure application in consideration, we assume that there is a correlation between the dust concentration in air and the amount of viable bacteria, as airborne bacteria from livestock production frequently adhere to dust (Zhao et al., 2014). Additionally, the abundant dust particles to

which the microorganisms adhere might have had a protective effect against biological decay (Milling et al., 2005).

Total viable bacteria counts detected in the air samples taken during manure application were also greatly influenced by the distance to the emission source for all types of manure pretreatment. Total viable bacteria counts in samples, taken in 20 m distance from the manure spreader, were three to almost four orders of magnitudes higher compared to the total viable bacteria counts in the samples taken in 100 m distance. Comparisons with PM_{10} concentrations at these distances were not possible because of the limited availability of EDMs.

Lower total viable bacteria counts were detected during manure incorporation compared to the manure application. The highest count was 4.4 LOG_{10} cfu/m^3 of air detected at a distance to the field edge of 50 m when the dried manure was incorporated. The ratio between bacteria counts to PM_{10} concentration is smaller compared to the application of manure. Especially, the ratio of the fresh manure decreased sharply. In contrast to the dust emissions during manure application, large amounts of soil mineral and organic particles were emitted by the incorporation of manure, to which fewer microorganisms adhered proportionally than to particles from manure. We also observed decreasing total viable bacteria counts with an increasing distance to the emission source for all types of manure pretreatment, but the effect was not as marked as for the manure application.

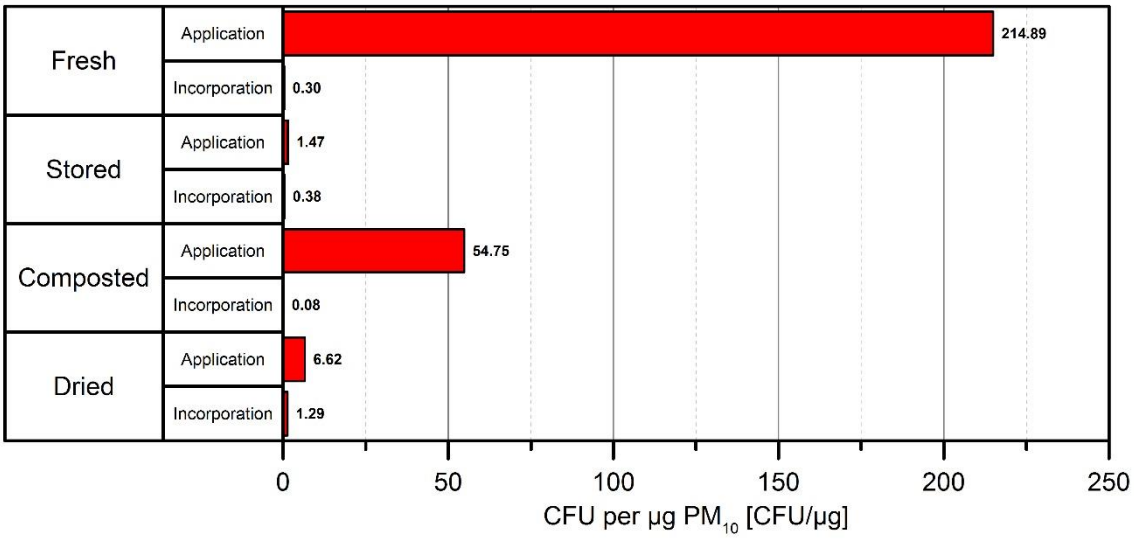

Fig. 2.10. Normalized bacteria counts to the summed PM_{10} concentration during the stationary manure application and incorporation of manure in PS.

2.3.2 Laboratory experiments

2.3.2.1 Particle size distribution of soils with different ratios of manure

The adding of manure changes the particle size distribution of soils. Here, we will tackle the issue, whether the added manure has influences on aggregation or binding of mineral dust and therefore affects PM emissions directly. A first simple dry sieving of the separated materials showed distinct differences in particle composition between the air-dried manure and the soils. The manure had a much lesser share in the dust fraction, with only 1.3% smaller 0.063 mm in diameter. The two soils had shares of 15% (MBG) and 11.1% (PS) in that fraction. Adding farmyard manure to soils resulted generally in a coarser structure (Fig. 2.11). Our results from the Malvern Mastersizer showed increasing median particle diameters of the samples, when manure in increasing shares was added to the soil. The decrease in particle diameter differed for both soils, when different air pressures were used to disperse the sample by shear stress or collision. The median particle diameter for the soil from MBG was even higher than for the soil from PS, although MBG is finer textured, independently from whether manure is added or not. The reason for the difference was the larger number of aggregates in that fine textured soil. For a typical application amount of manure (6 t/ha), the median particle diameter increased from 5% to 15% for the soil of MBG and only 0% – 4.4% for the coarser soil of PS. When we compare both soils and their diameter changes after manure application, the particle composition of the soil from MBG was more affected by adding manure than the soil from PS.

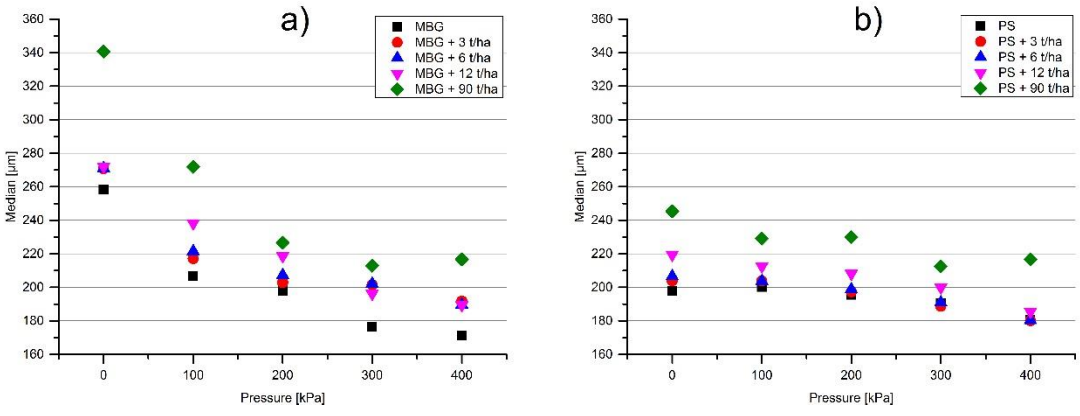

Fig. 2.11. Median particle diameter for different soil manure mixtures, representing application amounts of 3 t/ha, 6 t/ha, 12 t/ha and 90 t/ha with soils from Müncheberg-Friedrichshof (MBG) (a) and Potsdam-Bornim (PS) (b) depending on different dispersion intensities.

The adding of manure of MBG also changed the percentages share of particles smaller than 10 µm (Fig. 2.12). With increasing amounts of manure (3 t/ha, 6 t/ha, 12 t/ha), the PM_{10} share was reduced by 0.6% – 9.9% for MBG and by 0.7% – 12.3% for PS.

Manure as a fertilizer is not uniformly applied on fields on each square meter of soil. Therefore, soil samples from the field are characterized through an undefined mixture of soil and manure. In addition, only one application rate can be investigated, depending on the nutritional needs of a crop. In contrast, laboratory experiments can guarantee a much better homogenous mixture of manure with soil as realized during fertilization on a field. Furthermore, it is possible to investigate different manure-soil-mixtures (3 t/ha, 6 t/ha, 12 t/ha) to derive functional relationships.

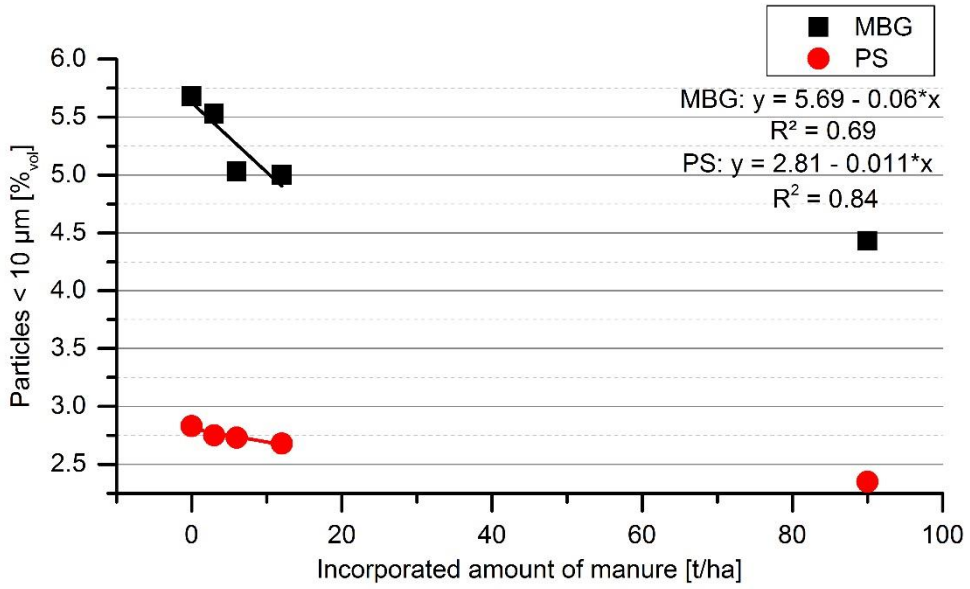

Fig. 2.12. Percentage of particles < 10 µm after incorporation of manure with different amounts of manure (3 t/ha, 6 t/ha, 12 t/ha, 90 t/ha) in soil samples from the two test fields, exemplary showed for a dispersion intensity of 2 bar.

2.4 Conclusion

The addition and incorporation of farmyard manure changes the composition in the top layer of soils with consequences on physical and chemical properties. This study focusses on the PM EF of the manure-soil-mixtures, which has not been considered in previous studies. Different pretreatments of the used manure result in distinct different PM_{10} emissions during application. Drying manure enhanced the release of PM_{10}, whereas the application of fresh, composted, or stored manure will reduce the PM_{10} emissions. As the drying of manure has a negative effect of bacteria survival, when the ratio (CFU/PM_{10}) between bacteria counts and PM_{10} emissions is considered, it results finally in a lower

risk potential for the spread of pathogenic bacteria. In contrast, the application of fresh manure with much lower PM_{10} emissions increased the CFU/PM_{10} ratio by 30 times. Hence, dust-producing processes of agricultural operations can be a possible atmospheric pathway for the spread of bacteria during and after organic fertilization. The problem arises with the application of organic fertilizers and continues as long following working steps produce dust, particularly by mixing tillage operations (e.g. incorporation of manure, seeding …). Particles from manure are always part of dust emissions from soils caused by tillage for a certain time. If contaminated with bacteria, the possible risk continues, depending on the survival rates of the bacteria and their tenacity on the soil surface, and needs further microbial investigations. However, with regard to the physical processes, possible PM emissions, and subsequent spread of bacteria from organic fertilizers could be determined.

CRediT authorship contribution statement

Steffen Münch: Investigation, Methodology, Formal analysis, Writing - original draft, Visualization. Natalie Papke: Resources, Visualization. Nadine Thiel: Resources, Investigation. Ulrich Nübel: Conceptualization, Project administration, Funding acquisition, Supervision, Writing - review & editing. Paul Siller: Formal analysis, Investigation, Writing - original draft. Uwe Roesler: Project administration, Funding acquisition, Supervision. Oliver Biniasch: Resources, Investigation. Roger Funk: Project administration, Funding acquisition, Supervision, Writing - original draft. Thomas Amon: Conceptualization, Project administration, Funding acquisition, Supervision, Writing - review & editing.

Declaration of competing interest

The authors declare that they have no known competing financial interests or personal relationships that could have appeared to influence the work reported in this paper.

Acknowledgements

The project “Spread of antibiotic resistance in an agrarian landscape” (SOARiAL) was funded by the Leibniz Association, Germany (SAW-2017-DSMZ-2). We thank the staff of the Leibniz Institute for Agricultural Engineering and Bioeconomy e.V. (ATB) for the conceptual design and preparation of the experimental plot at Potsdam-Bornim, where the stationary fertilization experiment and following soil tillage experiments took place.

Thanks to the anonymous reviewers, whose comments helped to improve the final version.

References

Acosta-Martínez, V., Van Pelt, S., Moore-Kucera, J., Baddock, M.C., Zobeck, T.M., 2015. Microbiology of wind-eroded sediments: Current knowledge and future research directions. Aeolian Res. 18, 99–113. https://doi.org/10.1016/j.aeolia.2015.06.001

Aimar, S.B., Mendez, M.J., Funk, R., Buschiazzo, D.E., 2012. Soil properties related to potential particulate matter emissions (PM10) of sandy soils. Aeolian Res. 3, 437–443.

Aloyan, A., Arutyunyan, V., Lushnikov, A., Zagaynov, V., 1997. Transport of coagulating aerosol in the atmosphere. J. Aerosol Sci. 28, 67–85.

Avecilla, F., Panebianco, J.E., Buschiazzo, D.E., 2017. Meteorological conditions during dust (PM10) emission from a tilled loam soil: Identifying variables and thresholds. Agric. For. Meteorol. 244–245, 21–32. https://doi.org/10.1016/j.agrformet.2017.05.016

Baker, J., Southard, R., Mitchell, J., 2005. Agricultural dust production in standard and conservation tillage systems in the San Joaquin Valley. J. Environ. Qual. 34, 1260–1269.

Birmili, W., Schepanski, K., Ansmann, A., Spindler, G., Tegen, I., Wehner, B., Nowak, A., Reimer, E., Mattis, I., Müller, K., Brüggemann, E., Gnauk, T., Herrmann, H., Wiedensohler, A., Althausen, D., Schladitz, A., Tuch, T., Löschau, G., 2008. An case of extreme particulate matter concentrations over Central Europe caused by dust emitted over the southern Ukraine. Atmospheric Chem. Phys. 8, 997–1016. https://doi.org/10.5194/acp-8-997-2008

Blanco-Canqui, H., Lal, R., Post, W.M., Izaurralde, R.C., Shipitalo, M.J., 2006. Organic Carbon Influences on Soil Particle Density and Rheological Properties. Soil Sci. Soc. Am. J. 70, 1407–1414. https://doi.org/10.2136/sssaj2005.0355

Bolte, K., Hartmann, P., Fleige, H., Horn, R., 2011. Determination of critical soil water content and matric potential for wind erosion. J. Soils Sediments 11, 209–220.

Borrelli, P., Ballabio, C., Panagos, P., Montanarella, L., 2014. Wind erosion susceptibility of European soils. Geoderma 232–234, 471–478. https://doi.org/10.1016/j.geoderma.2014.06.008

Burrows, S.M., Elbert, W., Lawrence, M.G., Poschl, U., 2009. Bacteria in the global atmosphere - Part 1: Review and synthesis of literature data for different ecosystems. Atmospheric Chem. Phys. 9, 9263–9280.

Buschiazzo, D.E., Funk, R., 2015. Wind erosion of agricultural soils and the carbon cycle., in: Banwart, S.A., Noellemeyer, E., Milne, E. (Eds.), Soil Carbon: Science, Management and Policy for Multiple Benefits. CABI, Wallingford, pp. 161–168. https://doi.org/10.1079/9781780645322.0161

CARB, 2003. Emission Inventory Procedural Manual Volume III: Methods for Assessing Area Source Emissions.

Carvacho, O.F., Ashbaugh, L.L., Brown, M.S., Flocchini, R.G., 2004. Measurement of PM2.5 emission potential from soil using the UC Davis resuspension test chamber. Geomorphology, Aeolian Research: processes, instrumentation, landforms and palaeoenvironments 59, 75–80. https://doi.org/10.1016/j.geomorph.2003.09.007

Cassel, T., Trzepla-Nabaglo, K., Flocchini, R., 2003. PM10 emission factors for harvest and tillage of row crops. Presented at the 12th International Emission Inventory Conference, San Diego, CA.

Chen, W., Tong, D.Q., Zhang, S., Zhang, X., Zhao, H., 2017. Local PM10 and PM2. 5 emission inventories from agricultural tillage and harvest in northeastern China. J. Environ. Sci. 57, 15–23.

Chen, W., Zhibao, D., Zhenshan, L., Zuotao, Y., 1996. Wind tunnel test of the influence of moisture on the erodibility of loessial sandy loam soils by wind. J. Arid Environ. 34, 391–402.

Countess, R.J., 1999. Development of a PM2 5 Emissions Inventory for the South Coast Air Basin. J. Air Waste Manag. Assoc. 49, 125–132.

Cowherd, C., 2006. Background document for revisions to fine fraction ratios used for AP-42 fugitive dust emission factors. Prep. Midwest Res. Inst. West. Gov. Assoc. West. Reg. Air Partnersh. Denver CO.

Cowherd, C., Donaldson, J., Hegarty, R., Ono, D., 2010. Proposed revisions to fine fraction ratios used for AP-42 fugitive dust emission factors.

Davidson, C.I., Phalen, R.F., Solomon, P.A., 2005. Airborne Particulate Matter and Human Health: A Review. Aerosol Sci. Technol. 39, 737–749. https://doi.org/10.1080/02786820500191348

Despres, V.R., Huffman, J.A., Burrows, S.M., Hoose, C., Safatov, A.S., Buryak, G., Frohlich-Nowoisky, J., Elbert, W., Andreae, M.O., Poschl, U., Jaenicke, R., 2012. Primary biological aerosol particles in the atmosphere: a review. Tellus Ser. B-Chem. Phys. Meteorol. 64, 58. https://doi.org/10.3402/tellusb.v64i0.15598

DIN 66118, 2016. Particle Size Analysis; Size Analysis by Air Classification; Fundamentals. Ger. Inst. Stand. Dtsch. Inst. Für Norm. EV Beuth Verl. GmbH.

DIN ISO 11277, 2002. Soil quality - Determination of particle size distribution in mineral soil material - Method by sieving and sedimentation. Ger. Inst. Stand. Dtsch. Inst. Für Norm. EV Beuth Verl. GmbH.

EFSA Panel on Biological Hazards (BIOHAZ), 2011. Scientific Opinion on the public health risks of bacterial strains producing extended-spectrum β-lactamases and/or AmpC β-lactamases in food and food-producing animals. EFSA J. 9, 2322.

FAO, 2014. World reference base for soil resources 2014: international soil classification system for naming soils and creating legends for soil maps. FAO, Rome.

Faulkner, W.B., Downey, D., Giles, D.K., Capareda, S.C., 2011. Evaluation of particulate matter abatement strategies for almond harvest. J. Air Waste Manag. Assoc. 61, 409–417.

Frielinghaus, M., Schmidt, R., 1993. Onsite and offsite damages by erosion in landscapes of east Germany. Farm land erosion. Template Plains Environ. Hills Elsevier Sci. Publ. BV 47–49.

Friese, A., Schulz, J., Laube, H., Von, C.S., Hartung, J., Roesler, U., 2013. Faecal occurrence and emissions of livestock-associated methicillin-resistant Staphylococcus aureus (laMRSA) and ESbl/AmpC-producing E. coli from animal farms in Germany. Berl. Munch. Tierarztl. Wochenschr. 126, 175–180.

Funk, R., Papke, N., Hör, B., 2019. Wind tunnel tests to estimate PM10 and PM2.5-emissions from complex substrates of open-cast strip mines in Germany. Aeolian Res. 39, 23–32. https://doi.org/10.1016/j.aeolia.2019.03.003

Funk, R., Reuter, H.I., Hoffmann, C., Engel, W., Öttl, D., 2008. Effect of moisture on fine dust emission from tillage operations on agricultural soils. Earth Surf. Process. Landf. J. Br. Geomorphol. Res. Group 33, 1851–1863.

Goossens, D., 2004. Wind erosion and tillage as a dust production mechanism on north European farmland. Wind Eros. Dust Dyn. Obs. Simul. Model. ESW Publ. Dep. Environ. Sci. Eros. Soil Water Conserv. Group Wagening. Univ. Wagening. 15–40.

Goossens, D., Gross, J., Spaan, W., 2001. Aeolian dust dynamics in agricultural land areas in lower Saxony, Germany. Earth Surf. Process. Landf. J. Br. Geomorphol. Res. Group 26, 701–720.

Griffin, D.W., Kellogg, C.A., Garrison, V.H., Shinn, E.A., 2002. The global transport of dust - An intercontinental river of dust, microorganisms and toxic chemicals flows through the Earth's atmosphere. Am. Sci. 90, 228–235. https://doi.org/10.1511/2002.9.781

Grimm, H., Eatough, D.J., 2009. Aerosol measurement: the use of optical light scattering for the determination of particulate size distribution, and particulate mass, including the semi-volatile fraction. J. Air Waste Manag. Assoc. 59, 101–107.

Hagen, L.J., Pelt, S.V., Zobeck, T.M., Retta, A., 2007. Dust deposition near an eroding source field. Earth Surf. Process. Landf. 32, 281–289. https://doi.org/10.1002/esp.1386

Hartmann, A., Amoureux, L., Locatelli, A., Depret, G., Jolivet, C., Gueneau, E., Neuwirth, C., 2012. Occurrence of CTX-M Producing Escherichia coli in Soils, Cattle, and Farm Environment in France (Burgundy Region). Front. Microbiol. 3. https://doi.org/10.3389/fmicb.2012.00083

Hinz, T., 2007. Particulate Matter in and from Agriculture. Bundesforschungsanstalt für Landwirtschaft (FAL).

Hoffmann, C., Funk, R., 2015. Diurnal changes of PM10-emission from arable soils in NE-Germany. Aeolian Res. 17, 117–127.

Hoffmann, C., Funk, R., Sommer, M., Li, Y., 2008. Temporal variations in PM10 and particle size distribution during Asian dust storms in Inner Mongolia. Atmos. Environ. 42, 8422–8431. https://doi.org/10.1016/j.atmosenv.2008.08.014

Holmén, B.A., James, T.A., Ashbaugh, L.L., Flocchini, R.G., 2001. Lidar-assisted measurement of PM10 emissions from agricultural tilling in California's San Joaquin Valley – Part II: emission factors. Atmos. Environ. 35, 3265–3277. https://doi.org/10.1016/S1352-2310(00)00519-7

Iturri, L.A., Funk, R., Leue, M., Sommer, M., Buschiazzo, D.E., 2017. Wind sorting affects differently the organo-mineral composition of saltating and particulate materials in contrasting texture agricultural soils. Aeolian Res. 28, 39–49. https://doi.org/10.1016/j.aeolia.2017.07.005

Jahne, M.A., Rogers, S.W., Holsen, T.M., Grimberg, S.J., Ramler, I.P., 2015. Emission and dispersion of bioaerosols from dairy manure application sites: human health risk assessment. Environ. Sci. Technol. 49, 9842–9849.

Kabelitz, T., Ammon, C., Funk, R., Münch, S., Biniasch, O., Nübel, U., Thiel, N., Rösler, U., Siller, P., Amon, B., Aarnink, A.J.A., Amon, T., 2020. Functional relationship of particulate matter (PM) emissions, animal species, and moisture content during manure application. Environ. Int. 143, 105577. https://doi.org/10.1016/j.envint.2020.105577

Kappos, A.D., Bruckmann, P., Eikmann, T., Englert, N., Heinrich, U., Höppe, P., Koch, E., Krause, G.H.M., Kreyling, W.G., Rauchfuss, K., Rombout, P., Schulz-Klemp, V., Thiel, W.R., Wichmann, H.-E., 2004. Health effects of particles in ambient air. Int. J. Hyg. Environ. Health 207, 399–407. https://doi.org/10.1078/1438-4639-00306

Kellogg, C.A., Griffin, D.W., 2006. Aerobiology and the global transport of desert dust. Trends Ecol. Evol. 21, 638–644.

Lal, R., 2003. Soil erosion and the global carbon budget. Environ. Int. 29, 437–450. https://doi.org/10.1016/S0160-4120(02)00192-7

Laube, H., Friese, A., Von Salviati, C., Guerra, B., Rösler, U., 2014. Transmission of ESBL/AmpC-producing Escherichia coli from broiler chicken farms to surrounding areas. Vet. Microbiol. 172, 519–527.

Lee, K., Lawson, R.J., Olenchock, S.A., Vallyathan, V., Southard, R.J., Thorne, P.S., Saiki, C., Schenker, M.B., 2004. Personal Exposures to Inorganic and Organic Dust in Manual Harvest of California Citrus and Table Grapes. J. Occup. Environ. Hyg. 1, 505–514. https://doi.org/10.1080/15459620490471616

Lelieveld, J., Evans, J.S., Fnais, M., Giannadaki, D., Pozzer, A., 2015. The contribution of outdoor air pollution sources to premature mortality on a global scale. Nature 525, 367.

Madden, N., Southard, R., Mitchell, J., 2008. Conservation tillage reduces PM10 emissions in dairy forage rotations. Atmos. Environ. 42, 3795–3808.

Maffia, J., Elio, D., Barbara, A., Paolo, B., 2020. PM emissions from open field crop management: Emission factors, assessment methods and mitigation measures–A review. Atmos. Environ. 117381.

Maki, T., Lee, K.C., Kawai, K., Onishi, K., Hong, C.S., Kurosaki, Y., Shinoda, M., Kai, K., Iwasaka, Y., Archer, S.D.J., Lacap-Bugler, D.C., Hasegawa, H., Pointing, S.B., 2019. Aeolian Dispersal of Bacteria Associated With Desert Dust and Anthropogenic Particles Over Continental and Oceanic Surfaces. J. Geophys. Res. Atmospheres 0. https://doi.org/10.1029/2018JD029597

Mastersizer, 2015. Mastersizer 3000 user manual (English) [WWW Document]. URL https://www.malvernpanalytical.com/en/learn/knowledge-center/user-manuals/MAN0474EN (accessed 10.22.19).

Meyer, E., Gastmeier, P., Deja, M., Schwab, F., 2013. Antibiotic consumption and resistance: data from Europe and Germany. Int. J. Med. Microbiol. 303, 388–395.

Milling, A., Kehr, R., Wulf, A., Smalla, K., 2005. Survival of bacteria on wood and plastic particles: Dependence on wood species and environmental conditions. Holzforschung 59, 72–81.

MLUL, 2016. Klimareport Brandenburg 2016 - Das Klima von gestern, heute und in Zukunft. Ministerium für Ländliche Entwicklung, Umwelt und Landwirtschaft des Landes Brandenburg (MLUL) Fachbeiträge des LfU.

Nerger, R., Funk, R., Cordsen, E., Fohrer, N., 2017. Application of a modeling approach to designate soil and soil organic carbon loss to wind erosion on long-term monitoring sites (BDF) in Northern Germany. Aeolian Res. 25, 135–147. https://doi.org/10.1016/j.aeolia.2017.03.006

Öttl, D., Funk, R., 2007. PM emission factors for farming activities by means of dispersion modeling. Presented at the International Conference “Particulate Matter in and from Agriculture.

Öttl, D., Kukkonen, J., Almbauer, R.A., Sturm, P.J., Pohjola, M., Härkönen, J., 2001. Evaluation of a Gaussian and a Lagrangian model against a roadside data set, with emphasis on low wind speed conditions. Atmos. Environ. 35, 2123–2132.

Proia, L., Anzil, A., Subirats, J., Borrego, C., Farrè, M., Llorca, M., Balcázar, J.L., Servais, P., 2018. Antibiotic resistance along an urban river impacted by treated wastewaters. Sci. Total Environ. 628–629, 453–466. https://doi.org/10.1016/j.scitotenv.2018.02.083

Renger, M., Bohne, K., Facklam, M., Harrach, T., Riek, W., Schäfer, W., Wessolek, G., Zacharias, S., 2008. Ergebnisse und Vorschläge der DBG-Arbeitsgruppe “Kennwerte des Bodengefüges” zur Schätzung bodenphysikalischer Kennwerte.

Royco Instruments, 1974. Characteristics of Particles and Particle Dispersoids. Royco Instrum. Menlo Park CA.

Rühlmann, J., Körschens, M., Graefe, J., 2006. A new approach to calculate the particle density of soils considering properties of the soil organic matter and the mineral matrix. Geoderma 130, 272–283. https://doi.org/10.1016/j.geoderma.2005.01.024

Schenker M, 2000. Exposures and health effects from inorganic agricultural dusts. Environ. Health Perspect. 108, 661–664. https://doi.org/10.1289/ehp.00108s4661

Seinfeld, J.H., Pandis, S.N., 2006. Atmospheric Chemistry and Physics: From Air Pollution to Climate Change, 2. ed. John Wiley & Sons, Hoboken, N.J.

SenUVK, 2018. PM10 Äquivalenznachweis für die automatischen Geräte des Typs FHIRund Grimm-EDM180 für das Jahr 2018 [WWW Document]. Senate Dep. Environ. Transp. Clim. Prot. Berl. URL https://www.berlin.de/senuvk/umwelt/luftqualitaet/de/messnetz/download/pm10-aequinachweis_berlin_2018.pdf

Shao, Y., 2008. Physics and Modelling of Wind Erosion. Springer Science & Business Media.

Sharratt, B., Wendling, L., Feng, G., 2010. Windblown dust affected by tillage intensity during summer fallow. Aeolian Res. 2, 129–134.

Siller, P., Daehre, K., Thiel, N., Nübel, U., Roesler, U., 2020. Impact of short-term storage on the quantity of extended-spectrum beta-lactamase–producing Escherichia coli in broiler litter under practical conditions. Poult. Sci. 99, 2125–2135. https://doi.org/10.1016/j.psj.2019.11.043

Stange, C., Sidhu, J.P.S., Tiehm, A., Toze, S., 2016. Antibiotic resistance and virulence genes in coliform water isolates. Int. J. Hyg. Environ. Health 219, 823–831. https://doi.org/10.1016/j.ijheh.2016.07.015

Statistisches Bundesamt, 2017. Publikation - Land- & Forstwirtschaft - Landwirtschaftliche Bodennutzung - Anbau auf dem Ackerland - Vorbericht - Ältere Ausgaben - Statistisches Bundesamt (Destatis) [WWW Document]. URL https://www.destatis.de/DE/Publikationen/Thematisch/LandForstwirtschaft/AlteAusgaben/AnbauAckerlandVorberichtAlt.html (accessed 12.12.18).

Steininger, M., Wurbs, D., 2017. Bundesweite Gefährdung der Böden durch Winderosion und Bewertung der Veränderung infolge des Wandels klimatischer Steuergrößen als Grundlage zur Weiterentwicklung der Vorsorge und Gefahrenabwehr im Bodenschutzrecht. Umweltbundesamt Texte | 13/2017, 119.

TA Luft, 1986. Erste allgemeine Verwaltungsvorschrift zum Bundes-Immissionsschutzgesetz–Technische Anleitung zur Reinhaltung der Luft (TA Luft) vom 7. Februar 1986. GMBl G 3191, 95.

Weber, A., 1976. Atmospheric dispersion parameters in Gaussian plume modeling. Part 1: Review of current systems and possible future developments. Rep. Sep 1975-Mar 1976 N. C. State Univ Raleigh Dept Geosci.

Zhang, Y., He, M., Wu, S., Zhu, Y., Wang, S., Shima, M., Tamura, K., Ma, L., 2015. Short-Term Effects of Fine Particulate Matter and Temperature on Lung Function among Healthy College Students in Wuhan, China. Int. J. Environ. Res. Public. Health 12, 7777–7793. https://doi.org/10.3390/ijerph120707777

Zhao, Y., Aarnink, A.J.A., Jong, M.C.M.D., Koerkamp, P.W.G.G., 2014. Airborne Microorganisms From Livestock Production Systems and Their Relation to Dust. Crit.

Rev. Environ. Sci. Technol. 44, 1071–1128. https://doi.org/10.1080/10643389.2012.746064

Zucker, B., Trojan, S., Müller, W., 2000. Airborne gram-negative bacterial flora in animal houses. J. Vet. Med. Ser. B 47, 37–46.

3 Airborne bacterial emission fluxes from manure-fertilized agricultural soil

Published in:

Thiel, N*., Münch, S.*, Behrens, W., Junker, V., Faust, M., Biniasch, O., Kabelitz, T., Siller, P., Boedeker, C., Schumann, P., Roesler, U., Amon, T., Schepanski, K., Funk, R., Nübel, U., 2020. Airborne bacterial emission fluxes from manure-fertilized agricultural soil. Microb. Biotechnol. 13, 1631–1647. https://doi.org/10.1111/1751-7915.13632

*equal contribution

Summary

This is the first study to quantify the dependence on wind velocity of airborne bacterial emission fluxes from soil. It demonstrates that manure bacteria get aerosolized from fertilized soil more easily than soil bacteria, and it applies bacterial genomic sequencing for the first time to trace environmental faecal contamination back to its source in the chicken barn. We report quantitative, airborne emission fluxes of bacteria during and following the fertilization of agricultural soil with manure from broiler chickens. During the fertilization process, the concentration of airborne bacteria culturable on blood agar medium increased more than 600 000-fold, and 1 m^3 of air carried 2.9×10^5 viable enterococci, i.e. indicators of faecal contamination which had been undetectable in background air samples. Trajectory modelling suggested that atmospheric residence times and dispersion pathways were dependent on the time of day at which fertilization was performed. Measurements in a wind tunnel indicated that airborne bacterial emission fluxes from freshly fertilized soil under local climatic conditions on average were 100-fold higher than a previous estimate of average emissions from land. Faecal bacteria collected from soil and dust up to seven weeks after fertilization could be traced to their origins in the poultry barn by genomic sequencing. Comparative analyses of 16S rRNA gene sequences from manure, soil and dust showed that manure bacteria got aerosolized preferably, likely due to their attachment to low-density manure particles. Our data show that fertilization with manure may cause substantial increases of bacterial emissions from agricultural land. After mechanical incorporation of manure into soil, however, the associated risk of airborne infection is low.

3.1 Introduction

Ambient air carries diverse bacteria at average concentrations of ~ 10^4 m^{-3} (Despres et al., 2012). Airborne bacteria have been studied for their potential adverse health effects (Fröhlich-Nowoisky et al., 2016) and for their impact on precipitation, as they may function as effective nuclei for cloud condensation and ice formation (Möhler et al., 2007). Most airborne bacteria are attached to other particles, e.g. soil fragments or agglomerates of other bacterial cells, with a median aerodynamic diameter of 4 µm (Despres et al., 2012). Due to their small size, bacteria remain suspended in the atmosphere for an average period of several days, and they can get transported over long distances (up to thousands of kilometers) during this time (Despres et al., 2012). For example, the long-distance transport of large quantities of dust derived from arid soils in Africa and Asia and its high microbial load upon deposition has been documented (Kellogg and Griffin, 2006). Molecular studies detected considerable microbial diversity associated with such desert dust (Barberán et al., 2014; Yamaguchi et al., 2012), and viable bacteria have been cultivated from it, including opportunistic pathogens (Hervàs et al., 2009; Kellogg et al., 2004; Prospero et al., 2005). However, bacterial emission fluxes from biologically more active regions, including grasslands and plant-covered agricultural fields, are many times stronger than those from desert soils, as indicated by direct measurements (Lighthart and Shaffer, 1994; Lindemann et al., 1982) and by flux modelling (Burrows et al., 2009b).

Estimates for global bacterial emissions range from 0.7 to 28 million tons annually (Despres et al., 2012). While concentrations and specific identities of airborne bacteria vary greatly over space and time (Bowers et al., 2011; Burrows et al., 2009a; Cáliz et al., 2018), the spatial and temporal variation of emission rates has been studied very little, limiting the precision of current numerical models of microbial transport (Burrows et al., 2009b; Despres et al., 2012). Moreover, aerosolized microorganisms have rarely been linked to their specific sources (Bowers et al., 2011), hindering investigations into the mechanisms and dynamics of microbial emission, transport and deposition. As a consequence, microbiology currently lacks a quantitative and mechanistic understanding of the aerial dispersal of environmental bacteria.

In the European Union, 14.5 million tons of chicken meat are produced annually and there are an additional 400 million laying hens (https://ec.europa.eu/agriculture), resulting

in the production of approximately 22 million tons of chicken litter per year (Chastain et al., 2002). The majority of this manure is disposed of as fertilizer onto agricultural land without any prior treatment. Solid manure from poultry production is prone to dust emissions due to its high dry matter content and small particle sizes (Kabelitz et al., 2020). It is currently not clear, however, which quantities of faecal bacteria from chicken manure get aerosolized during and after soil fertilization, over which distances these microorganisms may get transported atmospherically, or if they pose a risk of infection.

We here present quantitative measurements of bacterial emissions from soil fertilized with broiler manure, based on field trials and wind tunnel experiments. We assess the contribution of agricultural fertilization to bacterial emissions by modelling emission fluxes and transport routes of airborne bacteria and demonstrate how genomic sequencing can be applied to trace emitted faecal bacteria back to their sources. Finally, we provide an assessment of infection risk based on this data.

3.2 Results

3.2.1 Pathogenic bacteria in chicken faeces and manure

We sampled chicken faeces from two intensive broiler fattening farms and tested them for the presence of a variety of pathogenic bacteria by enrichment and by cultivation on selective agar media following dilution to extinction. All faeces samples carried *Ent. faecium* and ESBL-producing *E. coli*. No MRSA was detected, even by using a two-step enrichment procedure. As expected, manure delivered to the field site 13 days later contained abundant enterococci (Table 3.1). Interestingly, however, we were unable to recover any ESBL-producing *E. coli* from this manure, even though they had been abundant in chicken faeces just a few days before. Results from cultivation-independent analyses are described below.

Table 3.1 Bacterial concentrations in soil, manure and dust.

	Total bacteria (microscopy)	Blood agar counts (CFU)	Enterococci (CFU)
Manure, per g	$2.4 \times 10^{10} \pm 1.4 \times 10^{10}$	$5.2 \times 10^{8} \pm 1.4 \times 10^{8}$	$8.6 \times 10^{6} \pm 3.6 \times 10^{6}$
Unfertilized soil, per g	$1.0 \times 10^{9} \pm 3.9 \times 10^{8}$	$1.9 \times 10^{6} \pm 4.0 \times 10^{5}$	$1.5 \times 10^{3} \pm 5.7 \times 10^{2}$
Fertilized soil, per g	$1.3 \times 10^{9} \pm 3.1 \times 10^{8}$	$5.3 \times 10^{6} \pm 1.3 \times 10^{6}$	$1.1 \times 10^{5} \pm 6.4 \times 10^{4}$
Background air, per m^3	1.2×10^{6}[b]	113[b]	< Detection limit
Dust, manure application, per m^3	$4.9 \times 10^{8} \pm 1.5 \times 10^{8}$	$7.3 \times 10^{7} \pm 1.8 \times 10^{7}$	$2.9 \times 10^{5} \pm 6.2 \times 10^{4}$
Dust, manure incorporation, per m^3	$2.9 \times 10^{7} \pm 3.0 \times 10^{6}$	$8.4 \times 10^{5} \pm 1.6 \times 10^{5}$	9.4×10^{3}[a]
Dust from manure application, per g	$3.2 \times 10^{13} \pm 7.5 \times 10^{12}$	$5.1 \times 10^{12} \pm 1.1 \times 10^{12}$	$2.1 \times 10^{10} \pm 4.8 \times 10^{9}$
Dust from manure incorporation, per g	$1.7 \times 10^{11} \pm 2.6 \times 10^{10}$	$4.5 \times 10^{9} \pm 6.0 \times 10^{8}$	8.7×10^{7}[a]

Means and standard errors from three replicate samples are indicated

a. For enterococcal concentrations in dust during manure incorporation, triplicate measurements were not available due to contamination of agar plates.

b. Background air was sampled only once.

3.2.2 Emissions during manure application and incorporation

We measured emissions of dust and associated microorganisms during the application and incorporation of poultry manure in a field experiment. Details on the characteristics of particulate emissions from this experiment will be reported elsewhere (Münch et al., 2020). Briefly, the total measured PM_{10} concentrations consisted of the regional background and additional dust from agricultural activities. The background was measured and used to adjust PM_{10} concentrations for the share released by manure

application and incorporation. Each time the dust plume emitting from the tractor hit the measuring instruments, PM_{10} concentrations increased for a few seconds, to maximally 160 µg m^{-3} during manure application and to maximally 1300 µg m^{-3} during manure incorporation respectively (Fig. S3.2). Concentrations in dust plumes were used to calculate source strengths (Maffia et al., 2020) (Eq. 3.2 and Eq. 3.3), and total PM_{10} emissions were inferred considering processing times, assuming constant dust release (Table 3.2).

In parallel to recording particulate emissions, air samples were collected for microbiological analyses by impingement. The concentration of bacteria culturable on agar plates (blood agar counts) increased 600 000-fold to 7.3×10^7 per m^3 of air during application activity and 7000-fold to 8.4×10^5 per m^3 during incorporation of fertilizer into soil respectively (Table 3.1). Enterococci had not been detected at all in background air samples, but were found at concentrations of up to 2.9×10^5 per m^3 of air during manure application and 9.4×10^3 per m^3 during tillage (Table 3.1). Bacterial concentrations per gram of dust were consistently higher than per gram of soil or manure, respectively (Table 3.1), indicating the preferred aerosolization of bacteria.

Table 3.2 PM_{10} emissions and bacterial emission fluxes[a].

		PM_{10}	Bacterial cell counts (epifluor. microscopy)	Blood agar CFU	KAA agar CFU (Enterococci)
Fertilizer application	per ha	0.18 ± 0.12 kg	$5.5 \times 10^{16} \pm 3.6 \times 10^{16}$	$8.5 \times 10^{15} \pm 5.7 \times 10^{15}$	$3.5 \times 10^{13} \pm 2.4 \times 10^{13}$
Tillage	per ha	1.15 ± 0.59 kg	$1.8 \times 10^{14} \pm 9.3 \times 10^{13}$	$5.0 \times 10^{12} \pm 2.6 \times 10^{12}$	$2.9 \times 10^{10} \pm 1.5 \times 10^{10}$
Wind-driven emission, immediately following fertilization[b]	per ha per month	6.1 kg (41 kg)	9.6×10^{14} (6.4×10^{15})	2.7×10^{13} (1.8×10^{14})	1.5×10^{11} (1.0×10^{12})
	per m² per second		3.6×10^{4} (2.5×10^{5})	1×10^{3} (7.1×10^{3})	5.9 (38)
Wind-driven emission, four weeks after fertilization[c]	per ha per month	6.1 kg (41 kg)	4.7×10^{14} (3.2×10^{15})	3.9×10^{11} (2.6×10^{12})	5.3×10^{9} (3.6×10^{10})
	per m² per second		1.8×10^{4} (1.2×10^{5})	15 (100)	0.2 (1.3)

a. Emissions during fertilizer application and tillage were measured in the field. Wind-driven emissions were measured in a wind tunnel and projected to the field site considering long-term weather data.

b. Long-term mean (maximum) for March (Fig. 6_PM10release), based on bacterial load measured during tillage.

c. Long-term mean (maximum) for March (Fig. 6_PM10release), based on bacterial load measured 4 weeks after fertilization.

Microscopic cell counts and agar counts decreased with increasing distance from the dust sources (Fig. 3.1). Of note, enterococcal and blood agar counts were almost 10-fold higher during manure application than during subsequent incorporation into the soil, even though PM_{10} emissions were lower (Fig. 3.1). Based on dust concentrations and a Gaussian dispersion model, $5.5 \times 10^{16} \pm 3.6 \times 10^{16}$ total bacteria (as counted microscopically), including $3.5 \times 10^{13} \pm 2.4 \times 10^{13}$ culturable enterococci, were emitted per hectare during the fertilizer application process, and $1.8 \times 10^{14} \pm 9.3 \times 10^{13}$ bacteria and $2.9 \times 10^{10} \pm 1.5 \times 10^{10}$ enterococci were emitted per hectare during subsequent tillage activities (Table 3.2).

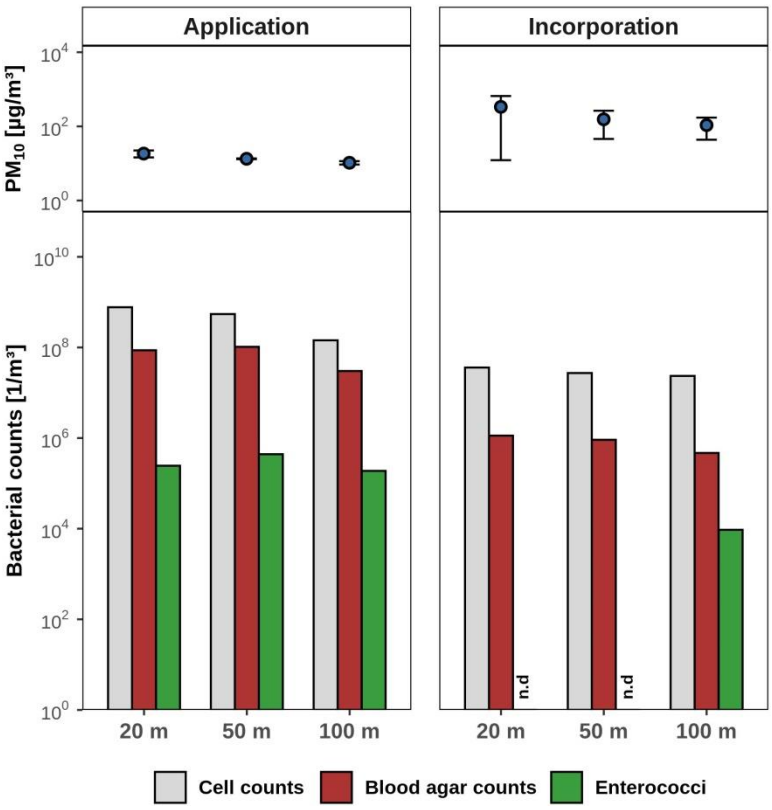

Fig. 3.1. PM_{10} (top) and microbial emissions (bottom) captured by the measuring instruments during manure application and incorporation processes at increasing distances to the tractor engine. Air samples were collected over 10 min for each distance, and particulate concentrations were monitored in parallel at a height of 1.5 m. Total bacteria were determined as microscopic cell counts, culturable bacteria as blood agar counts and enterococci as counts on KAA medium.

3.2.3 Modelling of dust transport

The transport of dust emitted during manure application and incorporation was simulated by using a dispersion model (Fig. 3.2). The turbulent nature of the atmospheric boundary layer resulted in an upward mixing of particles to up to 2500 m above ground level, and particles were removed from the atmosphere due to their gravitational settling and turbulent processes depending on their size. The results showed that the maximum

number of dust particles released during manure application got deposited within a distance of 20 km, whereas this maximum was at 200 km during subsequent manure incorporation due to a more mature atmospheric boundary layer in the afternoon (Fig. 3.2). However, during both manure application and incorporation, approximately 10% of dust got transported over > 300 km into a Southeastern direction, and 0.4% or 0.5%, respectively, got transported over > 1000 km (Fig. 3.2).

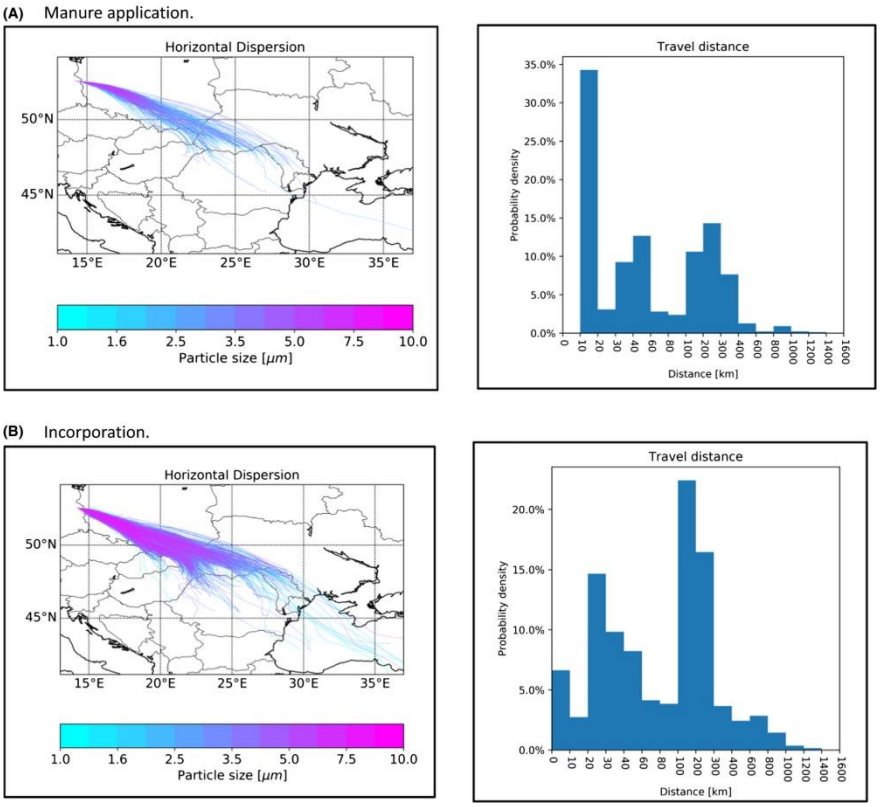

Fig. 3.2. Simulation of dust transport during field experiment. Probability densities for the height over ground and the distance from the emission source are shown. A. Simulation for emissions during manure application in the morning (10:49 – 12:15) of 31 May 2017. B. Simulation for emissions during incorporation of manure into soil (13:33 – 14:45).

3.2.4 Estimation of the potential for wind erosion induced PM_{10} emissions from the test field

We measured PM_{10} emissions and the associated release of bacteria from fertilized soil in wind tunnel experiments, assuming wind erosion occurs shortly after application and incorporation of manure (Fig. 3.3). Above the field-specific threshold wind velocity of 7.0 m s^{-1}, particles were released that initiated the so-called avalanching effect, resulting in an exponential increase of transport intensity at increasing wind velocity (Fig. 3.3 and Fig. 3.4A). Based on this correlation, we used historic weather data to calculate potential PM_{10} emissions from this field at an hourly basis for the period 1992 to 2018. Large differences between years were evident, with 0 – 354 kg of PM_{10} emitted from this field

annually (Fig. 3.4B). Calculated PM_{10} emissions correlated with the yearly course of the wind speed, with the highest values inferred for winter and spring (October to April; Fig. 3.4C). Fertilization is usually performed in spring (March to April) in this area. During this time period, we estimated that 6 ± 15 kg (April; mean, standard deviation) to 13 ± 23 kg (March) of PM_{10} got emitted from the test field per month in previous years (Fig. 3.4C). Due to weather variation between years, these estimates ranged from 0 kg to 268 kg per month and therefore were associated with large standard errors when averaged over 27 years. If the field had been fertilized with poultry manure as investigated here, these average dust emissions had been associated with emission fluxes of 3.6×10^4 $m^{-2}s^{-1}$ total bacteria (based on microscopic counts; range, 0 – 2.5×10^5 $m^{-2}s^{-1}$), 10^3 $m^{-2}s^{-1}$ bacteria culturable on blood agar (range, 0 – 7.1×10^3 $m^{-2}s^{-1}$) and 5.9 $m^{-2}s^{-1}$ enterococci (range, 0 – 38) respectively (Table 3.2).

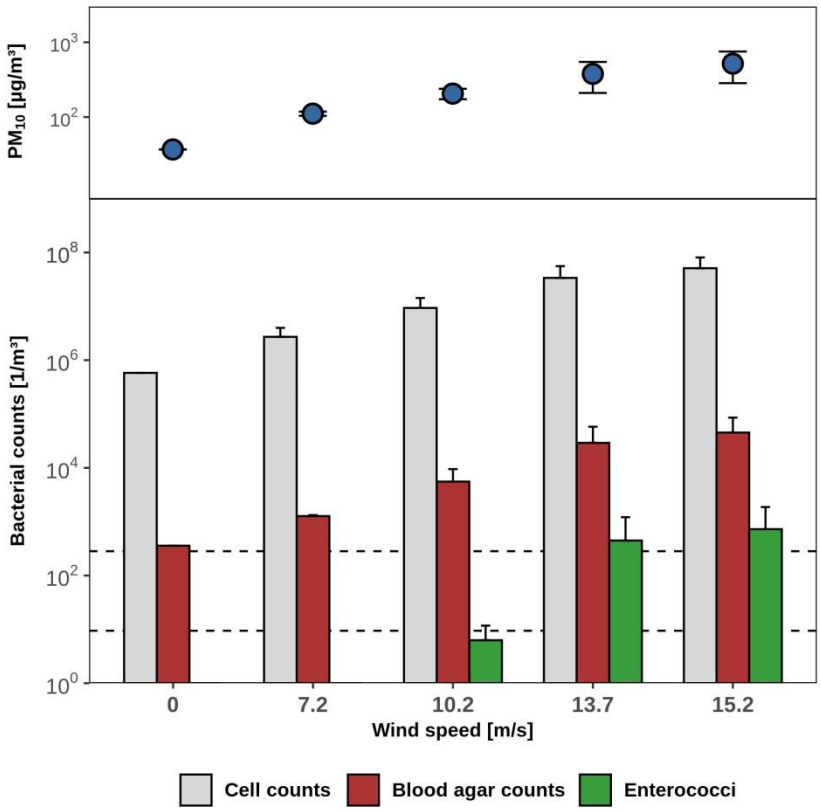

Fig. 3.3. Wind tunnel simulation of wind-driven release of bacteria from soil four weeks after fertilization. PM_{10} concentrations, microscopic cell counts and CFU for bacteria on blood agar and for enterococci at four different wind velocities and for background measurements (at 0 m s^{-1}) are depicted; means and standard deviations from three replicate experiments.

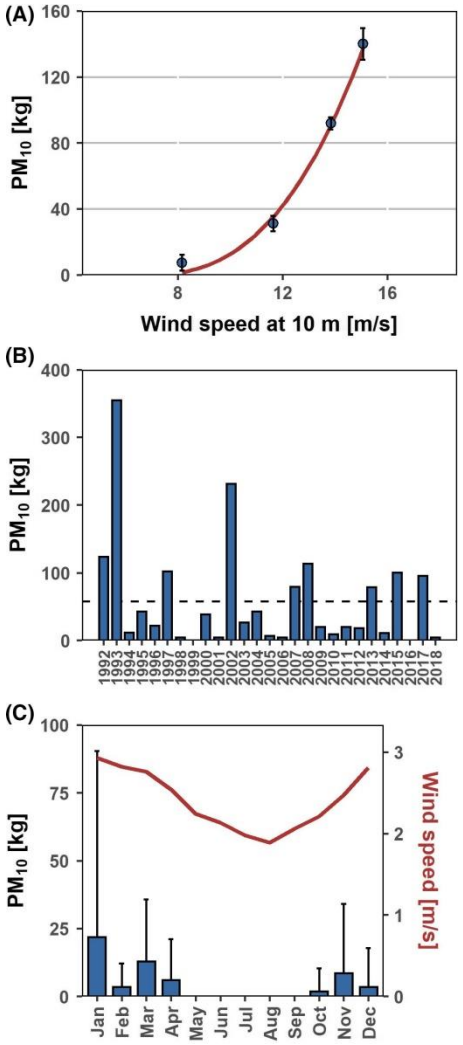

Fig. 3.4. Emissions of PM_{10} from the test field. (A) Calculated PM_{10} emission from wind tunnel experiments was plotted against wind velocity. (B,C) Estimated PM_{10} emissions from the test field (2.1 ha) in the last 27 years. (B) Annual sum, the dashed line indicates the mean annual emission, (C) monthly mean.

3.2.5 Survival of manure-derived enterococci in soil

We monitored numbers of bacteria (microscopy, blood agar counts) and enterococci (KAA agar) in soil prior to fertilization and thereafter in 2 – 5 weeks intervals until 19 weeks after fertilization (Fig. 3.5). In manure, microscopic cell counts were 50-fold larger than blood agar counts, indicating around 2% culturability of manure bacteria (Table 3.1). In contrast, culturability of soil bacteria was approximately 0.2% (Table 3.1). The number of enterococci was $8.6 \times 10^6 \pm 3.6 \times 10^6$ CFU g^{-1} in manure and $1.5 \times 10^3 \pm 5.7 \times 10^2$ CFU g^{-1} in non-fertilized soil (Table 3.1). Fertilization increased the number of enterococci in soil by more than 70-fold to $1.1 \times 10^5 \pm 6.4 \times 10^4$ CFU g^{-1} (Table 3.1). Seven weeks later, enterococci counts had decreased to background level (Fig. 3.5).

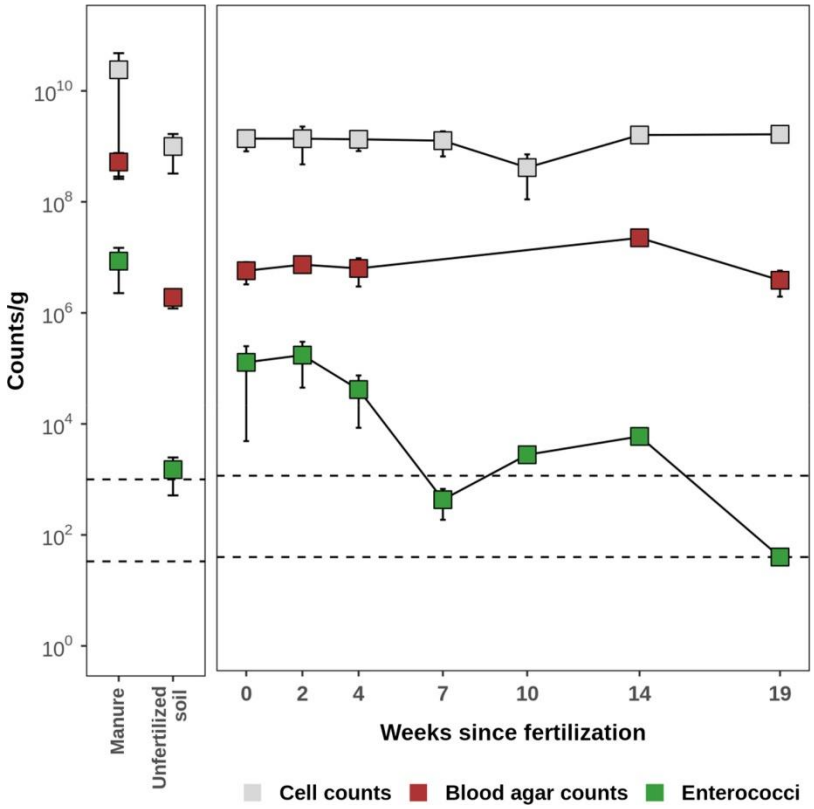

Fig. 3.5. Survival of enterococci in soil after fertilization. Mean bacterial counts from samples collected from three distinct spots on the field site; error bars: standard deviation. LoD, limit of detection; LoQ, limit of quantification.

The enteric pathogen *Ent. faecium* had not been found in soil samples prior to fertilization, but was consistently identified by species-specific PCR among enterococcal isolates from fertilized soil until 50 days after fertilization. Other predominant enterococci species were *Ent. Faecalis* and *Ent. casseliflavus* (identified by mass spectroscopy). Genomes from 92 *Ent. faecium* isolates, which had been collected from chicken stables (faeces), manure, fertilized soil and dust, got sequenced by using Illumina technology. While genome analyses indicated considerable phylogenetic diversity, encompassing multiple multilocus sequence types (STs), the *Ent. faecium* isolates were not closely related to strains which frequently cause healthcare- associated human infections (i.e. STs 17, 18, 117, 80, 192; Fig. 3.6). Importantly, we found multiple identical or near-identical *Ent. faecium* genomes (maximum difference, one core-genome allele; clades I to VI in Fig. 3.6) across all samples, including faeces, manure, fertilized soil and dust. Therefore, viable *Ent. faecium* detected in fertilized soil and dust indeed originated from applied manure, rather than from any environmental sources.

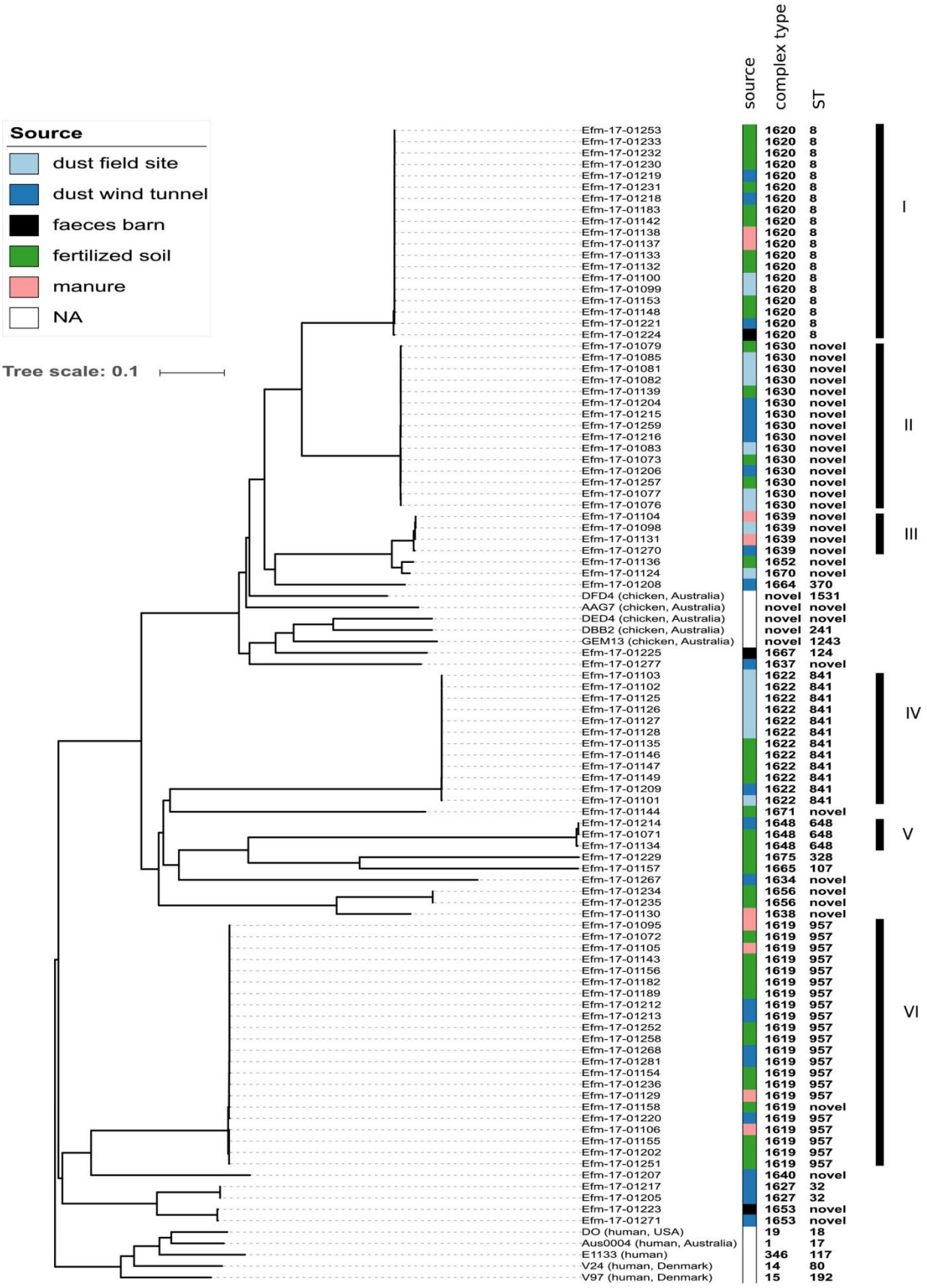

Fig. 3.6. Genome-based phylogenetic relationships among *Ent. faecium* isolates. A neighbor-joining tree was reconstructed from a matrix of core-genome allelic distances. Colors indicate the sampling sources as indicated. Six clusters with multiple near-identical genomes each (distance ≤ 1 core-genome allele) are labelled with roman numerals.

3.2.6 Bacterial diversity

To investigate the composition of bacterial communities in the different samples, we extracted their total DNA and PCR-amplified and sequenced the V4 region of 16S rDNA (Caporaso et al., 2011). Background air did not provide sufficient DNA for PCR amplification (not shown). The resulting 4.68×10^6 quality-filtered sequencing reads from 19 samples were assigned to 2.59×10^4 unique amplicon sequence variants (SV). Rarefaction analysis demonstrated that the sequencing depth for manure and almost all dust samples was sufficient to achieve saturation of the number of SVs (Fig. S3.3). Soil and dust (from wind tunnel experiments) carried greater bacterial diversity than chicken manure (Fig. 3.7). While only 775 ± 89 SVs were found in manure, numbers of SVs were consistently greater than 3000 in soil and soil-derived dust (Fig. 3.7, Fig. S3.3). Large bacterial diversity in soil and dust samples was also reflected by Shannon and Simpson indices (Fig. 3.7) and by the number of bacterial phyla and genera detected (Figs S4 and S5).

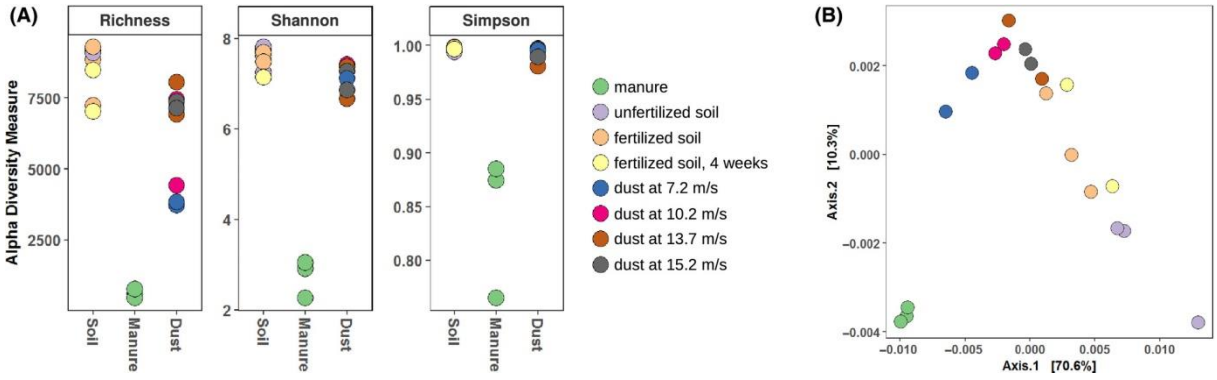

Fig. 3.7. Diversity analyses based on 16S rRNA gene sequencing. Colors indicate types of samples. A. Alpha diversity measures. B. Principal coordinate analysis of weighted UniFrac distances between samples.

At the level of individual sequence variants (SVs), 47 predominant SVs, affiliated to nine bacterial families, together accounted for 96% of 16S rDNA sequences from manure (Fig. 3.8). These SVs accounted for < 0.2% of 16S rDNA from soil prior to fertilization and for 2% of 16S rDNA from freshly fertilized soil (Fig. 3.8). Four weeks after fertilization, these 16S rDNA sequences had decreased to 0.7% in soil, yet they got enriched to up to 12% in dust emitted from this soil (Fig. 3.8).

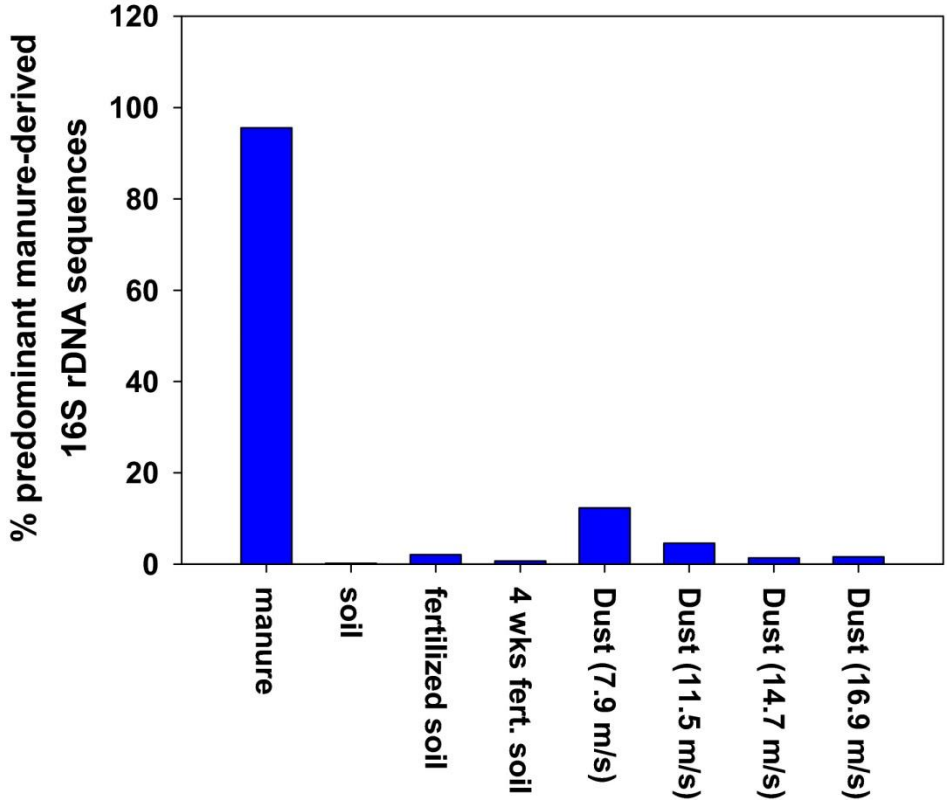

Fig. 3.8. Aggregated abundances of 47 sequence variants that each accounted for > 0.1% of 16S rRNA sequencing reads in chicken manure. These sequence variants were affiliated to Staphylococcaceae, Lactobacillaceae, Leuconostocaceae, Brevibacteriaceae, Corynebacteriaceae, Dermabacteraceae, Nocardiopsaceae, Bacillaceae, Enterobacteriaceae, Ruminococcaceae and Streptococcaceae (in the order of their proportional abundance in manure).

3.3 Discussion

3.3.1 Dust-associated bacterial emissions during fertilizer application and tillage operations

Emissions of PM_{10} during the process of manure application accounted for total losses of only 0.003% of the 12 tons of manure applied. Considerable numbers of viable bacteria were associated with these particulate emissions, however. Twenty meters downwind from the application site, the concentration in air of bacteria culturable on blood agar medium increased more than 105-fold compared to background levels. One m^3 of air carried 2.9 x 10^5 enterococci, which had been undetectable in background air.

Comparable data in the literature are scarce, and previously reported concentrations of aerosolized bacteria during the process of spreading liquid manure (cattle slurry) varied by five orders of magnitude, from 2×10^3 culturable bacteria per m^3 (Boutin et al., 1988) to 10^8 enterobacteria per m^3 (Hobbs et al., 2004). Our measurements were at the high range compared to this literature data, which were to be expected because poultry litter is

dryer (29% water content) and therefore more prone to aerosolization than liquid slurry (Kabelitz et al., 2020).

Measurements of airborne bacterial emissions during tillage operations have not previously been reported. In our field experiment, the quantities of particulate emissions during tillage activities incorporating fertilizer into the soil were in the range to be expected for a sandy clay loam soil with a water content of 9%. Tillage aerosolized 6.4 times larger amounts of PM_{10} than the preceding fertilizer spreading procedure. This larger amount of dust, however, carried less than 1% of the microscopically counted bacterial cells and only small fractions (< 0.1%) of blood agar plate counts and enterococcal (i.e. KAA agar) plate counts, compared to dust from fertilizer spread (Table 3.2). Obviously, tillage resulted in a dilution of manure in the soil. As a consequence, the majority of dust released during tillage was derived from the soil and hence contained a large proportion of inanimate mineral particles.

Not surprisingly, our sequence analyses of bacterial 16S rRNA genes revealed drastically different taxonomic compositions of the bacterial communities in soil and manure (Fig. 3.7 and Fig. 3.8). In the past, low culturability from soil dust had been ascribed to high proportions of dead bacterial cells (Lighthart, 1997). More recently, however, it has been well documented that the majority of soil bacteria cannot be readily cultivated on nutrient-rich agar media (Hugenholtz et al., 1998; Janssen et al., 2002). While 2% of bacteria from manure were successfully cultivated on blood agar in our hands, culturability of bacteria from soil was 10 times lower, at about 0.2% (Table 3.1). Hence, while large amounts of dust got emitted during tillage operations, it carried comparatively low concentrations of bacteria and particularly low numbers of those microorganisms that could be readily cultivated under standard conditions, including faecal bacteria. We conclude that the atmospheric release of manure-derived faecal bacteria during fertilizer spread was more quantitatively relevant than during subsequent tillage operations (more than 1000-fold in our experiments).

Considering real weather conditions on the day of the field experiment, modelling of dust transport indicated that the residence time of aerosolized microorganisms depended strongly on the boundary layer conditions during the emission and during transport. Afternoon conditions favored the elevation of aerosolized bacteria to greater altitudes. However, large proportions of dust particles released from both manure application and

incorporation were predicted to have prevailed in the atmosphere for several days and got transported over several hundred kilometers (Fig. 3.2), and fractions of 0.01% reached the Black Sea (1,600 km from the source) within 48 h. Assuming a survival rate that was previously measured for airborne Pseudomonas fluorescens, 0.3‰ of aerosolized bacteria would survive a two days atmospheric journey (Amato et al., 2015). This model suggests that of the blood agar detectable bacteria that got aerosolized from our test field during manure application activities (Table 3.2), 3×10^7 reached the Black Sea in a viable state, including 1×10^5 enterococci. Likewise, 2×10^8 of the total bacteria (microscopic counts) would have had a chance to survive this aerial transport, even though it is not known what proportion of these organisms had been viable when they got lifted from the soil.

3.3.2 Strong wind-driven bacterial emission fluxes from fertilized soil

Very few quantitative measurements of aerial microbial emission fluxes from soil have been reported throughout the literature. Available studies had presented point measurements, whereas the dependence on wind velocity and on weather conditions had not been investigated in the past. Our wind tunnel experiments provided soil-specific parameters for the functional relationship between wind velocity and bacterial emissions. Considering long-term precipitation and wind conditions, our data showed that bacterial emission fluxes from freshly fertilized soil, based on epifluorescence microscopy and averaged over 26 years, were 100-fold higher than previous mean estimates of fluxes from land (Burrows et al., 2009b; Lindemann et al., 1982). Peak bacterial fluxes during high-wind months were again almost seven-fold higher than the long-term average. Immediately following fertilization, even blood agar counts were eight-fold higher than previous cultivation-based estimates (Lindemann et al., 1982), although our cultivation conditions (blood agar, incubated aerobically at 37 °C) were not ideal for soil bacteria.

Previous investigations that had relied on bacterial cultivation on agar media alone (Lighthart and Shaffer, 1994; Lindemann et al., 1982) likely underestimated bacterial emission fluxes from soil severely. Our microscopic bacterial cell counts were up to three orders of magnitude higher than cultivation-based numbers (i.e. agar counts; Table 3.2), corroborating previous findings on the low culturability of soil bacteria by standard methods (Janssen et al., 2002). Our microscopic counts matched previously reported data from quantitative PCR, targeting bacterial 16S rRNA genes from aerosolized bacteria, which had been collected above agricultural soil following the spread of liquid dairy manure (Jahne et al., 2015).

Our data showed that wind-driven bacterial emissions from manure-fertilized soil were lower than those released during manure application, but were quantitatively about equally relevant as emissions caused by tillage (Table 3.2). Long-term weather data suggested that conditions for particulate and bacterial emissions from soil were most favorable during winter and spring, i.e. at times, when protective vegetation cover is scarce and fertilization gets performed. Temporal variations of climatic conditions and vegetation may alter the emission strength of soil and thereby contribute to the global, seasonal fluctuations of bacterial air concentrations that had been observed previously (Burrows et al., 2009b). This seasonal variability has as yet not been incorporated in atmospheric models of bacterial transport. Additional investigations are warranted to elucidate the dependence of bacterial emissions on soil type and soil moisture, which are known to influence particulate emissions (Funk et al., 2008).

We conclude that current models (Burrows et al., 2009b) underestimate bacterial emission fluxes from manure-fertilized agricultural soil about 100-fold to 670-fold, depending on actual weather conditions. Very likely, fertilization increased bacterial emission fluxes due to alterations of the soil composition. We observed that manure-derived bacteria got aerosolized preferably, which was probably due to their attachment to organic manure particles. Wind-driven erosion of soil causes organic matter to get suspended into the air more easily than mineral particles, leading to its relative enrichment at increasing height above ground (Iturri et al., 2017; Nerger et al., 2017).

3.3.3 Risk of infection

Enterococci are indicators of faecal contamination (Boehm and Sassoubre, 2014). Our comparative analysis of genome sequences demonstrated that *Ent. faecium* in fertilized soil up to seven weeks after manure application and in emitted dust originated from chicken faeces. While similar persistence of enterococci in manure-fertilized soil had been reported previously (Hodgson et al., 2016; Stocker et al., 2015), bacterial genome sequencing had not been applied in the past to trace any faecal contamination back to their source. Genome sequencing provides significantly better discriminatory power and specificity than analyses of 16S rRNA genes, which are more commonly applied for this purpose (Unno et al., 2018).

Surprisingly, ESBL-producing *E. coli* was below the detection limit in manure and dust, even though it had been abundant in litter collected from chicken barns. However, recent

experiments confirmed a rapid decline of ESBL-producing *E. coli* under aerobic composting conditions in manure heaps, suggesting that storage of poultry manure for 72 h was sufficient to effectively inactivate the majority of drug-resistant *E. coli* (Siller et al., 2020).

Most previous investigations of infection risks associated with the application of manure as agricultural fertilizer considered environmental contamination due to microbial runoff and impairment of stream and ground water quality (Blaustein et al., 2015; Bradford et al., 2013). Only limited research has measured emissions of bioaerosols from cattle and pig slurry during its land application (Boutin et al., 1988; Hobbs et al., 2004). One recent study had recommended a minimum distance of 160 m between manure application sites and any fields growing food crops, to avoid contamination with pathogens from manure (Jahne et al., 2016). Our atmospheric modelling results suggested, however, that transport trajectories of emissions depend on prevailing atmospheric conditions, which could change during the day and result in the transport of manure particles over hundreds of kilometers. In another study, the same authors had assessed the risk of airborne infection from a field fertilized with cattle manure, considering the exposure to manure-associated gastrointestinal pathogens through swallowing of inhaled bacteria after their deposition in the upper respiratory tract (Jahne et al., 2015). While that study reported a combined probability of infection of 1:500 at a distance of 100 m from the manure application site (Jahne et al., 2015), our measurements indicated 200-fold higher concentrations of enterococci within the dust plume during fertilizer application, suggesting an increased risk for those directly exposed, e.g. agricultural workers. In contrast, emissions of faecal bacterial were much lower during tillage and afterwards, indicating that the risk of airborne infection from properly prepared fields was low. Incorporation of manure into soil within few hours after application is required by law in Germany, to minimize runoff and gaseous emissions. Obviously, this policy also reduces the risk of airborne infection effectively.

3.4 Experimental procedures

3.4.1 Field experiment

A field experiment was performed on 31 May 2017 on 2.1 hectares of fallow land near Müncheberg-Friedrichshof (Brandenburg, Germany). The field consisted of sandy loam and had not been fertilized with animal waste for 15 years. Two days before the

experiment, the test field was pretreated with a chisel plow to subvert the plant cover. Manure for the field experiment was obtained from an intensive poultry-fattening farm in Brandenburg, housing about 19 000 animals per stable on wood pellets. Chicken housings had been sampled by collecting 30 chicken droppings from each stable. At the end of a fattening period, the stables were mucked out and the accumulated manure (water content, 30%) was transported to the field site, where it was stored in a heap overnight. From 10:49 h to 12:15 h (Central European Summer Time), 12 tons of manure got applied using a manure spreader 'Strautmann BE4' (spreading width 3 m). From 13:33 h to 14:45 h, the manure was incorporated into the soil by applying a field cultivator 'Lemken Smaragd 9' (working depth 8 cm, working width 3 m). Aerial samples were collected at the leeward side of the field when the tractor reached distances of 20, 50 and 100 m to the measuring point (Fig. S3.1). The experimental set-up consisted of two dust monitors (Environmental Dust Monitor EDM #164; Grimm Aerosol- Technik, Germany) at 1.50 m and 3.80 m height, each measuring particle concentrations continuously every 6 s at a flow rate of 1.2 l min^{-1}, and an XMX-CV aerosol collection system (Dycor, Canada) at 1.50 m, capturing particles by impingement into 5 ml phosphate-buffered saline (PBS) at a flow rate of 530 l min^{-1} for 10 min. After 10 min, the collection buffer was exchanged. Air temperature and relative humidity, wind velocity and wind direction were recorded by using a mobile weather station. Prior to and following fertilization, soil samples were collected at three representative, equally separated spots on the field site. Each of these samples was a mixture of five shovels of soil taken in a star-shaped pattern around the sampling spot. The same spots were sampled afterwards several times until October 2017 to determine the persistence of bacteria in the soil. Samples were stored at 4 °C for up to 24 h until they were analyzed for microbial content.

3.4.2 Gaussian dispersion model

To calculate the amount of dust produced during manure application and incorporation, a 'Gaussian dispersion model' was used, which describes the ambient air concentration of a pollutant from a continuous emitting point source including a deposition term (Seinfeld and Pandis, 2006; TA Luft, 1986; Weber, 1976):

$$C\ (x,y,z) = \frac{Q}{2\pi\sigma_y\sigma_z u_h}\exp\left(\frac{-y^2}{2\sigma_y^2}\right)\left(\exp\left(\frac{-(z-h)^2}{a}\right) + \exp\left(\frac{-(z+h)^2}{a}\right)\right)\exp\left[-\sqrt{\frac{2}{\pi}\frac{V_{di}}{u_h}\int_0^x \frac{1}{\sigma_z(\xi)}\exp\left(-\frac{h^2}{a(\xi)}\right)d\xi}\right] \quad \text{Eq. 3.1}$$

where C [µg m^{-3}] is the dust concentration, x [m], y [m] and z [m] are the distances from the source in downwind, crosswind and vertical directions, Q [µg s^{-1}] is the source strength (manure spreader or cultivator, respectively), u_h [m s^{-1}] is the wind speed at height h [m], σ_y [m] and σ_z [m] are the dispersion of dust in horizontal and vertical directions, V_{di} [m s^{-1}] is the deposition velocity of particles with different size classes ($V_{di}(PM_{10})$ = 0.07 m s^{-1}), and ξ is a non-dimensional stability parameter. Further, a = σ_z^2 is for tillage operations and a = $2\sigma_z^2$ for manure application. For tillage, the vertical dispersion parameter a is reduced to σ_z^2, because dust from tillage is emitted just above the ground and the dust plume develops only vertically upwards. Rearranging Eq. 3.1 enables the determination of the source strength from the concentration measurements:

$$Q = \frac{2\pi\sigma_y\sigma_z uC}{\exp\left(\frac{-y^2}{2\sigma_y^2}\right)\left(\exp\left(\frac{-(z-h)^2}{a}\right)+\exp\left(\frac{-(z+h)^2}{a}\right)\right)\exp\left[-\sqrt{\frac{2V_{di}}{\pi u_h}\int_0^x \frac{1}{\sigma_z(\xi)}\exp\left(-\frac{h^2}{a(\xi)}\right)d\xi}\right]} \quad \text{Eq. 3.2}$$

The released dust during each operation at the field is finally calculated by:

$$EF = \frac{Q \cdot t}{A} \quad \text{Eq. 3.3}$$

where EF [kg ha^{-1}] is the emission factor per unit area, t [s] is the duration of the operation, and A [ha] is the field size.

3.4.3 Modelling atmospheric transport of dust particles

Trajectory calculations are a commonly applied method to investigate the pathway of a particle through the atmosphere. In order to account for the atmosphere's strong turbulent fluctuations such as changes in wind speed and direction over time and space, a set of trajectories is calculated. Thereby, a single trajectory represents one statistically possible path of a group of particles. Consequently, a large number of trajectories together represent the most likely transport pathway of all particles emitted from one individual source through the atmosphere. In other words, this results in a distribution of likely dispersion pathways. In the framework of this study, we used the Lagrangian particle

simulation module 'itpas' (Faust et al., 2021) based on the COSMO-Model trajectory module (Miltenberger et al., 2013) to calculate the dispersion of dust-like particles (diameter, 1 – 10 µm) within the atmospheric boundary layer (lowest kilometers of the atmosphere). In order to describe the particle dust emission flux and particle size distribution, the model was initialized by particle size distributions and emission fluxes measured during the field experiment (Münch et al., 2020). In order to represent the different meteorological conditions during manure application and incorporation, respectively, two 48 h simulations were performed: 31 May 2017 at 10:50 and 13:30 (local time). Meteorological boundary data were taken from the European Center for Medium-range Weather Forecast ERA5 dataset.

3.4.4 Wind tunnel experiments

As measurements of wind erosion at the field site are quite uncertain due to unsteady weather conditions, we decided to investigate the test field soil's susceptibility to wind erosion in a wind tunnel as described previously (Funk et al., 2019). The boundary layer wind tunnel was operated as an open-circuit system, receiving ambient air from outside of the building. Twenty-eight days after manure application and incorporation, soil (500 l) from the upper 8 cm of the test field was collected and filled into the tunnel's working section of 7 m length × 0.7 m width, resulting in a soil layer of 0.1 m thickness. A EDM164 and a Dycor aerosol collector were placed in the tunnel's suspension chamber (Funk et al., 2019). For each experiment, dust (PM_{10}) and bacterial emissions were measured at wind velocities of 7.2, 10.2, 13.7 and 15.2 m s^{-1}. The wind velocity was increased within 30 s to the appropriate value and kept constant for 15 min. Because of the limited availability of erodible fractions of the soil, the surface was exhausted after a certain time, which always happened within the 10 min measuring interval of the Dycor. We estimated the wind velocity-dependent emissions as sum of the PM_{10} emitted during the 15 min runs in relation to the total tunnel floor (4.9 m^2) as mass per area. After each experiment, the soil surface was refreshed by mixing it with a rake.

3.4.5 Estimation of the potential for wind erosion induced PM_{10} emissions from the test field

Based on the wind tunnel tests, the following equation was derived, which follows the typical form of sand transport equations to describe the exponential increase of transport

intensity q with increasing wind velocity u or friction velocity u_* (Funk and Engel, 2015; Jarrah et al., 2020), with

$$q = A\, u_*(u_* - u_{*t})^2 \text{ for } u_* > u_{*t} \quad \text{Eq. 3.4}$$

where q is the soil flux [kg m^2 s^{-1}]; u_*, u_{*t} is friction velocity and threshold friction velocity [m s^{-1}] and A is a summarized coefficient of several empirical and physical parameter of influence.

As dust emissions arise from sand transport, there is a direct relationship between both transport modes (Marticorena and Bergametti, 1995). In the wind tunnel experiments, most parameters were kept constant, including soil composition and moisture, aggregation and roughness, so a simplified correlation between wind velocity (u) and PM_{10} emissions (F_{PM10}), which represents a specific part of the total soil flux q, was obtained by nonlinear regression:

$$F_{PM10} = Au(u - u_t)^{1.69} \quad \text{Eq. 3.5}$$

where F_{PM10} was calculated from concentration [µg m^{-3}], air flow rate [m^3 s^{-1}], wind tunnel floor area [4.9 m^2] and time (s). A = 1, will change if initial parameters are changed.

The wind tunnel results were transferred to natural open land conditions by converting wind velocities measured in the wind tunnel to the standard wind velocity at a measuring height of 10 m. The threshold wind velocity u_t was 7.0 m s^{-1}, valid for that field with a dry surface and roughness as after seedbed preparation (Funk and Engel, 2015). The total PM_{10} emissions of the test field were estimated considering its area of 21 000 m^2. On the basis of historic weather data [i.e. hourly values of wind velocity, precipitation, temperature, solar irradiation, air humidity from 1992 to 2018 (DWD, 2019a)], we estimated the potential extent of PM_{10} emissions from the test field during the last 27 years. Wind erosion and associated PM_{10} emissions were assumed when wind velocity exceeded the threshold of 7.0 m s^{-1}, and there had been no precipitation during the preceding 24 h (or when evapotranspiration was higher than precipitation). The vegetation cover was not considered for these estimations.

3.4.6 Cultivation-based enumeration of bacteria from manure, soil and dust samples

For enumeration of bacteria in manure and soil samples, 10 g of sample material was mixed with 90 g LB medium (Carl Roth). Samples were homogenized for 30 s with a bag mixer (Interscience, St. Nom la Bretèche, France) and left for sedimentation of coarse particles (30 min, room temperature). Dilutions of the supernatants and of impingement suspensions from the aerosol collector were diluted to extinction and streaked on Columbian blood agar (Oxoid) for quantification of total aerobe colony forming units (CFU) and on kanamycin-aesculin agar (KAA; Oxoid) for selection and quantification of Enterococci spp. Subsequent species identification of *Enterococcus faecium* was achieved by using a species specific PCR (Cheng et al., 1997) and verified by MALDI-TOF mass spectroscopy. Samples for mass spectroscopy were prepared by ethanol-formic acid extraction as described previously (Schumann and Maier, 2014) (Protocol 3), and spectra were recorded, evaluated and identified by using a MALDI Biotyper Smart System GP (Bruker Daltonik, Bremen, Germany). In addition, supernatants were streaked on 'Chromagar VRE' (Chromagar, France) for vancomycin-resistant enterococci and on 'Chromagar MRSA' (Chromagar, France) for methicillin-resistant Staphylococcus aureus (MRSA). Extended-spectrum beta-lactamase producing *E. coli* were isolated on McConkey agar No. 3 (Oxoid) supplemented with 1 mg l^{-1} cefotaxime, and species identification of E. coli was achieved by MALDI-TOF mass spectroscopy.

The limit of detection (LoD, 1 count per agar plate) was 10^2 CFU g^{-1} for soil and manure samples and 9.43 CFU m^{-3} for dust impingement samples. Accordingly, the limit of quantification (LoQ, 30 counts per agar plate) was 3×10^3 CFU g^{-1} for soil and 283 CFU m^{-3} for dust.

3.4.7 Microscopy

For determination of total bacterial counts, an aliquot of each sample was fixed in 1% glutardialdehyde and stored at 4 °C until analysis. Samples were stained with SYBR Green and filtered onto black 0.2 µm isopore membrane filters (Merck Millipore, Darmstadt, Germany) (Vieira et al., 2020). Filters were placed between object slide and coverslip and sealed with nail polish, and images were monitored employing a Nikon Eclipse Ti inverted microscope with GFP (485/20-525/30) filters. Fluorescence z-stacks were taken using a Nikon N Plan Apochromat λ × 100/1.45 oil objective and an ORCA

FLASH 4.0 HAMAMATSU camera. At least 10 fields of view (17 404.19 µm²) per sample were recorded. For quantification, ten fields of view were analyzed using the NIS-Elements software 4.30 (Nikon). Bacterial cells were identified automatically by using the object count tools (smooth: 4×, clean: 4×, fill holes: on, separate: 4×) and manually examined to account for background variation.

3.4.8 DNA extraction and 16S rRNA gene sequencing

Extraction of DNA from manure, soil and dust samples and subsequent PCR amplification of 16S rRNA gene segments were performed according to the 16S rDNA amplicon protocol of the Earth Microbiome Project (http://www.earthmicrobiome.org/protocols-and-standards/16s/). In brief, DNA was extracted using the DNeasy PowerSoil Kit (Qiagen, Hilden, Germany) according to the manufacturer's instructions. Primers used for amplification of the V4 region of the 16S rRNA gene were published previously (Caporaso et al., 2011; Parada et al., 2016). Forward primers contained sample-specific barcodes to enable multiplexing. PCR reactions were performed in triplicates, containing 0.8 x Platinum Hot Start PCR Master Mix (Thermo Fisher Scientific), 0.2 µM each of forward and reverse primer, and 1 ng of template DNA under the following conditions: 3 min at 94 °C, 35 cycles at 94 °C for 45 s, 50 °C for 60 s, 72 °C for 90 s and a final extension step at 72 °C for 10 min. Equimolar amounts of merged triplicates were pooled, purified by using QIAquick PCR purification columns (Qiagen) and sequenced on the MiSeq platform (MiSeq Reagent Kit v3, 600 cycle; Illumina).

3.4.9 Processing of 16S rRNA gene sequences

Amplicon sequences were analysed via the plugin-based QIIME2 pipeline (version 2018.4; Bolyen, (2019)). Demultiplexed forward reads were trimmed to 260 bases according to quality parameters using FASTX_TRIMMER (FASTX Toolkit Version 0.0.14). Truncated reads were loaded into the QIIME2 environment and processed by using implemented software tools. By using Deblur (Amir et al., 2017), sequences were error-filtered and unique sequence variants (SV) identified. Sequences were aligned with MAFFT (Katoh and Standley, 2013) and used to build a phylogenetic tree with FASTTREE (Price et al., 2009). Taxonomy was assigned to the respective SVs by alignment with the SILVA reference database, release 128 (Quast et al., 2013). Resulting BIOMtable, taxonomy and rooted tree were exported and further processed with R (version 3.4.3,

available at https://www.Rproject.org/) using the R package ‘phyloseq’ (McMurdie and Holmes, 2013). Rarefaction analysis was performed by plotting the number of SVs versus sequencing depth with the *R* package ‘ranacapa’ (version 0.1.0). For normalization, sequence counts were rarefied to the read count of the sample with the lowest total number of reads after error filtering (1.23×10^5 reads). As alpha diversity estimates, richness (observed number of SVs per sample) and Shannon and Simpson indices were computed. For estimation of beta diversity, unweighted and weighted UniFrac distance matrices were determined and subjected to principal coordinate analysis (PCoA) using the ‘phyloseq’ package.

3.4.10 Genome sequencing and phylogenetic analysis

DNA was purified from plate-grown *Ent. faecium* using the DNeasy Blood & Tissue Kit (Qiagen) according to the manufacturer’s instructions, except that bacterial cell lysis was performed with lysozyme (90 000 U) in 1% Triton X-100 for 45 min at 37°C. Sequencing libraries were prepared using a modified Nextera XT protocol (Baym et al., 2015; Steglich et al., 2018). The libraries were sequenced on a NextSeq machine with a NextSeq 500/550 midoutput v2 kit (Illumina). Illumina sequencing reads were assembled by using SPADES v3.13.0, and resulting contigs were processed in SEQSPHERE 6.0.2 for cgMLST allele calling and for determination of cgMLST-based complex types and classical MLST sequence types (STs; de Been et al., (2015)). Distances between cgMLST allelic profiles were used to construct a neighbor-joining phylogenetic tree, which was subsequently annotated with iTOL 4.0.3 (Letunic and Bork, 2016). Genome sequencing read data from 92 Enterococcus faecium isolates were submitted to the European Nucleotide Archive under accession number PRJEB36824.

Acknowledgements

We thank the farm owners for supporting this study, allowing sample collection at their facilities and donation of manure for experiments. We are grateful to U. Steiner for technical assistance, to J. Sikorski for help with Qiime2 and R and for helpful comments on the manuscript, D. Jacob for language editing, and to the Leibniz research alliance Infections ’21 for support. This study was funded by the Leibniz Association (grant number: SAW-2017-DSMZ-2). Open access funding enabled and organized by Projekt DEAL.

Conflict of interests

The authors declare no conflict of interest.

References

Amato, P., Joly, M., Schaupp, C., Attard, E., Möhler, O., Morris, C.E., Brunet, Y., Delort, A.-M., 2015. Survival and ice nucleation activity of bacteria as aerosols in a cloud simulation chamber. Atmospheric Chem. Phys. 15, 6455–6465. https://doi.org/10.5194/acp-15-6455-2015

Amir, A., McDonald, D., Navas-Molina, J.A., Kopylova, E., Morton, J.T., Zech Xu, Z., Kightley, E.P., Thompson, L.R., Hyde, E.R., Gonzalez, A., Knight, R., 2017. Deblur Rapidly Resolves Single-Nucleotide Community Sequence Patterns. mSystems 2, e00191-16. https://doi.org/10.1128/mSystems.00191-16

Barberán, A., Henley, J., Fierer, N., Casamayor, E.O., 2014. Structure, inter-annual recurrence, and global-scale connectivity of airborne microbial communities. Sci. Total Environ. 487, 187–195. https://doi.org/10.1016/j.scitotenv.2014.04.030

Baym, M., Kryazhimskiy, S., Lieberman, T.D., Chung, H., Desai, M.M., Kishony, R., 2015. Inexpensive Multiplexed Library Preparation for Megabase-Sized Genomes. PLOS ONE 10, e0128036. https://doi.org/10.1371/journal.pone.0128036

Blaustein, R.A., Pachepsky, Y.A., Shelton, D.R., Hill, R.L., 2015. Release and Removal of Microorganisms from Land-Deposited Animal Waste and Animal Manures: A Review of Data and Models. J. Environ. Qual. 44, 1338–1354. https://doi.org/10.2134/jeq2015.02.0077

Boehm, A.B., Sassoubre, L.M., 2014. Enterococci as indicators of environmental fecal contamination.

Bolyen, E., Rideout, J.R., Dillon, M.R., Bokulich, N.A., Abnet, C.C., Al-Ghalith, G.A., Alexander, H., Alm, E.J., Arumugam, M., Asnicar, F., Bai, Y., Bisanz, J.E., Bittinger, K., Brejnrod, A., Brislawn, C.J., Brown, C.T., Callahan, B.J., Caraballo-Rodríguez, A.M., Chase, J., Cope, E.K., Da Silva, R., Diener, C., Dorrestein, P.C., Douglas, G.M., Durall, D.M., Duvallet, C., Edwardson, C.F., Ernst, M., Estaki, M., Fouquier, J., Gauglitz, J.M., Gibbons, S.M., Gibson, D.L., Gonzalez, A., Gorlick, K., Guo, J., Hillmann, B., Holmes, S., Holste, H., Huttenhower, C., Huttley, G.A., Janssen, S., Jarmusch, A.K., Jiang, L.,

Kaehler, B.D., Kang, K.B., Keefe, C.R., Keim, P., Kelley, S.T., Knights, D., Koester, I., Kosciolek, T., Kreps, J., Langille, M.G.I., Lee, J., Ley, R., Liu, Y.-X., Loftfield, E., Lozupone, C., Maher, M., Marotz, C., Martin, B.D., McDonald, D., McIver, L.J., Melnik, A.V., Metcalf, J.L., Morgan, S.C., Morton, J.T., Naimey, A.T., Navas-Molina, J.A., Nothias, L.F., Orchanian, S.B., Pearson, T., Peoples, S.L., Petras, D., Preuss, M.L., Pruesse, E., Rasmussen, L.B., Rivers, A., Robeson, M.S., Rosenthal, P., Segata, N., Shaffer, M., Shiffer, A., Sinha, R., Song, S.J., Spear, J.R., Swafford, A.D., Thompson, L.R., Torres, P.J., Trinh, P., Tripathi, A., Turnbaugh, P.J., Ul-Hasan, S., van der Hooft, J.J.J., Vargas, F., Vázquez-Baeza, Y., Vogtmann, E., von Hippel, M., Walters, W., Wan, Y., Wang, M., Warren, J., Weber, K.C., Williamson, C.H.D., Willis, A.D., Xu, Z.Z., Zaneveld, J.R., Zhang, Y., Zhu, Q., Knight, R., Caporaso, J.G., 2019. Reproducible, interactive, scalable and extensible microbiome data science using QIIME 2. Nat. Biotechnol. 37, 852–857. https://doi.org/10.1038/s41587-019-0209-9

Boutin, P., Torre, M., Serceau, R., Rideau, P.-J., 1988. Atmospheric bacterial contamination from landspreading of animal wastes: Evaluation of the respiratory risk for people nearby. J. Agric. Eng. Res. 39, 149–160. https://doi.org/10.1016/0021-8634(88)90092-3

Bowers, R.M., McLetchie, S., Knight, R., Fierer, N., 2011. Spatial variability in airborne bacterial communities across land-use types and their relationship to the bacterial communities of potential source environments. ISME J. 5, 601–612. https://doi.org/10.1038/ismej.2010.167

Bradford, S.A., Morales, V.L., Zhang, W., Harvey, R.W., Packman, A.I., Mohanram, A., Welty, C., 2013. Transport and Fate of Microbial Pathogens in Agricultural Settings. Crit. Rev. Environ. Sci. Technol. 43, 775–893. https://doi.org/10.1080/10643389.2012.710449

Burrows, S.M., Elbert, W., Lawrence, M.G., Poschl, U., 2009a. Bacteria in the global atmosphere - Part 1: Review and synthesis of literature data for different ecosystems. Atmospheric Chem. Phys. 9, 9263–9280.

Burrows, S.M., Butler, T., Joeckel, P., Tost, H., Kerkweg, A., Poeschl, U., Lawrence, M.G., 2009b. Bacteria in the global atmosphere - Part 2: Modeling of emissions and transport between different ecosystems. Atmospheric Chem. Phys. 9, 9281–9297.

Cáliz, J., Triadó-Margarit, X., Camarero, L., Casamayor, E.O., 2018. A long-term survey unveils strong seasonal patterns in the airborne microbiome coupled to general and regional atmospheric circulations. Proc. Natl. Acad. Sci. 115, 12229–12234.

Caporaso, J.G., Lauber, C.L., Walters, W.A., Berg-Lyons, D., Lozupone, C.A., Turnbaugh, P.J., Fierer, N., Knight, R., 2011. Global patterns of 16S rRNA diversity at a depth of millions of sequences per sample. Proc. Natl. Acad. Sci. 108, 4516–4522.

Chastain, J.P., Camberato, J.J., Skewes, P., 2002. Poultry Manure Production and Nutrient Content, Poultry Training Manual. Clemson University, College of Agriculture, Forestry and Life Sciences, Clemson, SC.

Cheng, S., McCleskey, F.K., Gress, M.J., Petroziello, J.M., Liu, R., Namdari, H., Beninga, K., Salmen, A., DelVecchio, V.G., 1997. A PCR assay for identification of Enterococcus faecium. J. Clin. Microbiol. 35, 1248–1250. https://doi.org/10.1128/jcm.35.5.1248-1250.1997

Despres, V.R., Huffman, J.A., Burrows, S.M., Hoose, C., Safatov, A.S., Buryak, G., Frohlich-Nowoisky, J., Elbert, W., Andreae, M.O., Poschl, U., Jaenicke, R., 2012. Primary biological aerosol particles in the atmosphere: a review. Tellus Ser. B-Chem. Phys. Meteorol. 64, 58. https://doi.org/10.3402/tellusb.v64i0.15598

DWD, 2019. German Weather Service. Download from the Climate Data Center. [WWW Document]. Clim. Data Cent. URL https://www.dwd.de/EN/ourservices/cdcftp/cdcftp.html

Fröhlich-Nowoisky, J., Kampf, C.J., Weber, B., Huffman, J.A., Pöhlker, C., Andreae, M.O., Lang-Yona, N., Burrows, S.M., Gunthe, S.S., Elbert, W., Su, H., Hoor, P., Thines, E., Hoffmann, T., Després, V.R., Pöschl, U., 2016. Bioaerosols in the Earth system: Climate, health, and ecosystem interactions. Atmospheric Res. 182, 346–376. https://doi.org/10.1016/j.atmosres.2016.07.018

Funk, R., Engel, W., 2015. Investigations with a field wind tunnel to estimate the wind erosion risk of row crops. Soil Tillage Res. 145, 224–232. https://doi.org/10.1016/j.still.2014.09.005

Funk, R., Papke, N., Hör, B., 2019. Wind tunnel tests to estimate PM10 and PM2.5-emissions from complex substrates of open-cast strip mines in Germany. Aeolian Res. 39, 23–32. https://doi.org/10.1016/j.aeolia.2019.03.003

Funk, R., Reuter, H.I., Hoffmann, C., Engel, W., Öttl, D., 2008. Effect of moisture on fine dust emission from tillage operations on agricultural soils. Earth Surf. Process. Landf. J. Br. Geomorphol. Res. Group 33, 1851–1863.

Hervàs, A., Camarero, L., Reche, I., Casamayor, E.O., 2009. Viability and potential for immigration of airborne bacteria from Africa that reach high mountain lakes in Europe. Environ. Microbiol. 11, 1612–1623. https://doi.org/10.1111/j.1462-2920.2009.01926.x

Hobbs, P., Davies, D., Williams, J., Bakewell, H., Smith, K., 2004. Measurement of pathogen transfer in aerosols following land application of manure. Sustain. Org. Waste Manag. Environ. Prot. Food Saf. 2, 25–28.

Hodgson, C.J., Oliver, D.M., Fish, R.D., Bulmer, N.M., Heathwaite, A.L., Winter, M., Chadwick, D.R., 2016. Seasonal persistence of faecal indicator organisms in soil following dairy slurry application to land by surface broadcasting and shallow injection. J. Environ. Manage. 183, 325–332. https://doi.org/10.1016/j.jenvman.2016.08.047

Hugenholtz, P., Goebel, B.M., Pace, N.R., 1998. Impact of Culture-Independent Studies on the Emerging Phylogenetic View of Bacterial Diversity. J. Bacteriol. 180, 4765–4774. https://doi.org/10.1128/JB.180.18.4765-4774.1998

Iturri, L.A., Funk, R., Leue, M., Sommer, M., Buschiazzo, D.E., 2017. Wind sorting affects differently the organo-mineral composition of saltating and particulate materials in contrasting texture agricultural soils. Aeolian Res. 28, 39–49. https://doi.org/10.1016/j.aeolia.2017.07.005

Jahne, M.A., Rogers, S.W., Holsen, T.M., Grimberg, S.J., 2015. Quantitative microbial risk assessment of bioaerosols from a manure application site. Aerobiologia 31, 73–87. https://doi.org/10.1007/s10453-014-9348-0

Jahne, M.A., Rogers, S.W., Holsen, T.M., Grimberg, S.J., Ramler, I.P., Kim, S., 2016. Bioaerosol Deposition to Food Crops near Manure Application: Quantitative Microbial Risk Assessment. J. Environ. Qual. 45, 666–674. https://doi.org/10.2134/jeq2015.04.0187

Janssen, P.H., Yates, P.S., Grinton, B.E., Taylor, P.M., Sait, M., 2002. Improved Culturability of Soil Bacteria and Isolation in Pure Culture of Novel Members of the Divisions Acidobacteria, Actinobacteria, Proteobacteria, and Verrucomicrobia. Appl. Environ. Microbiol. 68, 2391–2396. https://doi.org/10.1128/AEM.68.5.2391-2396.2002

Jarrah, M., Mayel, S., Tatarko, J., Funk, R., Kuka, K., 2020. A review of wind erosion models: Data requirements, processes, and validity. CATENA 187, 104388. https://doi.org/10.1016/j.catena.2019.104388

Kabelitz, T., Ammon, C., Funk, R., Münch, S., Biniasch, O., Nübel, U., Thiel, N., Rösler, U., Siller, P., Amon, B., Aarnink, A.J.A., Amon, T., 2020. Functional relationship of particulate matter (PM) emissions, animal species, and moisture content during manure application. Environ. Int. 143, 105577. https://doi.org/10.1016/j.envint.2020.105577

Katoh, K., Standley, D.M., 2013. MAFFT Multiple Sequence Alignment Software Version 7: Improvements in Performance and Usability. Mol. Biol. Evol. 30, 772–780. https://doi.org/10.1093/molbev/mst010

Kellogg, C.A., Griffin, D.W., 2006. Aerobiology and the global transport of desert dust. Trends Ecol. Evol. 21, 638–644.

Kellogg, C.A., Griffin, D.W., Garrison, V.H., Peak, K.K., Royall, N., Smith, R.R., Shinn, E.A., 2004. Characterization of Aerosolized Bacteria and Fungi From Desert Dust Events in Mali, West Africa. Aerobiologia 20, 99–110. https://doi.org/10.1023/B:AERO.0000032947.88335.bb

Letunic, I., Bork, P., 2016. Interactive tree of life (iTOL) v3: an online tool for the display and annotation of phylogenetic and other trees. Nucleic Acids Res. 44, W242–W245. https://doi.org/10.1093/nar/gkw290

Lighthart, B., 1997. The ecology of bacteria in the alfresco atmosphere. FEMS Microbiol. Ecol. 23, 263–274. https://doi.org/10.1111/j.1574-6941.1997.tb00408.x

Lighthart, B., Shaffer, B.T., 1994. Bacterial flux from chaparral into the atmosphere in mid-summer at a high desert location. Atmos. Environ. 28, 1267–1274. https://doi.org/10.1016/1352-2310(94)90273-9

Lindemann, J., Constantinidou, H.A., Barchet, W.R., Upper, C.D., 1982. Plants as sources of airborne bacteria, including ice nucleation-active bacteria. Appl. Environ. Microbiol. 44, 1059–1063.

Maffia, J., Elio, D., Barbara, A., Paolo, B., 2020. PM emissions from open field crop management: Emission factors, assessment methods and mitigation measures–A review. Atmos. Environ. 117381.

Marticorena, B., Bergametti, G., 1995. Modeling the atmospheric dust cycle: 1. Design of a soil-derived dust emission scheme. J. Geophys. Res. Atmospheres 100, 16415–16430. https://doi.org/10.1029/95JD00690

McMurdie, P.J., Holmes, S., 2013. phyloseq: An R Package for Reproducible Interactive Analysis and Graphics of Microbiome Census Data. PLOS ONE 8, e61217. https://doi.org/10.1371/journal.pone.0061217

Miltenberger, A.K., Pfahl, S., Wernli, H., 2013. An online trajectory module (version 1.0) for the nonhydrostatic numerical weather prediction model COSMO. Geosci. Model Dev. 6, 1989–2004. https://doi.org/10.5194/gmd-6-1989-2013

Möhler, O., DeMott, P., Vali, G., Levin, Z., 2007. Microbiology and atmospheric processes: the role of biological particles in cloud physics. Biogeosciences Discuss. 4, 2559–2591.

Münch, S., Papke, N., Thiel, N., Nübel, U., Siller, P., Roesler, U., Biniasch, O., Funk, R., Amon, T., 2020. Effects of farmyard manure application on dust emissions from arable soils. Atmospheric Pollut. Res. 11, 1610–1624. https://doi.org/10.1016/j.apr.2020.06.007

Nerger, R., Funk, R., Cordsen, E., Fohrer, N., 2017. Application of a modeling approach to designate soil and soil organic carbon loss to wind erosion on long-term monitoring sites (BDF) in Northern Germany. Aeolian Res. 25, 135–147. https://doi.org/10.1016/j.aeolia.2017.03.006

Parada, A.E., Needham, D.M., Fuhrman, J.A., 2016. Every base matters: assessing small subunit rRNA primers for marine microbiomes with mock communities, time series and global field samples. Environ. Microbiol. 18, 1403–1414. https://doi.org/10.1111/1462-2920.13023

Price, M.N., Dehal, P.S., Arkin, A.P., 2009. FastTree: Computing Large Minimum Evolution Trees with Profiles instead of a Distance Matrix. Mol. Biol. Evol. 26, 1641–1650. https://doi.org/10.1093/molbev/msp077

Prospero, J.M., Blades, E., Mathison, G., Naidu, R., 2005. Interhemispheric transport of viable fungi and bacteria from Africa to the Caribbean with soil dust. Aerobiologia 21, 1–19.

Quast, C., Pruesse, E., Yilmaz, P., Gerken, J., Schweer, T., Yarza, P., Peplies, J., Glöckner, F.O., 2013. The SILVA ribosomal RNA gene database project: improved data processing and web-based tools. Nucleic Acids Res. 41, D590–D596. https://doi.org/10.1093/nar/gks1219

Schumann, P., Maier, T., 2014. Chapter 13 - MALDI-TOF Mass Spectrometry Applied to Classification and Identification of Bacteria, in: Goodfellow, M., Sutcliffe, I., Chun, J. (Eds.), Methods in Microbiology, New Approaches to Prokaryotic Systematics. Academic Press, pp. 275–306. https://doi.org/10.1016/bs.mim.2014.06.002

Seinfeld, J.H., Pandis, S.N., 2006. Atmospheric Chemistry and Physics: From Air Pollution to Climate Change, 2. ed. John Wiley & Sons, Hoboken, N.J.

Siller, P., Daehre, K., Thiel, N., Nübel, U., Roesler, U., 2020. Impact of short-term storage on the quantity of extended-spectrum beta-lactamase–producing Escherichia coli in broiler litter under practical conditions. Poult. Sci. 99, 2125–2135. https://doi.org/10.1016/j.psj.2019.11.043

Steglich, M., Hofmann, J.D., Helmecke, J., Sikorski, J., Spröer, C., Riedel, T., Bunk, B., Overmann, J., Neumann-Schaal, M., Nübel, U., 2018. Convergent Loss of ABC Transporter Genes From Clostridioides difficile Genomes Is Associated With Impaired Tyrosine Uptake and p-Cresol Production. Front. Microbiol. 9. https://doi.org/10.3389/fmicb.2018.00901

Stocker, M.D., Pachepsky, Y.A., Hill, R.L., Shelton, D.R., 2015. Depth-Dependent Survival of Escherichia coli and Enterococci in Soil after Manure Application and Simulated Rainfall. Appl. Environ. Microbiol. 81, 4801–4808. https://doi.org/10.1128/AEM.00705-15

TA Luft, 1986. Erste allgemeine Verwaltungsvorschrift zum Bundes-Immissionsschutzgesetz–Technische Anleitung zur Reinhaltung der Luft (TA Luft) vom 7. Februar 1986. GMBl G 3191, 95.

Unno, T., Staley, C., Brown, C.M., Han, D., Sadowsky, M.J., Hur, H.-G., 2018. Fecal pollution: new trends and challenges in microbial source tracking using next-generation sequencing. Environ. Microbiol. 20, 3132–3140. https://doi.org/10.1111/1462-2920.14281

Vieira, S., Sikorski, J., Gebala, A., Boeddinghaus, R.S., Marhan, S., Rennert, T., Kandeler, E., Overmann, J., 2020. Bacterial colonization of minerals in grassland soils is selective and highly dynamic. Environ. Microbiol. 22, 917–933. https://doi.org/10.1111/1462-2920.14751

Weber, A., 1976. Atmospheric dispersion parameters in Gaussian plume modeling. Part 1: Review of current systems and possible future developments. Rep. Sep 1975-Mar 1976 N. C. State Univ Raleigh Dept Geosci.

Yamaguchi, N., Ichijo, T., Sakotani, A., Baba, T., Nasu, M., 2012. Global dispersion of bacterial cells on Asian dust. Sci. Rep. 2, 525. https://doi.org/10.1038/srep00525

Supporting information

Additional supporting information can be found online (https://sfamjournals.onlinelibrary.wiley.com/doi/full/10.1111/1751-7915.13632) in the supporting Information section at the end of the article.

Fig. S3.1. Experimental set-up. (A) Satellite image of test field in Brandenburg near Müncheberg. The blue arrow indicates the predominant wind direction on the day of the test field, the asterisk indicates the position of the measuring equipment, and the dotted lines mark the tractor tracks during air sample collection. (B) Tractor equipped with manure spreader during manure application. (C) Tractor equipped with field cultivator during manure incorporation. (D) Measuring equipment consisted of two dust monitors at different heights and an aerosol collection device. (E) Wind tunnel.

Fig. S3.2. PM_{10} concentrations measured during manure application and incorporation at heights of 3.80 m and 1.50 m, as indicated. Light blue shading indicates time periods of aerosol collection by impingement.

Fig. S3.3. Rarefaction curves indicating the number of 16S rDNA sequence variants (SV) detected as a function of sequencing depth. The dotted line highlights the number of reads used for rarefying (normalization, N = 120 000).

Fig. S3.4. Taxonomic composition of 16S rDNA sequencing data at phylum level.

Fig. S3.5. Taxonomic composition of 16S rDNA sequencing data at genus level.

4 Differences in the sediment composition of wind eroded sandy soils before and after fertilization with poultry manure

Under review in:

Münch, S., Papke, N., Leue, M., Faust, M., Schepanski, K., Siller, P., Roesler, U., Nübel, U., Kabelitz, T., Amon, T., Funk, R., 2021. Organic fertilization on arable lands affects the physical and chemical composition of wind eroded sediments. Soil Tillage Res. (under review)

Abstract

Wind erosion is known to be a gradual process of soil degradation on arable lands. Poultry manure fertilization is a common practice to improve physical, chemical and biological soil properties, and is thus an essential part to maintain soil fertility. Shortly after incorporation, poultry manure and soil particles are loosely adjacent without any bonding. This supposedly affects the susceptibility of soils to wind erosion and influence the physical and chemical composition of the wind-eroded sediment. Wind tunnel experiments were conducted with three wind speeds (8, 11, 14 m s^{-1}) and four sandy soils, each fertilized with poultry manure in a common rate of 6 t ha^{-1}. Incorporation of manure in the soils changed the particulate organic matter (POM) composition resulting in increased median particle diameters, carbon contents and hydrophobicity. Wind erosion caused a preferred release of manure particles already at wind speeds close above the threshold of 7 m s^{-1} with the greatest sorting effects in size, shape, and density of the particles. Thus, wind erosion immediately leads to losses of the added organic material. At higher wind speeds the sediment composition rather corresponds to the entire soil or soil-manure mixtures. Depending on the wind speed and total soil loss, potential manure losses between 101 and 854 kg ha^{-1} were accounted, which are 1.7 to 14% of the fertilization rate. The results indicate a risk of substantial loss or redistribution of poultry manure by wind erosion immediately after incorporation.

4.1 Introduction

Wind erosion and associated dust emissions from arable lands are a topic of increasing concern, as the composition and the properties of the released dust causes various

environmental problems (Zobeck and Van Pelt, 2015). The main problem is that wind erosion on agriculture fields is often not noticeable as only the upper millimeters of the topsoil are affected. Thus, large areas of erosion and deposition are difficult to recognize. According to Chepil (1960), up to 40 tons per hectare of soil material can be lost annually without any visible effects. Single wind erosion events caused soil losses of more than hundred tons per hectare, independent of different climatic conditions and land use systems (Fryrear, 1995; Funk et al., 2004; Hoffmann et al., 2011; Michelena and Irurtia, 1995). Climate change will exacerbate the situation, as long lasting droughts and strong winds can be expected in Central Europe during spring and summer (May, 2008; Spinoni et al., 2015; Steininger and Wurbs, 2017). Drier periods have been already determined for the last decades for these seasons in Central Europe (Hänsel et al., 2019; Zolina et al., 2013).

Land use is a further control parameter for wind erosion. Especially summer crops increase the wind erosion risk in spring, as their fields are prepared in the time of the highest erosivity of the year (low precipitation rates and highest mean wind speeds in the spring months) (Borrelli et al., 2015; Funk and Frielinghaus, 1998; Funk and Reuter, 2006; Goossens and Riksen, 2004; Hassenpflug, 1998). Between 2000 and 2018, the acreage for maize increased by 63% in Germany (DESTATIS, 2021) and led to more bare arable land areas in spring. Sandy soils are particularly more susceptible to mechanical stress than soils of finer textures (Lyles, 1985; Zobeck and Van Pelt, 2015). Tillage at low soil moisture can destabilize the structure of sandy soils completely, leaving a pulverized or single grain structure (Chepil and Woodruff, 1963; Stach and Podsiadłowski, 2002).

There is a close relationship between the size of particles and the critical minimum wind speed for the start of particle movement (Bagnold, 1941). It is lowest for the fine sand fraction (200 – 63 µm) and is increased for finer (< 63 µm) and coarser fractions (> 200 µm) due to particle bonding between fine particles and increased masses of coarser fractions. Based on German sieving standards, particles > 630 µm are considered as non-erodible fraction (nEF) (Neemann, 1991) that is analogous to the fraction > 840 µm as used in US classification schemes (Chepil, 1941).

Wind erosion is also a very effective sorting process of soil material. Particles of the silt and clay fraction are predominantly removed by transport in suspension mode in the atmosphere, whereas the sand fraction remains on the field or is deposited at the field

edge (Buschiazzo and Funk, 2015; Buschiazzo and Taylor, 1993; Li et al., 2009; Shahabinejad et al., 2019). Measurements of wind erosion have also shown enriched carbon contents in the eroded materials (Iturri et al., 2017; Lal, 2003; Li et al., 2018; Nerger et al., 2017; Olson et al., 2016). This is expressed by enrichment ratios (ER) of soil organic carbon (SOC), i.e., the SOC content in the wind-eroded sediment compared to that of the parent soil (Sterk et al., 1996). Sandy soils generally have a higher ER than finer textured soils, indicating an easier separation of organic and mineral components. Independent from the soil type, ER's increase with transport height and distance and ranged between 1.05 and 41.9 (Larney et al., 1998; Li et al., 2009; Sharratt et al., 2018; Webb et al., 2013, 2012). As organic matter and the fine mineral fractions are the carriers of nutrients, wind erosion also results in losses of soil quality (Lei et al., 2019).

Farmyard manure is used to maintain or increase SOC content of soils in order to improve physical, chemical and biological soil properties (Haynes and Naidu, 1998). This is mainly related to the long-term effects. But shortly after incorporation, it is present in the soil as a part of particulate organic matter (POM) and can have an immediate impact on physical soil properties such as water repellency, implicating decreasing infiltration rates or enhanced surface flow and runoff for a certain time (Doerr et al., 2000; Jarvis et al., 2008; McGhie, 1980).

The manure incorporation is concentrated in the top soil layer, i.e. in the tillage horizon. After mixture of manure and soil components, a loose side-by-side of the particles remains for the first period. Depending on soil moisture and microbial activity, different organo-mineral interactions are initiated at different rates. Thus, manure application can lead to a possible combination of two issues. In the long-term, physical soil properties are improved and the risk of soil erosion is reduced due to increased aggregation. In the short-term, susceptibility to wind erosion is temporarily increased by adding fine structured and dry material, i.e. from poultry barns. Specific studies about organic fertilizer losses on sandy soils by wind erosion are lacking to date. The present study focusses on this topic to address this gap from the physical point of view. Sandy soils and poultry manure were used for wind erosion experiments in a wind tunnel, simulating typical spring conditions in Germany, when soils are prepared for summer crops.

4.2 Material and methods

4.2.1 Soil and poultry manure samples

Soil samples were taken from the plough horizon of four agricultural fields in the Federal States of Mecklenburg-West Pomerania and Brandenburg (North-Eastern Germany), for which wind erosion is a frequently observed phenomenon. Landscapes are dominated by sandy soils (fluvial and aeolian sediments), which were deposited during the Weichselian glaciation of the Pleistocene ice age. Land use is dominated by arable farming. The northern part of the study region, close to the coastline of the Baltic Sea, is characterized by high wind speeds and higher precipitation rates (annual averages of 4.5 – 4.8 m s^{-1} and 650 – 700 mm yr^{-1}). The southern part of the study region has generally lower wind speeds and lower precipitation rates (annual averages of 3.6 – 3.9 m s^{-1} and 450 – 550 mm yr^{-1}). The entire region has a lower precipitation rate than the German average of 819 mm (DWD, 2019, 2018).

The soil samples were used to characterize the grain size distribution by dry sieving and the wet pipette method (DIN ISO 11277, 2002). In addition, subsamples were carefully dry-sieved by hand in order to determine the non-erodible fraction > 630 µm (Funk et al., 2019; Funk and Frielinghaus, 1998; Neemann, 1991). Soil water content (SWC) was measured by the gravimetric method (DIN ISO 11465, 1996). The used soils have sand contents (> 63 µm) of 85 to 91%, low SOC contents (< 1.8%) (Table 4.1) and are typical for large parts of wind erosion affected arable lands in the North-Eastern German Lowlands (Funk and Reuter, 2006; Steininger and Wurbs, 2017; UBA, 2011).

Table 4.1 Overview of the investigated soil locations and their basic properties.

Site name	Code	Longitude Latitude	Texture class	Sand [%] c/m/f**	Silt [%] c/m/f***	Clay [%]**	> 630 µm [%]	SOC [%]	pH ($CaCL_2$)	SWC [%]***
Gottesgabe	GG	14°11'39"	Loamy	87	7	6	12.2			
		52°39'03"	sand	3/30/54	5/1/1		11.1†	1.3	7	0.9
Klockenhagen	KH	12°23'15"	Sand	92	7	1	10.5			
		54°14'15"		2/19/71	3/1/3		7.2†	0.9	6.3	0.6
Kuhstorf	KT	11°18'00"	Sand	92	7	1	16			
		53°22'46"		2/46/44	3/2/2		16†	0.6	5	0.5
Paulinenaue	PA	12°43'10"	Sand	92	7	1	69.8			
		52°41'04"		0/12/80	4/2/1		32.4/ 9.8†	1.8	4.5	1.3

*hydromorphic influenced soil during soil formation

**soil texture: Sand: coarse sand (2000 – 630 µm)/middle sand (630 – 200 µm)/fine sand (200 – 63 µm), Silt: coarse silt (63 – 20 µm)/middle silt (20 – 6 µm)/fine silt (6 – 2 µm) and clay (< 2 µm)

***for air-dry conditions in the laboratory: 20 – 22 °C, 50% relative humidity

†soil samples with poultry manure

Before the wind tunnel experiments, the soils were air-dried at 20 – 22 °C and 50% relative humidity for several weeks to ensure similar moisture conditions for all soils.

Depending on the SOC content, water contents of the air-dried samples were between 0.5 to 1.3%. Large aggregates or stones (> 2 cm) were removed.

Poultry manure was obtained from a chicken breeding farm in the study region. The farm uses conventional management practice, with a high animal population density and a periodic use of antibiotics. Wooden chips and sawdust were used as bedding material. The manure was also air-dried for several weeks, resulting in a remaining water content of 10%, and sieved through a 2 mm mesh. The aim was to achieve the same preconditions for a uniform mixture of poultry manure and soil for the entire time of experiments. This pretreatment can also be seen as a reflection of the meteorological conditions in spring, resulting in a fast surface drying of the upper centimeters of a soil or the soil-manure mixtures.

4.2.2 Wind tunnel experiments

An open circuit push type wind tunnel was used for wind erosion experiments. Two axial fans generated wind speeds up to 18 m s^{-1} inside the working section. In front of the working section, a wind profile was formed with a straightener section, spikes and variable roughness elements made by LEGO^{TM} bricks. The air intake and exhaust took place on the roof of the hall in a height of about 10 m. The working section of the wind tunnel has a length of 6.5 m, a width of 0.7 m and a height of 0.7 m. The floor of the working section was filled with soil material with a depth of 5 cm.

Both transport modes of wind erosion, saltation and suspension, can be measured separately at the end of the working section. A 0.05 m wide and 0.3 m high saltation trap collected and separated the saltation transport in five height segments (0 – 1 cm, 4 – 5 cm, 9 – 10 cm, 19 – 20 cm, 29 – 30 cm). During the run, the collected material from the two lowest segments was weighed every 2 s on scales, which were connected to a data logger. An exemplary illustration of the recorded discharge of soil material is depicted in Fig. S4.1a. The material from the heights of 9 – 10 cm, 19 – 20 cm and 29 – 30 cm was also sampled and weighed in total after each run. The values were used to calculate the total soil losses by regression analysis:

$$q(z) = q_0 e^{-bz} \qquad \text{Eq. 4.1}$$

Where $q(z)$ is the transported material [g] with height z [cm], q_0 is the transported material [g] near the surface (0 – 1 cm) and b is the slope or the measure of the vertical concentration gradient.

Particles < 32 µm and transported in suspension were measured with one Environmental Dust Monitor (EDM 164, GRIMM Aerosol Technique, hereinafter EDM) in the vertical outlet tube of the chamber behind the working section. The EDM measures the number concentration [L^{-1}] between 0.25 and 32 µm in 6-seconds-intervals and converts the number concentration to mass concentration [µg m^{-3}] (PM_{10}, $PM_{2.5}$, PM_1). More details on the structure and design of the wind tunnel can be found in Funk et al. (2019).

Each experiment consisted of three runs with wind speeds of 8, 11 and 14 m s^{-1}. The wind speed was increased to the target level within 30 s and kept constant for 10 min. During the first run for each soil, wind speed in the wind tunnel was measured with a high precision hot wire anemometer (Lambrecht meteo GmbH, Göttingen, Germany) at four heights above the soil (0.05 m, 0.15 m, 0.30 m, 0.50 m) to calculate the friction velocity u_* from the vertical wind profile. By using u_*, the wind speed is determined at the standard height of 10 m according to standard requirements of the world meteorological organization (WMO, 2018). The wind speeds of 8, 11 and 14 m s^{-1} in the tunnel correspond to 10.7, 14.8 and 18 m s^{-1} at 10 m height.

After the third wind tunnel run with the highest wind speed level, the deposited saltation material was completely collected and weighed for comparison with the calculated soil losses. Before the experiments were repeated with the same soil, the soil surface was turned and refreshed by mixing the eroded soil material with the soil in the working section uniformly with a rake to achieve the original state of the soil. The same procedure has been repeated two times for each soil, resulting in three experiments per soil with same wind speeds.

After finishing the wind erosion experiment with the soils, the same experiments were repeated with soil-manure mixtures. The added poultry manure corresponded to a common fertilization rate of 6 tons per hectare and an incorporation depth of 0.1 m, resulting in a manure amount of 1.4 kg for the whole wind tunnel working section. Poultry manure was evenly distributed with a hand scoop and incorporated by a rake.

Before the first run, soil samples from the soil surface were taken at five different positions along the working section. The samples and the sediments in the saltation trap were used to analyse the carbon- (C_t) and nitrogen (N_t) content, POM quality and particle size. Since the carbon contents were mainly of organic origin (~ 99% SOC), it was sufficient to show the C_t content in the results. The C mass losses per area were calculated by using the mean weighted C_t content over all trap heights for the respective wind speed:

$$M_{C_tL} = M_{SL} * C_t \quad \text{Eq. 4.2}$$

Where M_{CtL} is the area related C loss [kg m^{-2}], M_{SL} is the area related soil loss [kg m^{-2}] and C_t is the dimensionless total carbon content.

By subtracting the area related C loss from soil-manure mixtures and soils, it is possible to determine the total loss of poultry manure through wind erosion.

$$M_{ML} = \frac{M_{C_tML} - M_{C_tL}}{C_{tManure}} \quad \text{Eq. 4.3}$$

Where M_{ML} is the total loss of poultry manure [kg m^{-2}], M_{CtML} is the total area related carbon loss of soil-manure mixtures [kg m^{-2}], M_{CtL} is the total area related C loss of soils [kg m^2] and $C_{tManure}$ is the dimensionless amount of carbon content of poultry manure.

The PM emissions [µg m^{-2}] were determined by summing up the product of the measured PM concentration c [µg m^{-3}] (Fig. S4.1b) with the air discharge V [m³] for a complete duration of t = 10 min (100 intervals (i) of 6-second-measurements) of each wind speed and dividing through the wind tunnel section area A (4.55 m²):

$$PM\ emission = \frac{\sum_{i=1}^{t} c_i * V_i}{A} \quad \text{Eq. 4.4}$$

Analogously to the calculation of total soil, the total PM emissions are the sum of all wind speeds.

4.2.3 Size analysis of primary particles and micro aggregates

The particle and aggregate size analyses for wind erosion studies need a different consideration compared to standard texture analyses as only limited conclusions of the transported grains or aggregates can be drawn from fully dispersed samples. Size analyses of the soils and sediments were carried out with the Malvern Mastersizer 3000 laser diffractometer (Malvern Panalytical ltd, Malvern, United Kingdom) and an automated dry powder dispersion unit (Aero S). The samples pass the measuring unit without any

additional dispersion. Each sample was investigated with the same setting to achieve comparable size distributions: *Particle type*: non-spherical, refractive (1.543) and absorption (0.01) index of Quartz, *background-measuring time*: 10 s, *measuring time*: 5 s, *number of runs*: 3 – 10 (depending on the amount of material) and *obscuration range*: 1 – 10% (recommended).

By default the Mastersizer measurement is fundamentally a measurement of the volume distribution (Mastersizer 3000 user manual, 2015). Therefore, the volume based size distribution of particles and aggregates was used to determine the particle size distribution. The particle size distributions, i.e. median particle diameter d_{p50}, were calculated using the Mastersizer 3000 software (Mastersizer v 3.71, Malvern Panalytical ltd, Malvern, United Kingdom).

4.2.4 Carbon and nitrogen content and organic matter composition

The total carbon content (C_t) and the nitrogen content (N_t) of the soils and the sediment material in the saltation trap was determined by dry combustion using an elemental analyzer (CNS928-MLC, Leco Instruments GmbH, Mönchengladbach, Germany) (DIN EN 15936, 2012). The measured carbon and nitrogen contents are corrected to "absolutely dry" by multiplying them with a water content factor.

The organic matter composition of the soils and sediment material was characterized by diffuse reflectance infrared Fourier transform (DRIFT) spectroscopy in the mid-infrared range with respect to its organic functional groups (aliphatic C-H, C=O, C-O-C) (Capriel, 1997; Capriel et al., 1995), using an FTIR spectrometer BioRad FTS 135 (Digilab, Randolph, MA, USA). To avoid micro-topographic effects on DRIFT spectra due to large particle sizes (Leue et al., 2010), the samples were finely ground using a swinging ball mill (Retsch GmbH, Haan, Germany). Spectra were measured between wave number (WN) 4000 and 400 cm^{-1} (wavelengths between 2.5 to 25 µm) by 16 co-added scans at a resolution of 1 cm^{-1}. The spectra were baseline corrected using the Software WIN-IR Pro (Digilab, Randolph, MA, USA) and converted to Kubelka-Munk (KM) units (Kubelka, 1948). The band intensities of C-H groups (WN 2927 and 2858 cm^{-1}) were measured at the vertical distance from a local baseline plotted between tangential points in order to avoid effects of the neighboring O-H band. The summed heights of the C-H bands were used as a parameter for the potential wettability or repellency of organic matter in the samples (Capriel et al., 1995).

4.2.5 Optical contact angle measurement and drop contour analysis

Droplet contact angles were determined to test soil samples of non-fertilized and fertilized soil samples on water repellency, as water repellency can be used as an indication of wind erosion susceptibility (Doerr et al., 2000). Aliquots of the soil samples were attached each on small glass plates, using double-sided adhesive tape (Bachmann et al., 2000). A water drop of 6 µL was set on the material by a thin syringe (dosage needle). In combination with a backlight source, the dissolving behavior of the droplet was recorded with a high-resolution camera (SCA 20, DataPhysics GmbH, Filderstadt, Germany), starting with the moment of the initial contact between droplet and surface. The contact angle (CA) between droplet and soil surface was measured as a function of time (Fér et al., 2016). Its exponential decrease was fitted by a power function:

$$CA = a + bt^c \qquad \text{Eq. 4.5}$$

where *CA* is the contact angle [°], *t* is the water droplet deliquescence time [ms], and *a*, *b*, *c* are fitting parameters, which can be used to compare the droplet deliquescence for different samples.

4.2.6 Statistical analysis

A Mann-Whitney-Test (significance level *P < 0.05) was used to examine significant variations in the carbon and nitrogen content, FTIR-signals and particle size values from triplicate samples between the soil-manure mixtures and soil samples. Regression analyses were performed using Origin (OriginPro 9.1.0G, OriginLab Corporation, Northampton, MA, USA).

4.3 Results

4.3.1 Wind driven loss of soil, poultry manure and particulate matter (PM_{10}; $PM_{2.5}$)

The wind erosion experiments in the wind tunnel showed a close dependency of the total soil loss on the non-erodible fraction (nEF > 630 µm) for both soil and soil-manure mixtures. They resulted in maximum soil losses of 14.7 kg m^{-2} for the soil with the lowest share of nEF of around 10% and 3.3 kg m^{-2} for the soil with the highest share of nEF of about 70% (Fig. 4.1a). There is an exponential decrease of soil loss with increasing nEF. The most drastic decrease is shown, if the nEF increased from 5 to 15%. Only small differences of total soil losses could be determined between soils and soil-manure

mixtures (GG, KH, KT). While the total soil loss of GG and KH increased from 5 to 6.4 kg m^{-2} and from 14.7 to 15.1 kg m^{-2} after fertilizing with poultry manure, the soil loss of KT decreased from 4.4 to 4.2 kg m^{-2}. The soil loss of PA increased during the runs from 3.3 to 10.1 kg m^{-2} and is caused by a gradual decrease of nEF during the runs (Table 1).

The total PM_{10} emissions ranged between 1.5 g m^{-2} and almost 8 g m^{-2}. Total $PM_{2.5}$ emissions ranged between 0.46 and 2.58 g m^{-2}, resulting in a mean $PM_{2.5}/PM_{10}$ ratio of 0.38 ± 0.14. PM_{10} emissions as well as the $PM_{2.5}$ emissions were linear and significantly correlated to the soil losses, whereas the PM_{10} emissions increased more with higher soil losses than the $PM_{2.5}$ emissions (Fig. 4.1b). Similar to the soil loss results, no differences in PM emissions could be determined between soils and soil-manure mixtures.

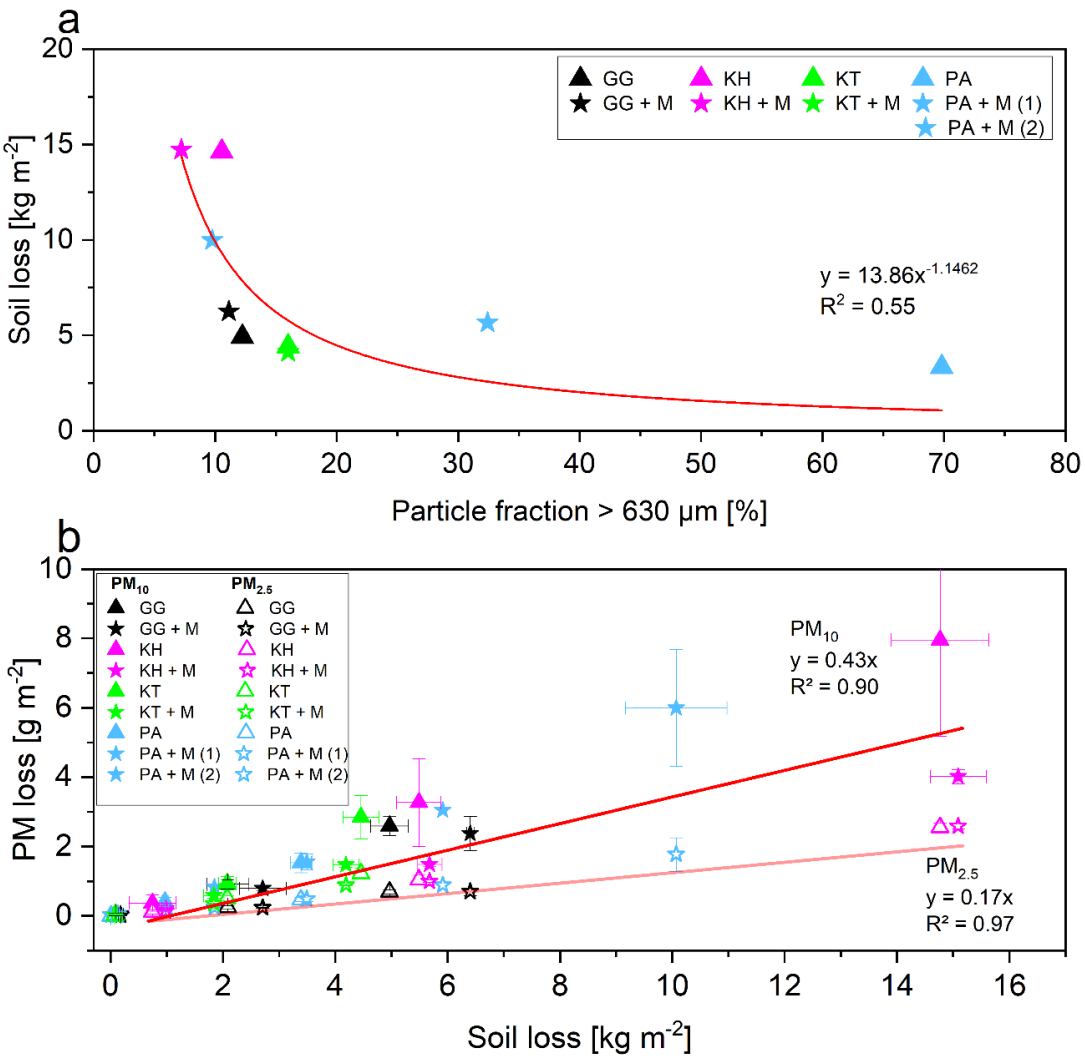

Fig. 4.1. (a) - Total soil loss in relation of non-erodible particles or aggregates with a diameter > 630 µm after the wind tunnel speed of 14 m s^{-1}, (b) - PM_{10} (solid symbols) and $PM_{2.5}$ (open symbols) losses in relation to the losses of the soils (triangle) and soil-manure mixtures (star) for the wind speeds in the wind tunnel.

Distinct differences between the soils and their mixtures with manure can be seen if the C_t losses are considered (Fig. 4.2). The relative C_t losses of the soil-manure mixtures are already enhanced at the lowest wind speed level of 8 m s^{-1}. If the relative C_t losses are compared, they increase from 3.5% to 8.1% for GG, from 6.8% to 9.5% for KH and from 5% to 13.8% for KT. The next wind speeds (11 and 14 m s^{-1}) yield to similar shares of relative C_t losses for soils and soil-manure mixtures.

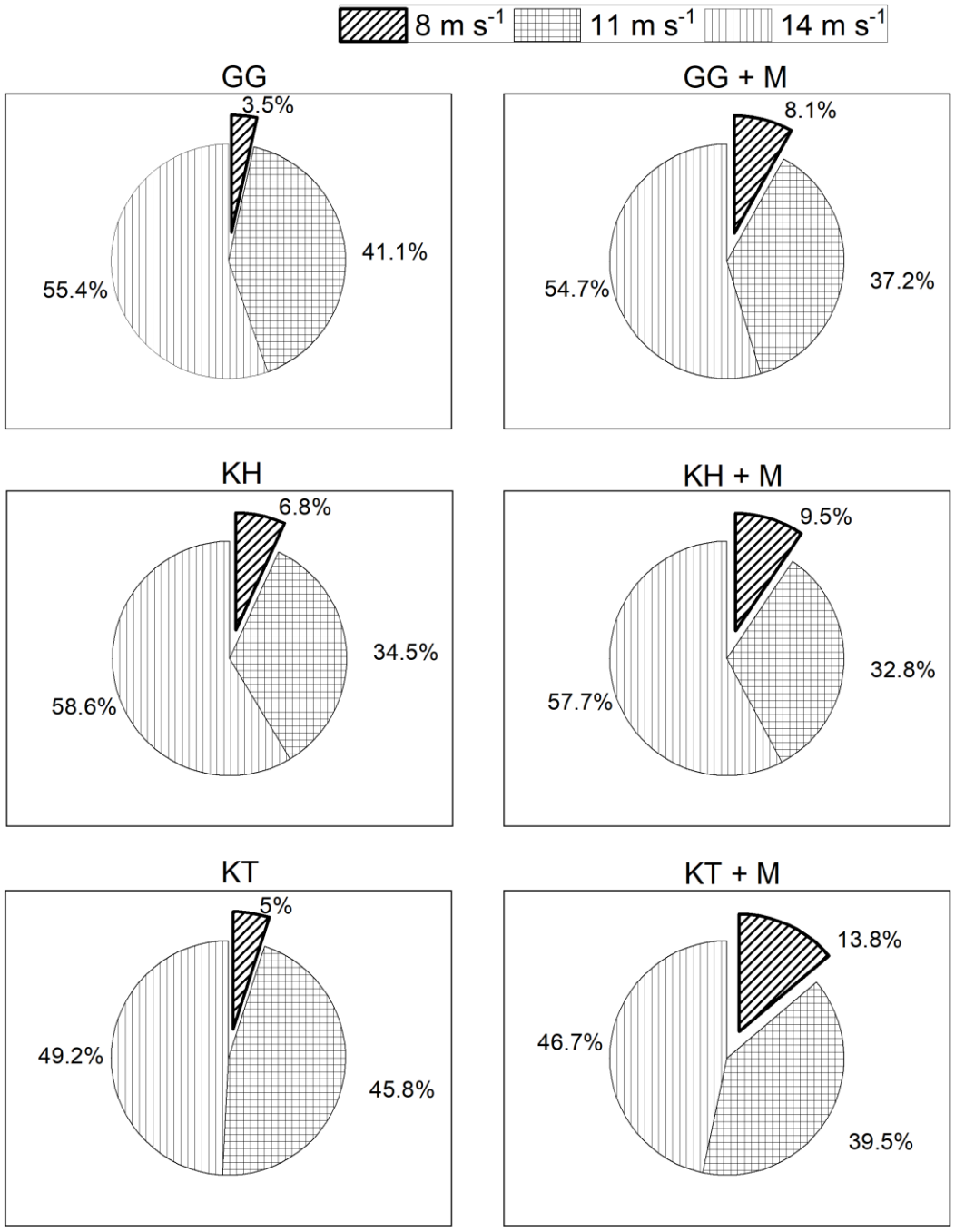

Fig. 4.2. Percentage of C_t losses in relation to the total C_t loss of the soils (GG, KH, KT) and soil-manure mixtures (GG +M, KH + M, KT+ M) after 14 m s^{-1}.

The absolute manure losses by wind erosion were calculated from the total soil losses and C_t losses of each experiment and were between 1.7 to 14% of the added amount of manure. This is equivalent to potential manure losses between 101 kg ha^{-1} and 854 kg ha^{-1} if related to the application amount of 6 tons per hectare (Table 4.2.). On the one hand, the highest relative losses of poultry manure occurred at the lowest wind speed level (8 m s^{-1}), where in particular, C was removed (KT, 13.8%). On the other hand, the highest

amount of C_t (KH, 854 kg ha^{-1}) gets lost at the highest wind speed (14 m s^{-1}) in correlation to the total soil losses. C_t losses for PA could not be calculated because of an insufficient amount of soil material in the saltation trap at the lowest wind speed.

Soil losses of the maximum wind speed level were 19 – 57 times larger compared to the minimum wind speed, whereas the poultry manure losses were about 3.7 – 6.1 times larger at 14 m s^{-1} compared to 8 m s^{-1}.

Table 4.2. Potential loss of poultry manure and soil at wind tunnel speeds of 8 m s^{-1} (10.7 m s^{-1}), 11 m s^{-1} (14.8 m s^{-1}) and 14 m s^{-1} (18 m s^{-1}) after a poultry manure incorporation of 6 t ha^{-1}.

Code	(8 m s^{-1}) [kg ha^{-1}]		(11 m s^{-1}) [kg ha^{-1}]		(14 m s^{-1}) [kg ha^{-1}]	
	Manure	Soil	Manure	Soil	Manure	Soil
GG	113	864	273	20 864	577	49 676
KH	140	7 473	381	54 879	854	147 656
KT	101	837	212	20 781	373	44 548
PA	N A*		N A*		N A*	

* Collected amount was insufficient and soil aggregates were broken due to low aggregate stability during wind tunnel runs

4.3.2 Effects of poultry manure on physical and chemical soil properties of soils and sediments

4.3.2.1 Soils and poultry manure – Particle sizes

The analyses of the samples regarding their non-dispersed grain and/or aggregate size distributions show significant differences between the soils, soil-manure mixtures and the manure (Fig. 4.3). The manure had a much coarser particle structure compared to the soils. The median diameter d_{p50} of the soils ranged between 177 and 242 µm, whereas the manure had a much larger d_{p50} between 1200 and 1300 µm. The soil-manure mixtures had d_{p50} between 190 and 290 µm.

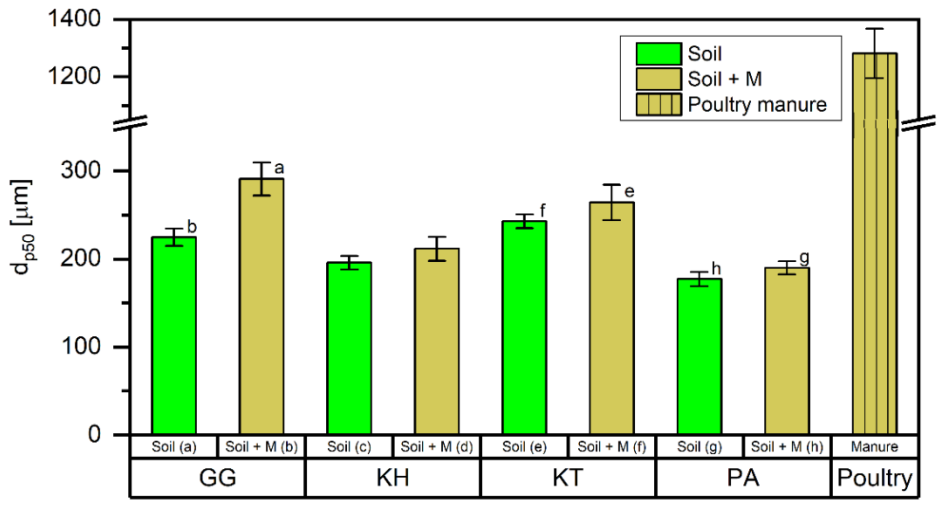

Fig. 4.3. Median diameter (d_{p50}) of the soil samples (soil, soil-manure mixtures (soil + M) and poultry manure). Please notice the break on the Y-axis. Data are mean values with error bars from triplicate measurements. Letters indicate statistical significance between the differences of soil and soil-manure mixtures of each side.

4.3.2.2 Soils and poultry manure – POM composition

The SOC contents of the four soils were between 0.6% (KT) and 1.8% (PA) (Fig. 4.4 and Table 4.1). In contrast, the manure had an OC-content of 41%, and a N_t content of 4.2%, resulting in a C/N ratio of about 10:1 and therefore ideal for use as organic fertilizer. Due to the relatively low SOC contents of sandy soils, the OC composition changed in quantity and quality when poultry manure of 6 tons per hectare was added to the top layer. Adding poultry manure to the soil resulted in a 1.25-fold increase of SOC for KT and KH and a 1.37-fold increase of OC for GG and PA.

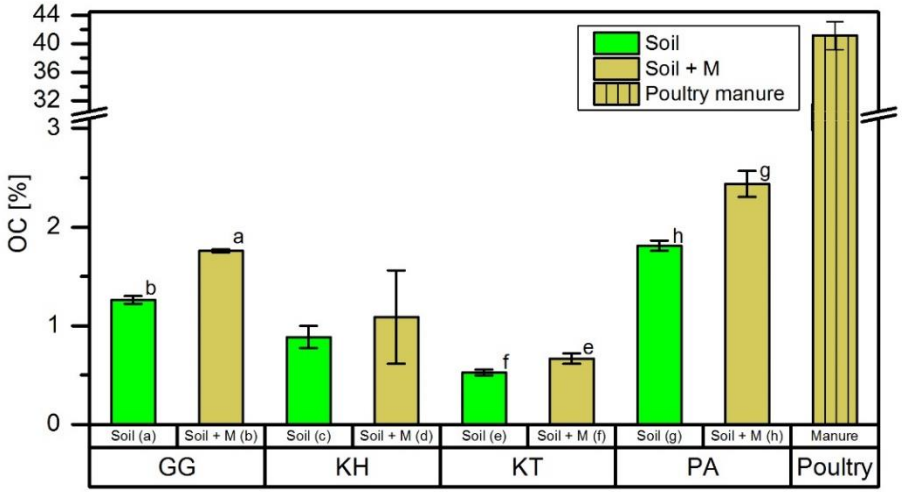

Fig. 4.4. Organic carbon (OC) contents of the soil samples (soil, soil-manure mixtures (soil + M), and poultry manure). Please notice the break on the Y-axis. Data are mean values with error bars from triplicate measurements. Letters indicate statistical significance between the differences of soil and soil-manure mixtures of each side.

The DRIFT spectra revealed changes in the OM composition after manure application, which can alter the physical and chemical soil properties. In all samples, the signal intensities of C-H groups were higher for the soil-manure mixtures compared to the corresponding soil samples (Fig. 4.5a), showing factors of 3.4 (KH), 1.9 (KT), 1.5 (GG), and 1.4 (PA).

As the C-H signal intensities of the soil-manure mixtures increased, it should also have an effect on soil wettability (Leue et al., 2015). The contact angles of the droplet decreased more rapidly for soils compared to soil-manure mixtures of all investigated sites (exemplarily shown for GG in Fig. 4.5b). As well, the initial droplet contact angle on the sample surface of the soil-manure mixture sample (110 ± 7.6°) was higher than for the soil sample (80.4 ± 8°) of GG. Following up, the slope of the contact angles from soil-manure mixtures was flatter than from the soil sample. This can be expressed by the parameter *c* of the power function (Eq. 5), which is a parameter for the curvature of the graph (soil: c = 0.68 ± 0.09; soil-manure mixture: c = 0.45 ± 0.01).

Summarizing the results of all soils, a relatively close relationship was found between the C-H signal intensities, the initial contact angle ($R^2 = 0.63$, *$P < 0.05$) (Fig. 4.5c), the C-H signal intensities and the parameter *c* of the power function (Eq. 5) ($R^2 = 0.59$, *$P < 0.05$) (Fig. 4.5d). Increasing C-H signal intensities were correlated with higher initial contact angles and higher values of the parameter *c* of the power function.

All soils revealed a change in POM composition towards higher OC contents with an increased share of non-decomposed material and increased hydrophobicity after manure application.

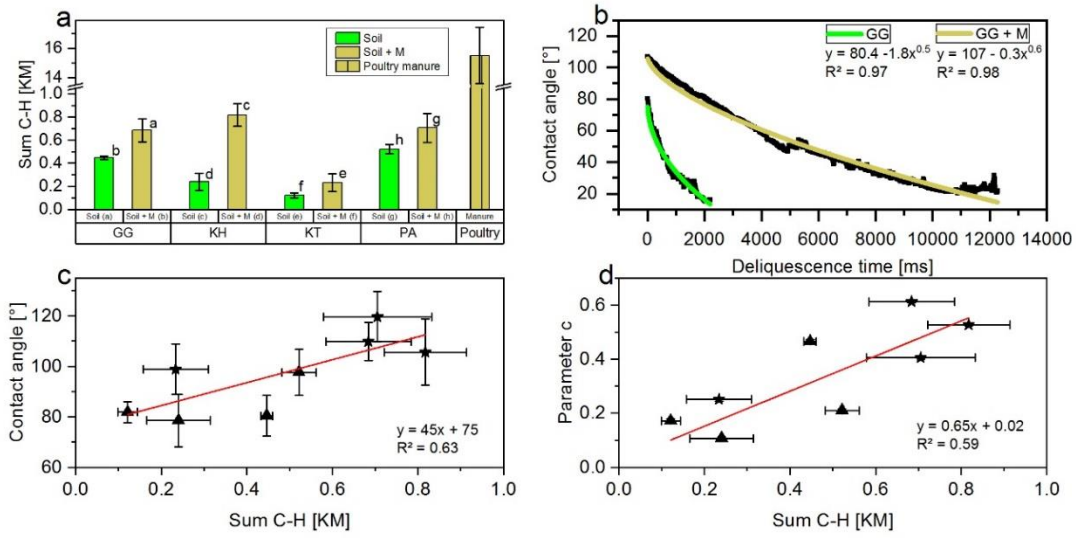

Fig. 4.5. (a) - FTIR signal intensities of the summed aliphatic C-H groups at WN 2927 and 2858 cm^{-1} of soil samples (soil, soil-manure mixtures (soil +M), and poultry manure) from triplicate measurements, (b) - mean contact angles, exemplary for the soil and soil-manure mixture of GG, (c) – relationship between the signal intensities of the summed aliphatic C-H groups and the first frame of the contact angle and (d) - as well as the parameter c of the power function (Eq. 5). Star symbols in (c) and (d) indicate soil-manure mixtures. Letters in (a) indicate statistical significance between the differences of soil and soil-manure mixtures of each side.

4.3.2.3 Sediments – Particle sizes

Fig. 4.6 shows the particle size compositions of the eroded material in relation to the wind speed and trapping heights. The median diameter d_{p50} of the eroded material varied considerably and increased especially near the surface (0 – 1 cm) at wind speeds of 8 m s^{-1} compared to the soils without manure. This is a first indication of the higher susceptibility and the preferred transport of particulate organic components by wind erosion. Although easily detached, they remain close to the surface and part of the saltation load. When the soil contains poultry manure, the d_{p50} of the transported sediment increased significantly at the surface from 242 to 306 µm (GG), from 214 to 511 µm (KT), from 162 to 196 µm (KH) and though not significantly, from 151 to 173 µm (PA). The same, but to lesser extent, were detected for the height of 4 – 5 cm. As the intensity of saltation was weak and friction velocity (u_*) was low at 8 m s^{-1}, no or only a very low amount of material was transported in heights above 5 cm. At the wind speeds of 11 m s^{-1} and 14 m s^{-1}, material was transported and measured at all heights. Here, no clear difference was determined between the d_{p50} of the eroded materials from the soils and

soil-manure mixtures. However, for both, the median particle diameter increased with increasing trapping heights. Particle diameters were in the range of 170 µm to 200 µm near the surface, and increased to diameters of over 300 µm at the maximum wind speed in the wind tunnel (14 m s^{-1}).

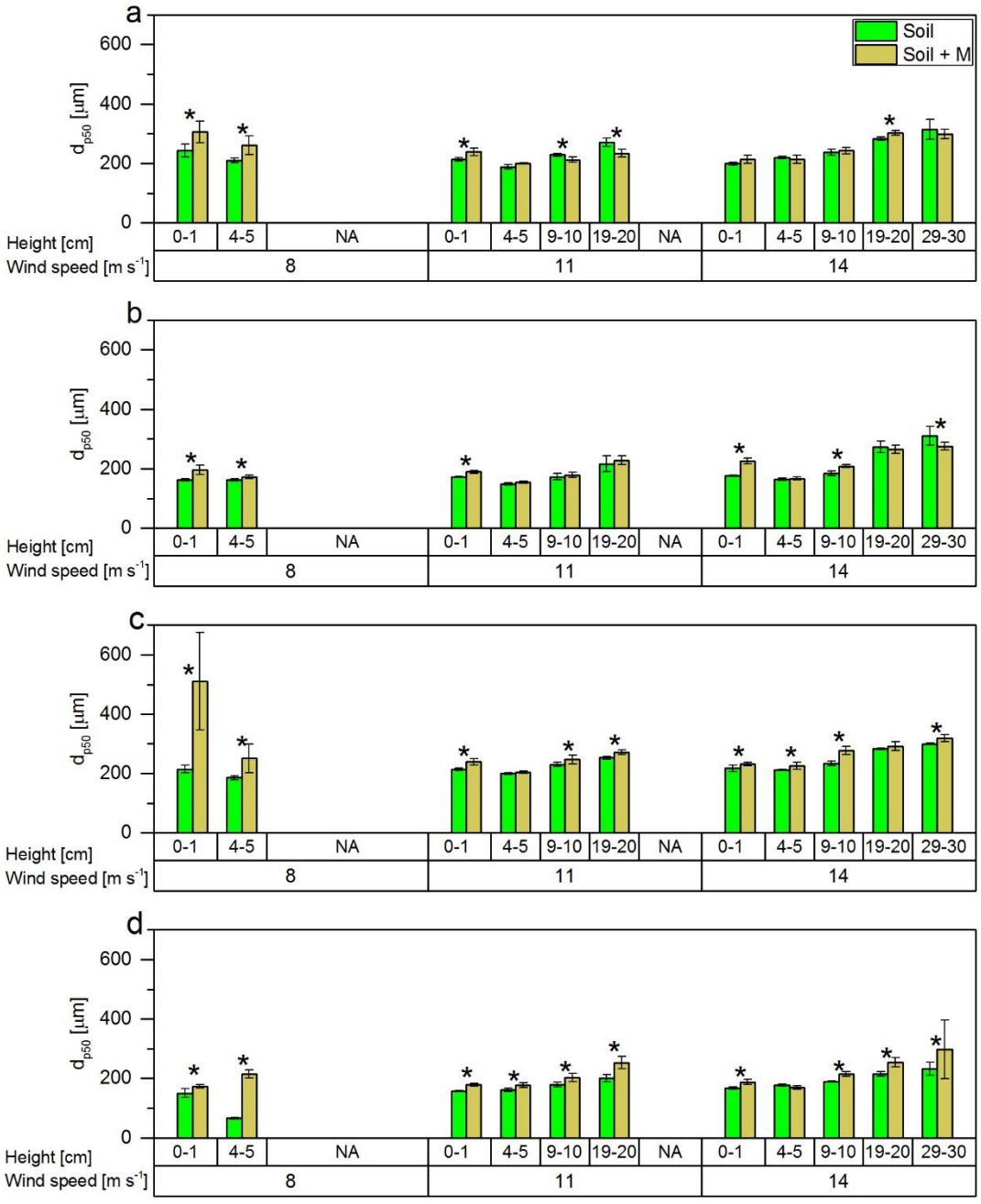

Fig. 4.6. Median diameter d_{p50} of the trapped sediments of each soil and soil-manure mixtures (soil + M) trapped at the height segments of 0 – 1, 4 – 5, 9 – 10, 19 – 20 and 29 – 30 cm at 8, 11 and 14 m s^{-1} in the wind tunnel from (a) GG, (b) KH, (c) KT and (d) PA. Stars indicate significance between soil-manure mixture and soils for each height.

4.3.2.4 Sediments – POM composition

The ER of C_t in the trapped sediments is a further indication of the origin of the POM. The highest ER's were found in sediments from soil-manure mixtures at the two lowest trap heights and minimum wind speed (Fig. 4.7). After incorporating poultry manure to the soil bed, the ER of C_t increased differently but significantly for GG from 1.99 to 2.63, for KT from 3.17 to 20.63 and for KH from 0.98 to 1.30. Increasing wind speed and correlated soil losses caused ER's tending to a value of 1, reflecting no further separation, and losses of the entire soils.

The ER for PA could not fully be determined because the traps did not catch enough material at the beginning of the wind tunnel runs due to a high share of aggregates (Table 4.1). But, because of a general low aggregate stability, a gradual aggregate destruction is visible by greater ER's during the wind tunnel runs for PA. The POM, previously retained in aggregates, was found in the traps at higher wind speeds (11 m s^{-1}, 14 m s^{-1}).

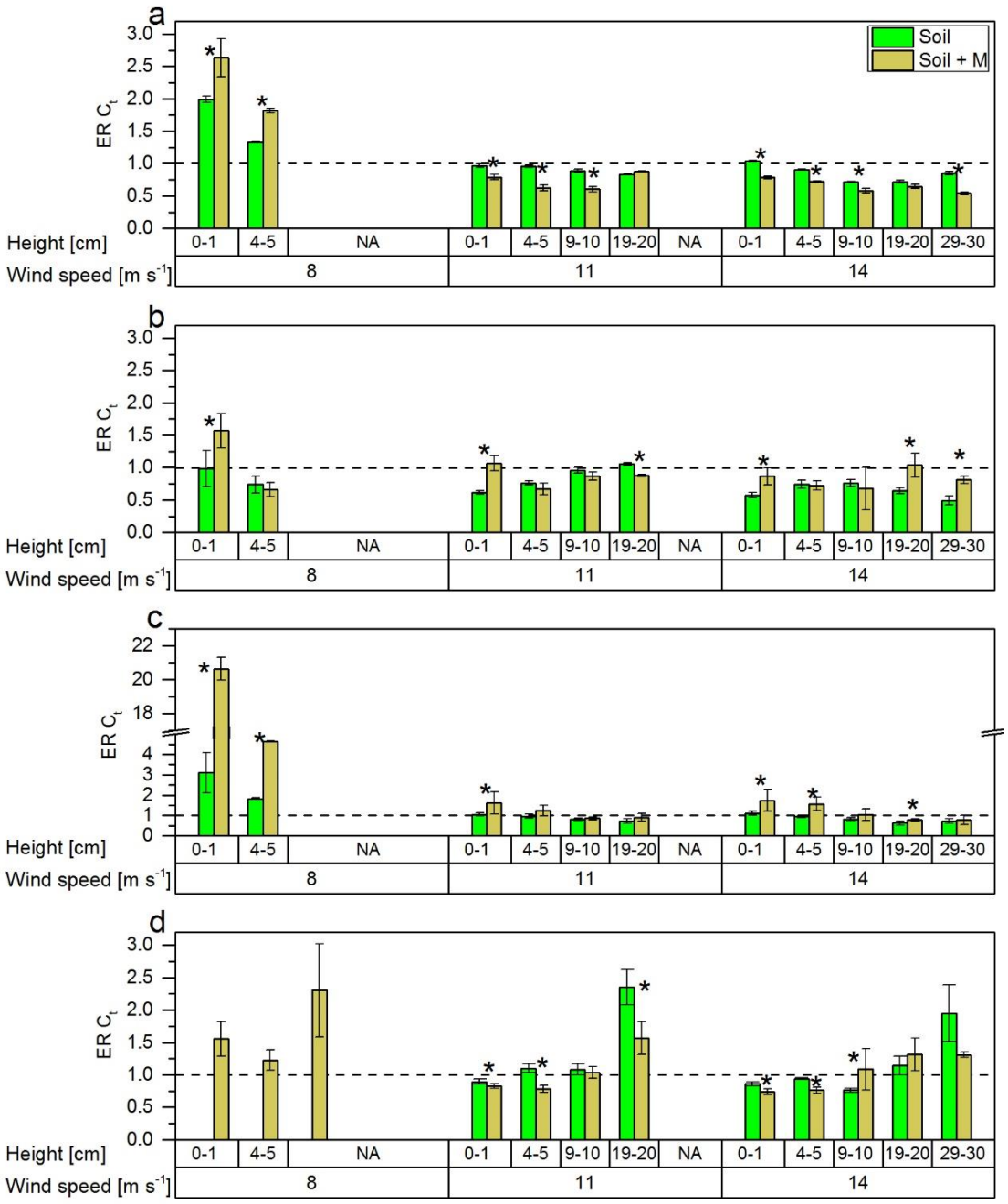

Fig. 4.7. Carbon (C_t) enrichment ratios (ER's) of the sediments trapped of each soil and soil-manure mixtures (Soil + M) at the height segments of 0 – 1, 4 – 5, 9 – 10, 19 – 20 and 29 – 30 cm at 8, 11 and 14 m s^{-1} in the wind tunnel from (a) GG, (b) KH, (c) KT and (d) PA. The dotted line indicated the threshold between enrichment (ER > 1) and reduction (ER < 1) of carbon in the sedimentation trap compared to the soil. Stars indicate significance between soil-manure mixture and soils for each height.

The FTIR signal intensities show the composition of the POM (Fig. 4.8). The signal intensities of the C-H groups for the eroded sediments of each soil generally increase for the soil-manure mixtures. This concerns mainly the lowest heights at the lowest wind speed (8 m s^{-1}). At 11 and 14 m s^{-1}, increased signal intensities were measured after manure application for all heights. The highest signal intensities in KM were 1.41 for GG at 8 m s^{-1} and 0 – 1 cm height, 0.7 for KH at 8 – 11 m s^{-1} and 0 – 1 cm height, 2 for KT at

8 m s^{-1} and 4 – 5 cm height and 1.26 for PA at 11 – 14 m s^{-1} and 19 – 20 cm height. The signal intensity of the C-H groups increased in most of the eroded sediments and show that manure residues were found at almost all heights at each wind speeds. PA is again an exception, since here the higher signal intensities are also due to increasing aggregate decay.

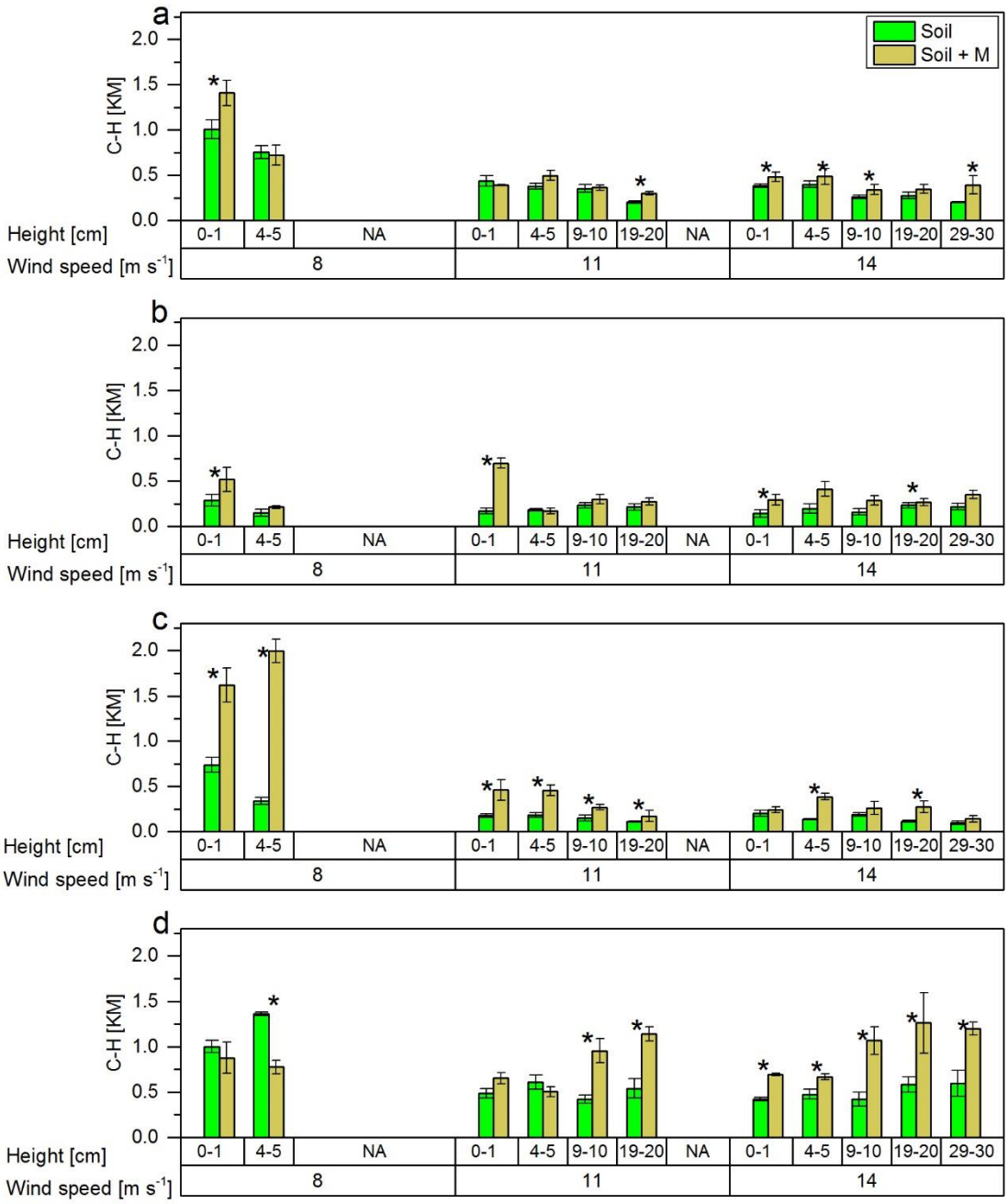

Fig. 4.8. FTIR signal intensities of the summed aliphatic C-H groups at WN 2927 and 2858 cm^{-1} of the sediments of each soil and soil-manure mixtures (soil + M) trapped at the height segments of 0 – 1, 4 – 5, 9 – 10, 19 – 20 and 29 – 30 cm at 8, 11 and 14 m s^{-1} in the wind tunnel from (a) GG, (b) KH, (c) KT and (d) PA. Stars indicate significance between soil-manure mixture and soils for each height.

Wind speed depending separation effects between mineral and organic particles are also revealed by the relation of particle sizes (d_{p50}) to the C_t content of the eroded sediments (Fig. 4.9). There is only a clear linear relationship between increasing d_{p50} and increasing C_t at the lowest wind speed of 8 m s^{-1} (Fig. 4.9a). This applies to the entire data set (large diagram) as well as to the one cleared of the outlier (small diagram in the upper left corner). R^2 only changes slightly from 0.96 to 0.8. This relationship shows the sorting effects between mineral and organic particles, especially at wind speeds close above the threshold. With increasing wind speeds and soil losses, a correlation could not be determined (Fig. 4.9b).

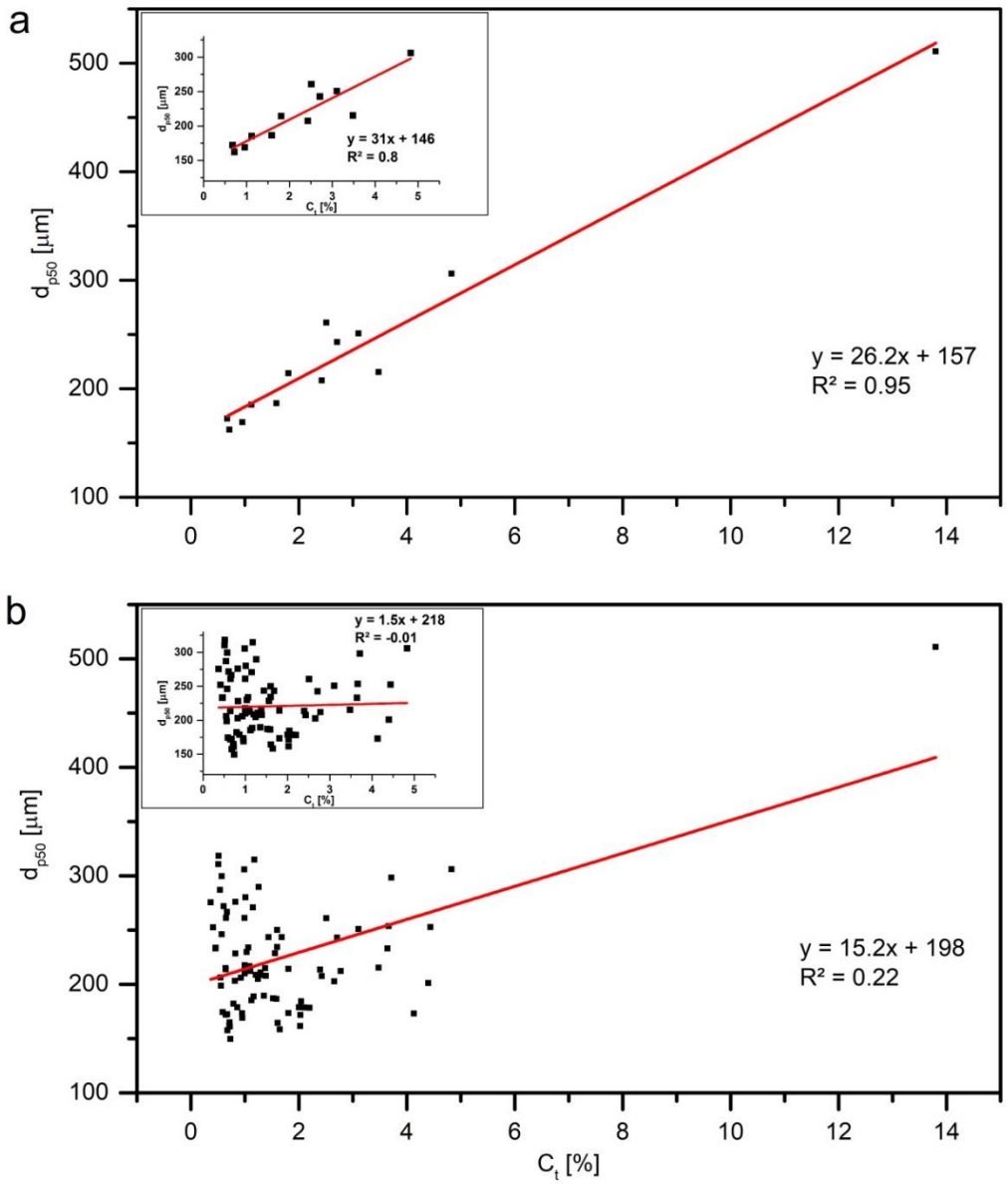

Fig. 4.9. Mass weighted median particle diameter in relation to C_t from (a) wind tunnel runs at the lowest wind speed (8 m s^{-1}) and from (b) all wind tunnel runs. The small graphics in (a) and (b) showed the relation without the outlier at C_t = 13.8%.

Since wind erosion generally leads to a separation between organic and mineral particles, which particularly affect the labile organic matter, it can be further proven via the correlation of the C_t content and the C-H signal intensities. Fig. 4.10 shows that eroded sediments, independent if fertilized or not, are containing higher amounts of labile organic matter with increasing C_t contents, indicated by higher aliphatic C-H signal intensities. The removal of the outlier improves the correlation between the C-H signal intensities and C_t content (small diagram in the upper left corner). The slightly lower R^2

resulted from the fact that only the second highest signal intensity was measured for the highest C_t content of the sediment load.

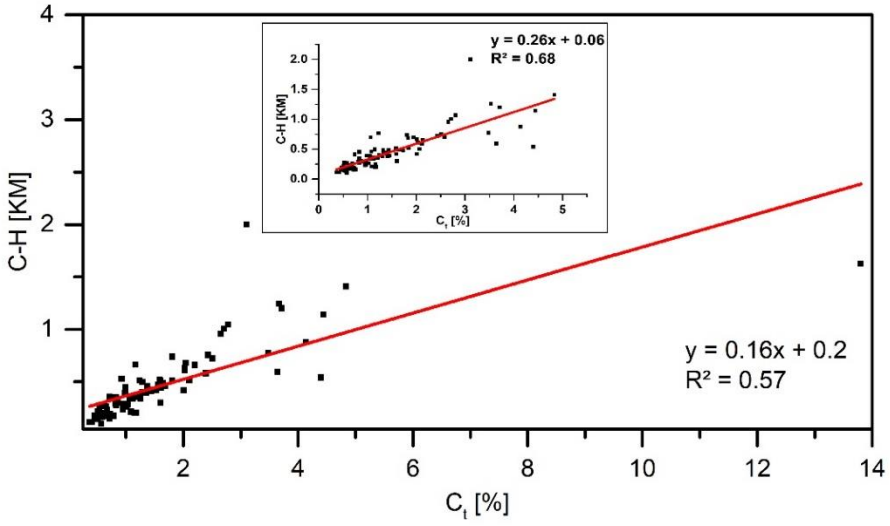

Fig. 4.10. Mass weighted signal intensities of the summed aliphatic C-H groups at WN 2927 and 2858 cm^{-1} in relation to C_t. The smaller graphic showed the relation without the outlier at C_t = 13.8%.

4.4 Discussion

Soils, fertilized with poultry manure, have been identified as a source of fecal bacteria release during wind erosion, being a risk of infections with enterococci (Thiel et al., 2020), *Escherichia coli* (Siller et al., 2021) and *Clostridioides difficile* (Frentrup et al., 2021). The specific properties of poultry manure are a drier consistence and a fine crumbled structure compared to other fertilizers. After manure application and incorporation into soils, a loose side-by-side of organic and mineral particles remains for a certain time if both substrates are relatively dry. Herewith, the manure becomes directly part of the POM of the soil. Application amounts of several tons per hectare can influence physical properties of soils with consequences for wind erosion susceptibility which has not been investigated so far under this focus.

4.4.1 Potential wind driven loss of soil, poultry manure, and particulate matter

Total soil losses, measured in this study in a wind tunnel, were in the range of 3.3 – 14.7 kg m^{-2} and are comparable to reported soil losses in the literature (Bach, 2008; Funk et al., 2004; Goossens, 2004; Nerger et al., 2017). Differences in absolute soil losses from soils and soil-manure mixtures could not be detected. This is mainly due to the very low density of the manure, which has only a minor influence, as losses are based on the

parameter *mass*. Differences between the grain size distributions of soils and soil-manure mixtures could be detected by optical measures and the added manure leads to a general coarser particle structure (Münch et al., 2020). The much lower density of the manure also resulted in only slight changes of the particle size distributions (Table 1), if again based on mass per mesh size after sieving.

Susceptibility of sandy soils to wind erosion is determined by the texture, mainly the non-erodible particle fraction (> 630 µm) as aggregate stability is low. This is in accordance with several wind erosion studies (Chepil, 1960; Funk et al., 2019; Rezaei et al., 2019; Skidmore, 1988; Tatarko, 2001). Three of the soils (GG, KH, KT) were mostly present in the single grain structure, whereas the results of the soil PA show the influence of even weak aggregation. The soil losses of PA increased during the repeated wind tunnel runs, independent if fertilized or not. At the beginning, PA had many aggregates (> 630 µm) resulting from a high soil water content during sampling. Finally, due to a low soil aggregate stability, the aggregates broke by saltation bombardment and repeated mechanical disturbance between the wind tunnel runs, which resulted in gradual increasing losses, finally exceeding the other soils.

The mass share of the added poultry manure, assuming an application amount of 6 t ha^{-1} and an incorporation depth of 10 cm, is only 0.4 percent of the mass of that layer. Based on soil losses and the C_t contents of the sediments, 1.7 to 14% of poultry manure gets lost by wind erosion. The highest manure losses were measured at the highest wind speed in the wind tunnel, whereas the highest relative losses of manure were determined at the lowest wind speed close above the threshold. Here, the density differences of the organic and mineral particles have the most distinct effect on the beginning of transport, resulting in a preferential release of the organic particles (SOM and manure) from the soil surface. Because of the great differences in u_{*t} for mineral and organic particles, it can be assumed, that, once airborne, organic particles are less affected by saturation effects (erosion and deposition in equilibrium) of the saltation transport mode than mineral ones. This is often visible on wind erosion affected fields, where onsite and offsite depositions are characterized by a much lighter color than the original soil (Hassenpflug, 1992). This fact is also confirmed by numerous field studies (Bach, 2008; Larney et al., 1998; Sterk et al., 1996; Webb et al., 2012), where clear correlations were reported between the ER for C_t and the transport height, which can be seen as a proxy for the transport distance. Limitations of the wind tunnel experiments are revealed by the result of the higher wind

speeds. A saturation of the transport is not reached in the short measuring section and a separation similar to field lengths of hundreds of meters is not feasible. However, wind speed depending potential losses of a certain area can be derived in a quite easy way.

In contrast to significantly increased dust emissions during the application of dry poultry manure (Kabelitz et al., 2021, 2020; Münch et al., 2020), wind erosion had in this study neither a strengthening nor a reducing effect on the emissions of particulate matter after the incorporation of poultry manure. Similar PM_{10} and $PM_{2.5}$ -emissions were detected between soils and soil-manure mixtures. The total PM emissions, their linear correlation to the soil losses and the ratio of $PM_{2.5}/PM_{10}$ agrees with other wind tunnel studies (Funk et al., 2019; Li et al., 2015; Panebianco et al., 2016).

4.4.2 Properties of the investigated soils and sediments before and after adding manure

The added manure leads to increased particle and aggregate sizes in the soil, which has already been reported for short-term by Münch et al. (2020). Due to the low C_t content of the sandy soils, poultry manure fertilization had considerable effects on the momentary C_t contents of all soils (relative increase of 25 – 37%). Because effects of manuring are often considered over the long-term, short-term effects are missing from the literature. But long-term monitoring also shows impacts on soil properties by manuring (including poultry manure), such as an increase of mean aggregate diameters and C_t (Agbede et al., 2008; Bhogal et al., 2009; Blanco-Canqui et al., 2005).

Adding manure to the soils changed the composition of POM by increasing the proportion of labile organic compounds, reflected by increased signal intensities of the C-H absorption bands (Iturri et al., 2017). A stronger hydrophobic character was also proven by higher initial contact angles (Leue et al. 2015; Fér et al. 2016). It is widely accepted that soil water repellency is caused by organic compounds derived from living or decomposing plants or microorganisms, when most severe soils are dry (Doerr et al., 2000). The stronger hydrophobicity increases the soil susceptibility to wind erosion, especially for the POM.

In order to initiate wind erosion, a critical threshold value for wind speed or shear stress must first be exceeded. Following Bagnold (1941), the threshold friction velocity u_{*t} is a function of particle diameter and particle density. u_{*t} is lower for particles with a lower

density (POM) and increase with increasing particle diameter, whereas the absolute difference of u_{*t} between particles with different densities increase likewise (Fig. S4.2). It shows that the aerodynamic diameter of a poultry manure particle of about 1200 µm (median particle diameter of poultry manure) is the same as for a particle of mineral origin of 250 – 300 µm. This is the physical reason for the separation of poultry manure particles and mineral particles during wind erosion and becomes particularly obvious at the lowest wind speed above the threshold.

Significant coarser particle compositions were found to be transported near the surface layer resulting in increased ER of C_t. The largest ER was observed for the soils with the lowest SOC - content (KT) (Fig. 4.7, Table 4.1), which is in accordance with Webb et al. (2013). Other studies determined increased ER of C_t also in greater heights because of general higher wind speeds during the experiments (e.g. Iturri et al., 2017). In our study, most of the POM got already lost at the wind speed of 8 m s^{-1}, therefore POM losses at 11 m s^{-1} and 14 m s^{-1} were a corresponding part of the total losses with less separation.

The preferential losses of poultry manure, as a part of POM, were also verified by increased signal intensities of the C-H groups with FTIR analyses. An exception is the soil PA, where the aggregate decay led to a steady resupply of POM in the runs, indicated by higher ER's and C-H signal intensities at higher wind speeds.

4.4.3 Short-term effects vs. long-term effects of poultry manure on wind erosion

Manure application mitigates land degradation and improves the soil properties due to the addition of organic matter at long-term (Liu et al., 2020). Manuring has several benefits to soil properties, such as improving soil structure, higher water adsorption capacity, enhancing biological activity, soil fertility etc. (Blanco and Lal, 2008).

Manure is applied in a variety of forms, from liquid to solid, in coarse or fine structure. Relevant for wind erosion issues are fine structured, dry manures as poultry manure. Before manure can develop its positive long-term effects, it is incorporated into the soil by mixing tools as cultivators or disc harrows. Depending on the meteorological and soil moisture conditions the soil-manure mixture can be affected first by tillage (Faust et al., 2021) and then by wind erosion shortly after fertilization. As wind erosion is not only a removing but also sorting process, our study provides information of the preferential

removal of poultry manure incorporated in sandy soils, depending on the erosion intensity.

Based on this wind tunnel study, it can be concluded that wind erosion may reduce the beneficial effects of poultry manuring. Strong wind erosion events do not occur every year in mid-latitudes and wind erosion does not necessarily occur directly after fertilization. However, it has already been shown that weather systems, including dry spells, may remain more stationary in mid-latitudes due to climate change (Krüger et al., 2020; Nakamura and Huang, 2018; Stendel et al., 2021). Dry spells decrease the soil moisture and promote the wind erosion risk during high wind intensity, when agricultural fields were fresh tilled.

4.5 Conclusion

Wind erosion is an effective process of sorting soil particles by size and density removed from sandy arable fields. This also includes freshly incorporated poultry manure. Our wind tunnel experiments showed that the manure particles in sandy soils are additional material for wind erosion. We showed that poultry manure changes physical and chemical properties in the upper soil layer as well as in the wind-eroded sediments. The particularly strong wind events are not decisive in this case. The selective blow-out of the organic fertilizer particles is mainly caused by wind speeds near the wind erosion threshold of 7 m s^{-1}, which occur more frequently (77 – 86%) than higher wind speeds over the study region in Northeast Germany. Therefore, from the physical point of view, application of a fine structured organic fertilizer, as poultry manure, increases the soil susceptibility to wind erosion. This is particular under the focus, when tillage of dry sandy soil already promotes a single-grain structure. Either the soil or the poultry manure should contain sufficient water to allow binding between the different particles and initiate aggregation.

Acknowledgements

The project “Spread of antibiotic resistance in an agrarian landscape” (SOARiAL) was funded by the Leibniz Association, Germany (SAW-2017-DSMZ-2). The authors thank the cooperating poultry farm staff for providing the poultry manure.

References

Agbede, T., Ojeniyi, S., Adeyemo, A., 2008. Effect of poultry manure on soil physical and chemical properties, growth and grain yield of sorghum in southwest, Nigeria. Am.-Eurasian J. Sustain. Agric. 2, 72–77.

Bach, M., 2008. Äolische Stofftransporte in Agrarlandschaften: experimentelle Untersuchungen und räumliche Modellierung von Bodenerosionsprozessen durch Wind.

Bachmann, J., Ellies, A., Hartge, K.H., 2000. Development and application of a new sessile drop contact angle method to assess soil water repellency. J. Hydrol. 231–232, 66–75. https://doi.org/10.1016/S0022-1694(00)00184-0

Bagnold, R.A., 1941. Bagnold, R.A. 1941: The physics of blown sand and desert dunes. London: Methuen. Prog. Phys. Geogr. - PROG PHYS GEOG 18, 91–96. https://doi.org/10.1177/030913339401800105

Bhogal, A., Nicholson, F.A., Chambers, B.J., 2009. Organic carbon additions: effects on soil bio-physical and physico-chemical properties. Eur. J. Soil Sci. 60, 276–286. https://doi.org/10.1111/j.1365-2389.2008.01105.x

Blanco, H., Lal, R., 2008. Principles of soil conservation and management. Springer New York.

Blanco-Canqui, H., Lal, R., Owens, L.B., Post, W.M., Izaurralde, R.C., 2005. Strength Properties and Organic Carbon of Soils in the North Appalachian Region. Soil Sci. Soc. Am. J. 69, 663–673. https://doi.org/10.2136/sssaj2004.0254

Borrelli, P., Panagos, P., Hessel, R., Riksen, M., Stolte, J., 2015. Soil erosion by wind in Europe, EU RECARE Project. pp. 27–38. https://doi.org/10.2788/488050

Buschiazzo, D.E., Funk, R., 2015. Wind erosion of agricultural soils and the carbon cycle., in: Banwart, S.A., Noellemeyer, E., Milne, E. (Eds.), Soil Carbon: Science, Management and Policy for Multiple Benefits. CABI, Wallingford, pp. 161–168. https://doi.org/10.1079/9781780645322.0161

Buschiazzo, D.E., Taylor, V., 1993. Efectos de la erosión eólica sobre algunas propiedades de suelos de la Región Semiárida Pampeana Central. Cienc. Suelo 10, 46–53.

Capriel, P., 1997. Hydrophobicity of organic matter in arable soils: influence of management. Eur. J. Soil Sci. 48, 457–462. https://doi.org/10.1111/j.1365-2389.1997.tb00211.x

Capriel, P., Beck, T., Borchert, H., Gronholz, J., Zachmann, G., 1995. Hydrophobicity of the organic matter in arable soils. Soil Biol. Biochem. 27, 1453–1458. https://doi.org/10.1016/0038-0717(95)00068-P

Chepil, W.S., 1960. Conversion of Relative Field Erodibility to Annual Soil Loss by Wind. Soil Sci. Soc. Am. J. 24, 143–145. https://doi.org/10.2136/sssaj1960.03615995002400020022x

Chepil, W.S., 1941. Relation of Wind Erosion to the Dry Aggregate Structure of a Soil. Sci. Agric. 21, 488–507. https://doi.org/10.4141/sa-1941-0029

Chepil, W.S., Woodruff, N.P., 1963. The Physics of Wind Erosion and its Control11Contribution from Soil and Water Conservation Research Division, Agricultural Research Service, USDA, with Kansas Agricultural Experiment Station cooperating. Department of Agronomy Contribution No. 795., in: Norman, A.G. (Ed.), Advances in Agronomy. Academic Press, pp. 211–302. https://doi.org/10.1016/S0065-2113(08)60400-9

DESTATIS, 2021. Statistisches Bundesamt - Branchen und Unternehmen - Produktionsmethoden - Landwirtschaftliche Betriebe, Fläche: Deutschland, Jahre, Bodennutzungsarten [WWW Document]. Fed. Stat. Off. Wiesb. URL https://www-genesis.destatis.de/genesis/online?operation=abruftabelleBearbeiten&levelindex=0&levelid=1619353913280&auswahloperation=abruftabelleAuspraegungAuswaehlen&auswahlverzeichnis=ordnungsstruktur&auswahlziel=werteabruf&code=41141-0001&auswahltext=&werteabruf=Werteabruf#abreadcrumb (accessed 25 May 2021).

DIN EN 15936:2012-11, Schlamm, behandelter Bioabfall, Boden und Abfall_-Bestimmung des gesamten organischen Kohlenstoffs (TOC) mittels trockener Verbrennung; Deutsche Fassung EN_15936:2012, 2012. Beuth Verlag GmbH. https://doi.org/10.31030/1866720

DIN ISO 11277, 2002. Soil quality - Determination of particle size distribution in mineral soil material - Method by sieving and sedimentation. Ger. Inst. Stand. Dtsch. Inst. Für Norm. EV Beuth Verl. GmbH.

DIN ISO 11465, 1996. DIN ISO 11465 Bodenbeschaffenheit-Bestimmung der Trockensubstanz und des Wassergehaltes auf Grundlage der Masse-Gravimetrisches Verfahren). Beuth Berl.

Doerr, S.H., Shakesby, R.A., Walsh, R.P.D., 2000. Soil water repellency: its causes, characteristics and hydro-geomorphological significance. Earth-Sci. Rev. 51, 33–65. https://doi.org/10.1016/S0012-8252(00)00011-8

Dreisiebner-Lanz, S., Matzer, R., 2019. Organische Dünger. Fachgruppe Technik.

DWD, 2021a. DWD Climate Data Center (CDC): Vieljährige Stationsmittelwerte für die Klimareferenzperiode 1981-2010, für aktuellen Standort und Bezugsstandort, Version V0.x. [WWW Document]. URL https://www.dwd.de/DE/leistungen/cdc/cdc_ueberblick-klimadaten.html (accessed 21 February 2021).

DWD, 2021b. Windkarten und Winddaten für Deutschland Bezugszeitraum 1981 – 2000 [WWW Document]. URL https://www.dwd.de/DE/leistungen/windkarten/deutschland_und_bundeslaender.html# (accessed 21 February 2021).

DWD, 2019. Klimareport Brandenburg. 1 Aufl. Dtsch. Wetterd. Offenb. Am Main Dtschl. 40.

DWD, 2018. Klimareport Mecklemburg-Vorpommern. 1 Aufl. Dtsch. Wetterd. Offenb. Am Main Dtschl. 52.

Faust, M., Wolke, R., Münch, S., Funk, R., Schepanski, K., 2021. A new Lagrangian in-time particle simulation module (Itpas v1) for atmospheric particle dispersion. Geosci. Model Dev. 14, 2205–2220. https://doi.org/10.5194/gmd-14-2205-2021

Fér, M., Leue, M., Kodešová, R., Gerke, H.H., Ellerbrock, R.H., 2016. Droplet infiltration dynamics and soil wettability related to soil organic matter of soil aggregate coatings and interiors. J. Hydrol. Hydromech. 64, 111–120.

Frentrup, M., Thiel, N., Junker, V., Behrens, W., Münch, S., Siller, P., Kabelitz, T., Faust, M., Indra, A., Baumgartner, S., Schepanski, K., Amon, T., Roesler, U., Funk, R., Nübel, U., 2021. Agricultural fertilization with poultry manure results in persistent environmental contamination with the pathogen Clostridioides difficile. Environ. Microbiol. https://doi.org/10.1111/1462-2920.15601

Fryrear, D.W., 1995. Soil Losses by Wind Erosion. Soil Sci. Soc. Am. J. 59, 668–672. https://doi.org/10.2136/sssaj1995.03615995005900030005x

Funk, R., Frielinghaus, M., 1998. Winderosion, in: Handbuch Der Bodenkunde. American Cancer Society, pp. 1–24. https://doi.org/10.1002/9783527678495.hbbk1998003

Funk, R., Papke, N., Hör, B., 2019. Wind tunnel tests to estimate PM10 and PM2.5-emissions from complex substrates of open-cast strip mines in Germany. Aeolian Res. 39, 23–32. https://doi.org/10.1016/j.aeolia.2019.03.003

Funk, R., Reuter, H.I., 2006. Wind Erosion, in: Soil Erosion in Europe. John Wiley & Sons, Ltd, pp. 563–582. https://doi.org/10.1002/0470859202.ch41

Funk, R., Skidmore, E.L., Hagen, L.J., 2004. Comparison of wind erosion measurements in Germany with simulated soil losses by WEPS. Environ. Model. Softw., Modelling of Wind Erosion and Aeolian Processes 19, 177–183. https://doi.org/10.1016/S1364-8152(03)00120-8

Goossens, D., 2004. Wind erosion and tillage as a dust production mechanism on north European farmland. Wind Eros. Dust Dyn. Obs. Simul. Model. ESW Publ. Dep. Environ. Sci. Eros. Soil Water Conserv. Group Wagening. Univ. Wagening. 15–40.

Goossens, D., Riksen, M., 2004. Wind Erosion and Dust Dynamics: Observations, Simulations, Modelling. ESW Publications.

Hänsel, S., Ustrnul, Z., Łupikasza, E., Skalak, P., 2019. Assessing seasonal drought variations and trends over Central Europe. Adv. Water Resour. 127, 53–75. https://doi.org/10.1016/j.advwatres.2019.03.005

Hassenpflug, W., 1998. Bodenerosion durch wind. Bodenerosion–Analyse Bilanz Eines Umweltprobl. Wiss. Buchgesellschaft Darmstadt 69–82.

Hassenpflug, W., 1992. Winderosion. Handb. Bodenschutzes Kap 2, 200–215

Haynes, R.J., Naidu, R., 1998. Influence of lime, fertilizer and manure applications on soil organic matter content and soil physical conditions: a review. Nutr. Cycl. Agroecosystems 51, 123–137. https://doi.org/10.1023/A:1009738307837

Hoffmann, C., Funk, R., Reiche, M., Li, Y., 2011. Assessment of extreme wind erosion and its impacts in Inner Mongolia, China. Aeolian Res. 3, 343–351. https://doi.org/10.1016/j.aeolia.2011.07.007

Iturri, L.A., Funk, R., Leue, M., Sommer, M., Buschiazzo, D.E., 2017. Wind sorting affects differently the organo-mineral composition of saltating and particulate materials in contrasting texture agricultural soils. Aeolian Res. 28, 39–49. https://doi.org/10.1016/j.aeolia.2017.07.005

Jarvis, N., Etana, A., Stagnitti, F., 2008. Water repellency, near-saturated infiltration and preferential solute transport in a macroporous clay soil. Geoderma 143, 223–230. https://doi.org/10.1016/j.geoderma.2007.11.015

Krüger, J., Pilch Kedzierski, R., Bumke, K., Matthes, K., 2020. Impact of North Atlantic SST and Jet Stream anomalies on European Heat Waves. Weather Clim. Dyn. Discuss. 1–21. https://doi.org/10.5194/wcd-2020-32

Kabelitz, T., Ammon, C., Funk, R., Münch, S., Biniasch, O., Nübel, U., Thiel, N., Rösler, U., Siller, P., Amon, B., Aarnink, A.J.A., Amon, T., 2020. Functional relationship of particulate matter (PM) emissions, animal species, and moisture content during manure application. Environ. Int. 143, 105577. https://doi.org/10.1016/j.envint.2020.105577

Kabelitz, T., Biniasch, O., Ammon, C., Nübel, U., Thiel, N., Janke, D., Swaminathan, S., Funk, R., Münch, S., Rösler, U., Siller, P., Amon, B., Aarnink, A.J.A., Amon, T., 2021. Particulate matter emissions during field application of poultry manure - The influence of moisture content and treatment. Sci. Total Environ. 146652. https://doi.org/10.1016/j.scitotenv.2021.146652

Kubelka, P., 1948. New Contributions to the Optics of Intensely Light-Scattering Materials. Part I. JOSA 38, 448–457. https://doi.org/10.1364/JOSA.38.000448

Lal, R., 2003. Soil erosion and the global carbon budget. Environ. Int. 29, 437–450. https://doi.org/10.1016/S0160-4120(02)00192-7

Larney, F.J., Bullock, M.S., Janzen, H.H., Ellert, B.H., Olson, E.C.S., 1998. Wind erosion effects on nutrient redistribution and soil productivity. J. Soil Water Conserv. 53, 133–140.

Lei, L., Zhang, K., Zhang, X., Wang, Y.-P., Xia, J., Piao, S., Hui, D., Zhong, M., Ru, J., Zhou, Z., Song, H., Yang, Z., Wang, D., Miao, Y., Yang, F., Liu, B., Zhang, A., Yu, M., Liu, X., Song, Y., Zhu, L., Wan, S., 2019. Plant Feedback Aggravates Soil Organic Carbon Loss Associated With Wind Erosion in Northwest China. J. Geophys. Res. Biogeosciences 124, 825–839. https://doi.org/10.1029/2018JG004804

Leue, M., Ellerbrock, R.H., Bänninger, D., Gerke, H.H., 2010. Impact of Soil Microstructure Geometry on DRIFT Spectra: Comparisons with Beam Trace Modeling. Soil Sci. Soc. Am. J. 74, 1976–1986. https://doi.org/10.2136/sssaj2009.0443

Leue, M., Gerke, H.H., Godow, S.C., 2015. Droplet infiltration and organic matter composition of intact crack and biopore surfaces from clay-illuvial horizons. J. Plant Nutr. Soil Sci. 178, 250–260. https://doi.org/10.1002/jpln.201400209

Li, J., Okin, G.S., Epstein, H.E., 2009. Effects of enhanced wind erosion on surface soil texture and characteristics of windblown sediments. J. Geophys. Res. Biogeosciences 114. https://doi.org/10.1029/2008JG000903

Li, H., Tatarko, J., Kucharski, M., Dong, Z., 2015. PM2.5 and PM10 emissions from agricultural soils by wind erosion. Aeolian Res., Eight International Conference on Aeolian Research – ICAR 8 19, 171–182. https://doi.org/10.1016/j.aeolia.2015.02.003

Li, P., Liu, L., Wang, J., Wang, Z., Wang, X., Bai, Y., Chen, S., 2018. Wind erosion enhanced by land use changes significantly reduces ecosystem carbon storage and carbon sequestration potentials in semiarid grasslands. Land Degrad. Dev. 29, 3469–3478. https://doi.org/10.1002/ldr.3118

Liu, S., Wang, J., Pu, S., Blagodatskaya, E., Kuzyakov, Y., Razavi, B.S., 2020. Impact of manure on soil biochemical properties: A global synthesis. Sci. Total Environ. 745, 141003. https://doi.org/10.1016/j.scitotenv.2020.141003

Lyles, L., 1985. Predicting and Controlling Wind Erosion. Agric. Hist. 59, 205–214.

Mastersizer 3000 user manual (English) [WWW Document], 2015. URL https://www.malvernpanalytical.com/en/learn/knowledge-center/user-manuals/MAN0474EN (accessed 22 October 2019).

May, W., 2008. Potential future changes in the characteristics of daily precipitation in Europe simulated by the HIRHAM regional climate model. Clim. Dyn. 30, 581–603. https://doi.org/10.1007/s00382-007-0309-y

McGhie, D.A., 1980. The origins of water repellence in some Western Australian soils.

Michelena, R.O., Irurtia, C.B., 1995. Susceptibility of soil to wind erosion in La Pampa province, Argentina. Arid Soil Res. Rehabil. 9, 227–234. https://doi.org/10.1080/15324989509385891

Münch, S., Papke, N., Thiel, N., Nübel, U., Siller, P., Roesler, U., Biniasch, O., Funk, R., Amon, T., 2020. Effects of farmyard manure application on dust emissions from arable soils. Atmospheric Pollut. Res. 11, 1610–1624. https://doi.org/10.1016/j.apr.2020.06.007

Nakamura, N., Huang, C.S.Y., 2018. Atmospheric blocking as a traffic jam in the jet stream. Science 361, 42–47. https://doi.org/10.1126/science.aat0721

Neemann, W., 1991. Bestimmung des Bodenerodierbarkeitsfaktors für winderosionsgefährdete Böden Norddeutschlands: ein Beitrag zur Quantifizierung der Bodenverluste ; mit 53 Tabellen. Schweizerbart.

Nerger, R., Funk, R., Cordsen, E., Fohrer, N., 2017. Application of a modeling approach to designate soil and soil organic carbon loss to wind erosion on long-term monitoring sites (BDF) in Northern Germany. Aeolian Res. 25, 135–147. https://doi.org/10.1016/j.aeolia.2017.03.006

Olson, K.R., Al-Kaisi, M., Lal, R., Cihacek, L., 2016. Impact of soil erosion on soil organic carbon stocks. J. Soil Water Conserv. 71, 61A-67A. https://doi.org/10.2489/jswc.71.3.61A

Panebianco, J.E., Mendez, M.J., Buschiazzo, D.E., 2016. PM10 Emission, Sandblasting Efficiency and Vertical Entrainment During Successive Wind-Erosion Events: A Wind-

Tunnel Approach. Bound.-Layer Meteorol. 161, 335–353. https://doi.org/10.1007/s10546-016-0172-7

Rezaei, M., Riksen, M.J.P.M., Sirjani, E., Sameni, A., Geissen, V., 2019. Wind erosion as a driver for transport of light density microplastics. Sci. Total Environ. 669, 273–281. https://doi.org/10.1016/j.scitotenv.2019.02.382

Rühlmann, J., Körschens, M., Graefe, J., 2006. A new approach to calculate the particle density of soils considering properties of the soil organic matter and the mineral matrix. Geoderma 130, 272–283. https://doi.org/10.1016/j.geoderma.2005.01.024

Shahabinejad, N., Mahmoodabadi, M., Jalalian, A., Chavoshi, E., 2019. In situ field measurement of wind erosion and threshold velocity in relation to soil properties in arid and semiarid environments. Environ. Earth Sci. 78, 501. https://doi.org/10.1007/s12665-019-8508-5

Sharratt, B.S., Kennedy, A.C., Hansen, J.C., Schillinger, W.F., 2018. Soil Carbon Loss by Wind Erosion of Summer Fallow Fields in Washington's Dryland Wheat Region. Soil Sci. Soc. Am. J. 82, 1551–1558. https://doi.org/10.2136/sssaj2018.06.0214

Siller, P., Daehre, K., Rosen, K., Münch, S., Bartel, A., Funk, R., Nübel, U., Amon, T., Roesler, U., 2021. Low airborne tenacity and spread of ESBL-/AmpC-producing Escherichia coli from fertilized soil by wind erosion. Environ. Microbiol. n/a. https://doi.org/10.1111/1462-2920.15437

Skidmore, E., 1988. Wind erosion. Soil Eros. Res. Methods 203–233.

Spinoni, J., Naumann, G., Vogt, J., 2015. Spatial patterns of European droughts under a moderate emission scenario. https://doi.org/10.5194/asr-12-179-2015

Stach, A., Podsiadłowski, S., 2002. Pulverizing and wind erosion as influenced by spatial variability of soils texture. Quaest. Geogr. 22, 67–78.

Steininger, M., Wurbs, D., 2017. Bundesweite Gefährdung der Böden durch Winderosion und Bewertung der Veränderung infolge des Wandels klimatischer Steuergrößen als Grundlage zur Weiterentwicklung der Vorsorge und Gefahrenabwehr im Bodenschutzrecht. Umweltbundesamt Texte | 13/2017, 119.

Stendel, M., Francis, J., White, R., Williams, P.D., Woollings, T., 2021. Chapter 15 - The jet stream and climate change, in: Letcher, T.M. (Ed.), Climate Change (Third Edition). Elsevier, pp. 327–357. https://doi.org/10.1016/B978-0-12-821575-3.00015-3

Sterk, G., Herrmann, L., Bationo, A., 1996. Wind-blown nutrient transport and soil productivity changes in southwest Niger. Land Degrad. Dev. 7, 325–335. https://doi.org/10.1002/(SICI)1099-145X(199612)7:4<325::AID-LDR237>3.0.CO;2-Q

Tatarko, J., 2001. Soil aggregation and wind erosion: processes and measurements. Ann. Arid Zone 40, 251–264.

Thiel, N., Münch, S., Behrens, W., Junker, V., Faust, M., Biniasch, O., Kabelitz, T., Siller, P., Boedeker, C., Schumann, P., Roesler, U., Amon, T., Schepanski, K., Funk, R., Nübel, U., 2020. Airborne bacterial emission fluxes from manure-fertilized agricultural soil. Microb. Biotechnol. 13, 1631–1647. https://doi.org/10.1111/1751-7915.13632

Webb, N.P., Chappell, A., Strong, C.L., Marx, S.K., McTainsh, G.H., 2012. The significance of carbon-enriched dust for global carbon accounting. Glob. Change Biol. 18, 3275–3278. https://doi.org/10.1111/j.1365-2486.2012.02780.x

Webb, N.P., Strong, C.L., Chappell, A., Marx, S.K., McTainsh, G.H., 2013. Soil organic carbon enrichment of dust emissions: magnitude, mechanisms and its implications for the carbon cycle. Earth Surf. Process. Landf. 38, 1662–1671. https://doi.org/10.1002/esp.3404

WMO, 2018. Guide to Instruments and Methods of Observation, 2018 Edition. ed, WMO. WMO, Geneva.

UBA, 2011. Die Böden Deutschlands. Umweltbundesamt.

Zobeck, T.M., Pelt, R.S.V., 2015. Wind Erosion, in: Soil Management: Building a Stable Base for Agriculture. John Wiley & Sons, Ltd, pp. 209–227. https://doi.org/10.2136/2011.soilmanagement.c14

Zolina, O., Simmer, C., Belyaev, K., Gulev, S.K., Koltermann, P., 2013. Changes in the Duration of European Wet and Dry Spells during the Last 60 Years. J. Clim. 26, 2022–2047. https://doi.org/10.1175/JCLI-D-11-00498.1

Differences in the sediment composition of wind eroded sandy soils before and after fertilization with poultry manure

Supporting information

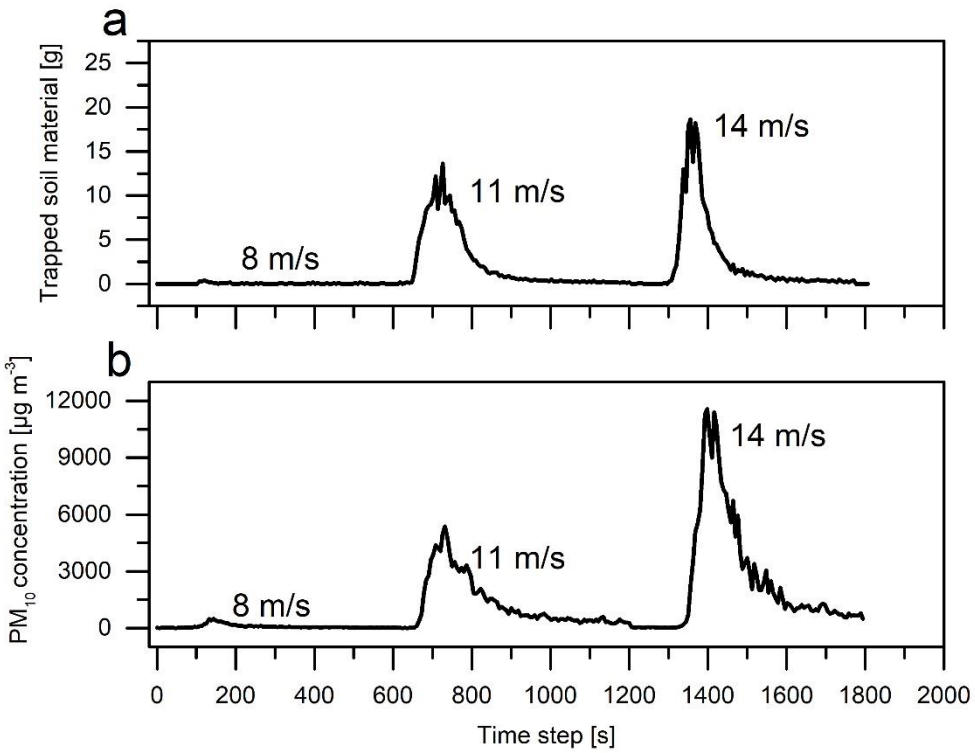

Fig. S4.1. Exemplarily illustration of the wind tunnel measurements; (a) - discharge per time unit of soil material in the saltation trap at the height of 0 – 1 cm and (b) - PM_{10} concentration in the chamber behind the working section.

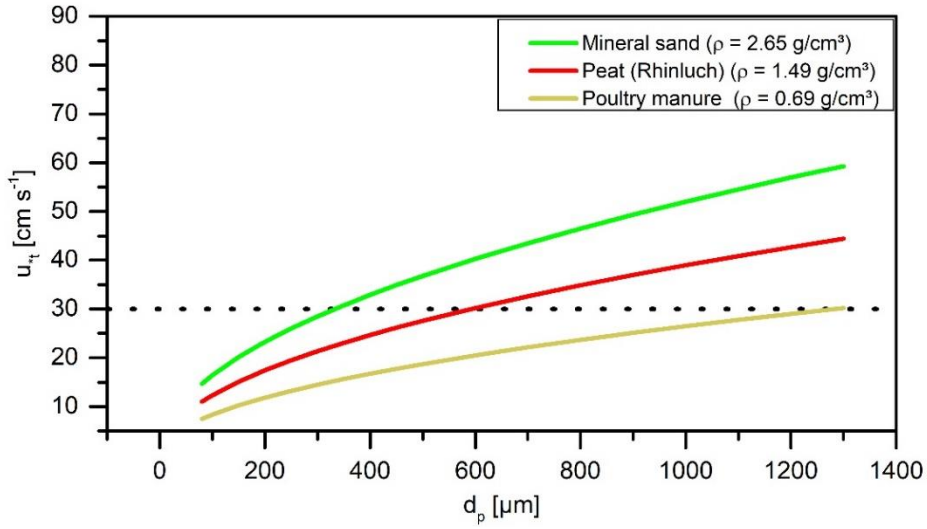

Fig. S4.2. Threshold friction velocity u_{*t} in dependence to the particle diameter d_p with particle densities of mineral origin (2.65 g cm^{-3}), peat origin (1.49 g cm^{-3}) (Rühlmann et al., 2006), and poultry manure origin (0.69 g cm^{-3}) (Dreisiebner-Lanz and Matzer, 2019). The dotted line corresponds to the threshold friction velocity of poultry manure particles with a median particle diameter of 1281 µm.

5 Discussion

According to the World Health Organization, the prevalence of ARB has become a global emerging issue since the last century (WHO, 2015). It is well known, that ARB enter the environment from human or animal sources (Sharma et al., 2016). The increased application of antibiotics in agriculture results in an increased prevalence of ARB (Silbergeld et al., 2008). It has been well documented, that ARB are released into the air, water and soil from contaminated feces in or near livestock production sites (Blaak et al., 2015; Falgenhauer et al., 2019; Gao et al., 2015, 2014; Laube et al., 2014; Lee et al., 2020; von Salviati et al., 2015). However, it is unclear to what extent the use of contaminated farmyard manure may lead to an increased prevalence of ARB in the environment. As ARB were detected in fertilized arable soils (Hartmann et al., 2012; Zheng et al., 2017), the environment of arable lands may represent a further transmission source to other ecosystems.

The work concentrates on the atmospheric dispersal of bacteria via the dust fraction, because bacteria are spread over long distances with dust particles serving as carriers (Maki et al., 2019). The focus was on characterizing the conditions that favor dust emissions, and qualifying and quantifying the dust released from agricultural operations and through wind erosion. We used solid manure from poultry livestock farms under conventional management. On the one side, solid manure from poultry production is prone to dust emissions (Aarnink and Ellen, 2007; Kabelitz et al., 2020). On the other side, conventional management of poultry production performs a periodic use of antibiotics, resulting in a potential load of ARB in feces and manure (Bezerra et al., 2017).

Field experiments started with the first step of an agricultural process chain, producing dust emissions: The application of poultry manure with different pretreatments. Although the process of manure application is a known contributor of primary PM emissions, there are still no information on emission factors in the literature yet (Maffia et al., 2020; Sharratt and Auvermann, 2014).

By using the Gaussian dispersion model inversely, it was possible to predict emission factors (amount of size-dependent released dust of a dust source per surface area) from different agricultural operations at downwind concentration measurements. For the first

time, area-related PM_{10} emission factors were provided for the agricultural operation of poultry manure application. The work demonstrates that the application of manure contributes to PM_{10} emissions significantly. In addition to quantifying emissions from manure application, it was possible to calculate PM emission factors for the other operations of the process chain (e.g. incorporation of manure) with the same dispersion model.

Bogman et al., (2007) suggested that PM_{10} emissions from fertilization are an order of magnitude lower than from land preparation operations (Sharratt and Auvermann, 2014). With the exception of the dried pretreatment, the PM_{10} emissions from the application of poultry manure were indeed an order of magnitude lower than the PM_{10} emissions of land preparation, as was reported in this work and compared to the values given in the literature (e.g. Sharratt and Auvermann, 2014). By comparing surface friction velocity as an upward flux and sink velocities as a downward flux of different particles sizes, it was shown that particles of the PM_{10} fraction remain in suspension and leave the field area during all field operations.

Importantly, no ESBL-producing *E. coli* were found in manure, fertilized soil and air samples on the field side, although ESBL-producing *E. coli* (*bla*$_{\text{CTX-M}}$ gene resistant against Penicillin, Cephalosporin and Aztreonam) had been detected in the poultry feces in high concentration (2×10^5 colony forming unit (CFU) per gram feces), when sampling the poultry stables prior to the field experiments. This finding is in line with the results of short-term storage experiments of contaminated poultry litter within the project, in which a rapid decline of the amount of ESBL-producing *E. coli* in poultry litter was shown within 36 – 72 h, indicating, that storage is an efficient method for inactivating ESBL-producing *E.coli* (Siller et al., 2020).

By comparing soils and soil-manure mixtures (poultry manure) with respect to their soil properties, it was found that manuring changes the soil characteristics in the soil top layer immediately after manure incorporation. Wind tunnel experiments showed that wind erosion causes a preferred detachment of poultry manure on recently fertilized sandy soils because poultry manure has similar physical properties to SOM, which is likewise prone to wind erosion (Iturri et al., 2017). Parallel studies of Siller et al., (2021) and of this work assessed a likewise low risk of airborne infection due to ARB during wind erosion.

5.1 Research Questions

Based on the results of the current work, the research questions (RQ), raised in the introduction (see chapter 1.3.2), can be answered as followed.

(RQ 1): To what extent poultry manure application contributes to PM_{10} emissions, compared to land preparation, and how do the pretreatments of manure influence PM_{10} emissions?

Chapter 2 focused on the PM emissions of manure application and subsequent further agricultural operations on fertilized arable lands. Manure application is to be considered as the first working step of an agricultural process chain, producing dust emissions on arable lands. PM_{10} emissions of poultry manure application were at large range and depended on the water content, which was influenced by the manure pretreatment. The water content (WC) ranged between 20.1% for dried manure and 51.1% for fresh manure. Whereas drying of manure (heated up 48 h with a hot air dryer) enhanced the PM_{10} emissions up to more than 160-fold compared to the other pretreatments (fresh, stored, composted), the PM_{10} emissions from the application of fresh, composted or stored manure were lower and ranged between 0.05 and 0.15 kg ha^{-1}. Further, dust emissions of manure application also depended on the application intensity of the manure spreader. A high spreading intensity is responsible for higher PM_{10} emissions (8.4 kg ha^{-1}, WC = 20.1%, field experiment in Potsdam), whereas a lower spreading intensity accounts for lower PM_{10} emissions (0.18 kg ha^{-1}, WC = 28.7%, field experiment in Müncheberg), although the water contents did not differ very much from each other.

PM_{10} emissions of land preparation ranged between 0.35 and 1.15 kg ha^{-1} at a SWC between 2 and 10%. No dust emissions were determined for sowing at a SWC of 12%, may indicating a threshold of SWC for dust emissions between 10 and 12% for this soil. Compared to the WC of the manure, the SWC were obviously lower. It indicates an organic-related moisture threshold for generating dust emissions from agricultural operations, that was previously determined in wind tunnel studies (e.g. Funk et al., 2008).

(RQ 2): Does the different pretreatments of poultry manure have an effect on the bacterial spread during the application of manure?

Different pretreatments of manure result in different total bioaerosol emissions. There is a relation between the dust emissions and the total viable bacteria during manure

application, because bacteria adhere to dust particles. Despite the low dust emissions during fresh manure application, bacterial concentrations of fresh manure were close to them from dried manure. Normalizing dust and bacterial concentration (CFU per µg PM_{10}) resulted in a 30 times higher bacterial concentration per µg PM_{10} during the application of fresh manure and a 10 times higher bacterial concentration per µg PM_{10} during composted manure application compared to dried manure application. Using dried manure resulted in an apparent inactivation of total bacteria, despite heavier dust particle generating. A study within the project showed, that drying of poultry manure also reduced the amounts of pathogens considerably compared to the fresh samples of manure (Kabelitz et al., 2020).

(RQ 3): To which extent ARB are released from poultry manure fertilized soils and what are the differences between application and incorporation of manure?

No ESBL-producing *E. coli* were found in the manure, soil and air samples at the field side, although they had been detected in fecal samples a few days before in the stables. MRSA and VRE were only detected in isolated cases in the stables. Nonetheless, distinct differences in concentrations and airborne emission fluxes of bacteria were reported during the application and incorporation of poultry manure. During the manure application in Müncheberg, concentrations of airborne bacteria (culturable on blood agar medium) increased up to 600 000 times and increased bacterial concentration continued with the incorporation (up to 7000 times), both compared to background concentration. Enterococci, an indicator for fecal contamination, had not been detected at background level, but concentrations had been increased of more than 10^5 per m^3 air for application and more than 10^3 per m^3 air for incorporation. As poultry manure is in general dryer and tend to higher aerosolization than other fertilizer (Kabelitz, 2020), our measurements of aerosolized bacteria were at the upper edge during application compared to the literature (e.g. Jahne et al., 2015). Although PM_{10} emissions were 6.4 times higher when manure was incorporated than when manure was applied, fecal bacterial emissions were more than 1000 times lower when manure was incorporated than when manure was applied, concluding a larger concern for bacterial release during application and a dilution of manure in soil due to tillage. Particles of manure origin were still part of dust emissions in the subsequent land preparations, but due to the dilution, they only take a percentage of less than 1% of total PM_{10} emissions.

Despite lower PM_{10} emissions during application of fresh, stored, and composted manure compared to PM_{10} emissions during subsequent incorporation, larger concern of bacterial release was also observed during application than during incorporation of the field experiments in Potsdam.

(RQ 4): Is it possible to trace back fecal contamination to its source?

By sequencing the genomes, it was possible to retrace fecal bacteria to its primary source in the poultry stables for the first time. Identical bacterial genomes (*Enterococcous faecium*) were found across all samples from feces, manure, dust and fertilized soils up to 7 weeks after the field experiments with manure application. Hence, bacteria of fecal origin from all samples had to descend from the poultry stables.

(RQ 5): What are the effects on soil properties after poultry manure incorporation at short-term?

Organic fertilizers are used to maintain or improve soil properties on arable lands. Incorporating poultry manure as a common fertilizer caused a modified soil composition and changed the physical and chemical properties in the soil top layer already at short-term conditions. In detail, the incorporation of manure changed the POM composition with consequences to increased particle sizes, carbon contents and hydrophobicity in the soil-manure mixtures. Organic carbon, as the main component of humus, is a storage and buffer medium for water, nutrients and pollutants and essentially controls the nutrient and pollutant retention capacity of the soil. But at short-term, the adding of incompletely decomposed organic matter (poultry manure) is responsible for increased hydrophobicity in the soil-manure mixture. This leads to a weaker soil moisture penetration in the soil layer, which increases soil erodibility (Doerr et al., 2000).

(RQ 6): How does the incorporated poultry manure affect the wind-eroded sediment and how much is lost due to wind erosion?

Wind erosion is not only a soil removing process, but also a particle sorting process between mineral and organic soil particles. Organic carbon is concentrated in the soil top layer. It is vulnerable to wind erosion in its particulate form, because it has a lower particle density compared to the mineral particles in the soil (Buschiazzo and Funk, 2015). Similar wind-induced sorting effects were determined for recently fertilized sandy soils. The focus was on the undecomposed poultry manure with its single particle

structure. Under dry and windy conditions, which are typical in spring months, sandy soils are vulnerable to a preferred detachment of particulate poultry manure material due to the lower density of manure particle. The selective release occurred at wind speeds closely above the threshold velocity of wind erosion (7 m s^{-1}) and was expressed in enriched material of poultry manure origin in the eroded sediment material. Depending on total soil loss and wind speeds, 1.7 – 14% of the total applied poultry manure was detached from the fertilized soil surface due to wind erosion.

The preferential release of manure particles also implies a preferential release of bacteria of fecal origin during wind erosion, as they adhere to the manure particles of lower density.

5.2 Synthesis of the results

The work contributes to a better understanding of the dispersion dynamics of particles and bacteria from agricultural soils. The work addresses the extent to which ARB of fecal origin and dust emissions during poultry manure application, land preparation and wind erosion enter the environment through dispersal from agricultural land. It clearly demonstrates that poultry manure application can contribute to dust pollution in the atmosphere. Drying of manure reduces the number of pathogens but is associated with a significant dust burden. Due to the lower density of manure particles compared to mineral particles, they can not only be transported over longer distances in the atmosphere after manure application and land preparation, but are also preferentially discharged by wind erosion (as well as bacteria of fecal origin). However, from the experiments of this work, it can be said that the risk of infection by ARB can be considered as low, since ARB were not detected in any of the dust samples.

5.3 Outlook

The present work shows physical and microbial investigations of dust emissions, bacterial fluxes and wind-induced erosion of farmyard manure and of fertilized soils, which has not been investigated so far. The work focuses on the common use of poultry manure, which is one of the solid organic fertilizers. However, farmyard manure does not only involve poultry manure but also other livestock manure such as from pigs. Solid pig manure also contributes to dust emissions, which was shown for animal housing systems or in wind tunnel studies (Cambra-López et al., 2010; Kabelitz et al., 2020), but emission factors from field experiments are missing (Maffia et al., 2020). According to the Food and

Agricultural Organization of the United Nations (FAO), livestock accounts for 850 million of Pigs and 27 billion of poultry (chickens, ducks geese and guinea fowls) worldwide (FAO, 2019), showing the potential of a prevalence of ARB. From this, it can be deduced that studies of ARB will also be of great importance in the future worldwide.

Solid manure is not the only fertilizer, used on arable lands, which is susceptible for dust generating particles. Sewage sludge is also used for fertilizing arable lands worldwide and has to be considered regarding the release of pathogens and pollutants (Maffia et al., 2020). Emission factors of sewage sludge are still not available in the literature.

Bacterial fluxes and dust emissions of soils fertilized with liquid manure are scarce or missing in literature and should be considered in further investigations. Liquid manure (e.g. slurry) does not contribute to primary dust emissions during the application. But fibrous residues of incorporated liquid manure in a dry soil-manure mixture may contribute to a preferential aerosolization because low moisture prohibits a binding between fertilizer residues and mineral soil components. The trend towards a drier spring due to more frequent and longer dry spells in Central Europe leads to an earlier and more severe decline in soil moisture in spring (Hänsel et al., 2019), when soils are susceptible to wind erosion. Further, stronger winds will increase due to climate change and enhance the risk of wind erosion (Steininger and Wurbs, 2017).

Thus, the fertilizer types, mentioned above, should be linked to emission studies of agricultural operations and also to wind erosion studies, to get a detailed view of this distribution path, as both account for dust emissions and bacterial fluxes. Worldwide studies (including aircraft measurement campaigns) are necessary in order to be able to make statements about spreading of ARB from arable lands on a global level.

An initial step to reduce the risk of antibiotic resistance at continental level is the “European Green Deal”, which is presented by the European Commission and entered into force in June 2021. The overall aim is to become the first climate neutral continent till 2050. The central part of the European Green Deal is the “Farm to fork” strategy, which deals with the challenges of sustainable food system. As conventional food systems are one of the drivers of climate change and land degradation, it is necessary to reduce among others excess fertilization and dependency of antibiotics. To reach the goal, the strategy is to lower the antibiotic sales to livestock animals by 50% and use of fertilizers by at least 20% by 2030 (European Green Deal, 2021). The implementation of

the strategy would not only lower the prevalence of antibiotic resistance in livestock but also contribute to reduced annual dust emissions by organic solid fertilizers.

6 Summary

The overall aim of the work was to determine the risk of a possible dust-associated spread of antibiotic-resistant bacteria from fertilized agricultural land. This was done by field experiments and wind tunnel studies with different soils and fertilizers from poultry barns from industrial poultry fattening facilities. In the samples from the poultry barns, *E. coli* had been detected in high concentration (2 x 10^5 CFU per gram feces) that have the capability to produce extended-spectrum beta-lactamases (ESBLs), making most beta-lactam antibiotics resistant (ESBL-producing *E. coli*).

The degree of aerosolization during poultry manure application depends on the water content of the manure and was heavy at low water contents. This was shown in this work, in parallel studies under field conditions (Kabelitz et al., 2021) and in wind tunnel experiments (Kabelitz et al., 2020). A preferred detachment and losses of poultry manure components by wind erosion were found in this work, after soils were experimentally fertilized with poultry manure. Typical sorting effects between low-density manure particles and soil particles of mineral origin were already detected at wind speeds close above the threshold wind speed of 7 m s^{-1}.

By genomic sequencing of feces, manure, soil and dust, it was demonstrated, that the bacteria of fecal origin in the fertilized soil were indeed identical to those in the manure, dust and in the feces from the poultry barns. We showed a more relevant release of bacteria during manure application than during manure incorporation and the dependence of airborne bacterial emissions from soils on wind speeds. Further, it was shown that manure bacteria were preferentially released during wind erosion because they were attached on low-density manure particles. Although ESBL-producing bacteria were detected in the poultry barns, no viable ESBL-producing *E. coli* could be detected in the dust during manure application, land preparation and wind erosion in this work and in parallel studies of Siller et al. (2021). This corresponds to short-term storage experiments of contaminated poultry litter within the project, showing a rapid decline of ESBL-producing *E.coli* in poultry manure within 36 – 72 h (Siller et al., 2020). The rapid death of ESBL-producing *E.coli* could explain the lack of detection in the dust. In contrast to ESBL-producing *E.coli*, vancomycin-resistant enterococci (VRE) and methicillin-resistant Staphylococcus aureus (MRSA) were only detected in fecal samples sporadically and not at all in the dust samples.

Bibliography

Aarnink, A., Ellen, H., 2007. Processes and factors affecting dust emissions from livestock production. Improve Air Qual.

Acosta-Martínez, V., Van Pelt, S., Moore-Kucera, J., Baddock, M.C., Zobeck, T.M., 2015. Microbiology of wind-eroded sediments: Current knowledge and future research directions. Aeolian Res. 18, 99–113. https://doi.org/10.1016/j.aeolia.2015.06.001

Aimar, S.B., Mendez, M.J., Funk, R., Buschiazzo, D.E., 2012. Soil properties related to potential particulate matter emissions (PM10) of sandy soils. Aeolian Res. 3, 437–443.

Avecilla, F., Panebianco, J.E., Buschiazzo, D.E., 2017. Meteorological conditions during dust (PM10) emission from a tilled loam soil: Identifying variables and thresholds. Agric. For. Meteorol. 244–245, 21–32. https://doi.org/10.1016/j.agrformet.2017.05.016

Bagnold, R.A., 1941. Bagnold, R.A. 1941: The physics of blown sand and desert dunes. London: Methuen. Prog. Phys. Geogr. - PROG PHYS GEOG 18, 91–96. https://doi.org/10.1177/030913339401800105

Bell, B.G., Schellevis, F., Stobberingh, E., Goossens, H., Pringle, M., 2014. A systematic review and meta-analysis of the effects of antibiotic consumption on antibiotic resistance. BMC Infect. Dis. 14, 13. https://doi.org/10.1186/1471-2334-14-13

Bezerra, W.G.A., Horn, R.H., Silva, I.N.G., Teixeira, R.S.C., Júnior, E.S.L., Albuquerque, Á.H., Cardoso, W.C., 2017. Antibiotics in the poultry industry: a review on antimicrobial resistance. Arch. Zootec. 66, 301–307.

Birmili, W., Schepanski, K., Ansmann, A., Spindler, G., Tegen, I., Wehner, B., Nowak, A., Reimer, E., Mattis, I., Müller, K., Brüggemann, E., Gnauk, T., Herrmann, H., Wiedensohler, A., Althausen, D., Schladitz, A., Tuch, T., Löschau, G., 2008. An case of extreme particulate matter concentrations over Central Europe caused by dust emitted over the southern Ukraine. Atmospheric Chem. Phys. 8, 997–1016. https://doi.org/10.5194/acp-8-997-2008

Blaak, H., Hoek, A.H.A.M. van, Hamidjaja, R.A., Plaats, R.Q.J. van der, Heer, L.K., Husman, A.M. de R., Schets, F.M., 2015. Distribution, Numbers, and Diversity of ESBL-Producing E. coli in the Poultry Farm Environment. PLOS ONE 10, e0135402. https://doi.org/10.1371/journal.pone.0135402

Bogman, P., Cornelis, W., Rollé, H., Gabriels, D., 2007. Prediction of TSP and PM10 emissions from agricultural operations in Flanders, Belgium. Presented at the 14th International Conference “Transport and Air Pollution”, Graz, Austria.

Borrelli, P., Ballabio, C., Panagos, P., Montanarella, L., 2014. Wind erosion susceptibility of European soils. Geoderma 232–234, 471–478. https://doi.org/10.1016/j.geoderma.2014.06.008

Borrelli, P., Panagos, P., Hessel, R., Riksen, M., Stolte, J., 2015. Soil erosion by wind in Europe, EU RECARE Project. pp. 27–38. https://doi.org/10.2788/488050

Buschiazzo, D.E., Funk, R., 2015. Wind erosion of agricultural soils and the carbon cycle., in: Banwart, S.A., Noellemeyer, E., Milne, E. (Eds.), Soil Carbon: Science, Management and Policy for Multiple Benefits. CABI, Wallingford, pp. 161–168. https://doi.org/10.1079/9781780645322.0161

Bush, K., Courvalin, P., Dantas, G., Davies, J., Eisenstein, B., Huovinen, P., Jacoby, G.A., Kishony, R., Kreiswirth, B.N., Kutter, E., Lerner, S.A., Levy, S., Lewis, K., Lomovskaya, O., Miller, J.H., Mobashery, S., Piddock, L.J.V., Projan, S.,

Thomas, C.M., Tomasz, A., Tulkens, P.M., Walsh, T.R., Watson, J.D., Witkowski, J., Witte, W., Wright, G., Yeh, P., Zgurskaya, H.I., 2011. Tackling antibiotic resistance. Nat. Rev. Microbiol. 9, 894–896. https://doi.org/10.1038/nrmicro2693

Cambra-López, M., Aarnink, A.J.A., Zhao, Y., Calvet, S., Torres, A.G., 2010. Airborne particulate matter from livestock production systems: A review of an air pollution problem. Environ. Pollut. 158, 1–17. https://doi.org/10.1016/j.envpol.2009.07.011

Clausnitzer, H., Singer, M.J., 1996. Respirable-Dust Production from Agricultural Operations in the Sacramento Valley, California. J. Environ. Qual. 25, 877–884. https://doi.org/10.2134/jeq1996.00472425002500040032x

Doerr, S.H., Shakesby, R.A., Walsh, R.P.D., 2000. Soil water repellency: its causes, characteristics and hydro-geomorphological significance. Earth-Sci. Rev. 51, 33–65. https://doi.org/10.1016/S0012-8252(00)00011-8

European Green Deal, 2021. Farm to Fork Strategy. For a fair, healthy and environmentally-friendly food system.

Falgenhauer, L., Schwengers, O., Schmiedel, J., Baars, C., Lambrecht, O., Heß, S., Berendonk, T.U., Falgenhauer, J., Chakraborty, T., Imirzalioglu, C., 2019. Multidrug-Resistant and Clinically Relevant Gram-Negative Bacteria Are Present in German Surface Waters. Front. Microbiol. 0. https://doi.org/10.3389/fmicb.2019.02779

FAO, 2019. Food and Agriculture Organization of the United Nations. FAOSTAT Statistical Database. [Rome].

Frielinghaus, M., Schmidt, R., 1993. Onsite and offsite damages by erosion in landscapes of east Germany. Farm land erosion. Template Plains Environ. Hills Elsevier Sci. Publ. BV 47–49.

Friese, A., Schulz, J., Laube, H., Von, C.S., Hartung, J., Roesler, U., 2013. Faecal occurrence and emissions of livestock-associated methicillin-resistant Staphylococcus aureus (laMRSA) and ESbl/AmpC-producing E. coli from animal farms in Germany. Berl. Munch. Tierarztl. Wochenschr. 126, 175–180.

Funk, R., 2004. Viel wind um nichts? forschungen zur winderosion in Brandenburg: Much wind about nothing? wind erosion research in Brandenburg. Arch. Agron. Soil Sci. 50, 309–317. https://doi.org/10.1080/03650340410001663855

Funk, R., 1995. Quantifizierung der Winderosion auf einem Sandstandort Brandenburgs unter besonderer Berücksichtigung der Vegetationswirkung. Zentrum für Agrarlandschafts-und Landnutzungsforschung.

Funk, R., Reuter, H.I., Hoffmann, C., Engel, W., Öttl, D., 2008. Effect of moisture on fine dust emission from tillage operations on agricultural soils. Earth Surf. Process. Landf. J. Br. Geomorphol. Res. Group 33, 1851–1863.

Gao, L., Hu, J., Zhang, X., Ma, R., Gao, J., Li, S., Zhao, M., Miao, Z., Chai, T., 2014. Dissemination of ESBL-Producing Escherichia coli of Chicken Origin to the Nearby River Water. Microb. Physiol. 24, 279–285. https://doi.org/10.1159/000365786

Gao, L., Tan, Y., Zhang, X., Hu, J., Miao, Z., Wei, L., Chai, T., 2015. Emissions of Escherichia coli Carrying Extended-Spectrum β-Lactamase Resistance from Pig Farms to the Surrounding Environment. Int. J. Environ. Res. Public. Health 12, 4203–4213. https://doi.org/10.3390/ijerph120404203

Goossens, D., 2004. Wind erosion and tillage as a dust production mechanism on north European farmland. Wind Eros. Dust Dyn. Obs. Simul. Model. ESW Publ. Dep. Environ. Sci. Eros. Soil Water Conserv. Group Wagening. Univ. Wagening. 15–40.

Goossens, D., Gross, J., Spaan, W., 2001. Aeolian dust dynamics in agricultural land areas in lower Saxony, Germany. Earth Surf. Process. Landf. J. Br. Geomorphol. Res. Group 26, 701–720.

Goossens, D., Riksen, M., 2004. Wind Erosion and Dust Dynamics: Observations, Simulations, Modelling. ESW Publications.

Hänsel, S., Ustrnul, Z., Łupikasza, E., Skalak, P., 2019. Assessing seasonal drought variations and trends over Central Europe. Adv. Water Resour. 127, 53–75. https://doi.org/10.1016/j.advwatres.2019.03.005

Hartmann, A., Amoureux, L., Locatelli, A., Depret, G., Jolivet, C., Gueneau, E., Neuwirth, C., 2012. Occurrence of CTX-M Producing Escherichia coli in Soils, Cattle, and Farm Environment in France (Burgundy Region). Front. Microbiol. 3. https://doi.org/10.3389/fmicb.2012.00083

Hassenpflug, W., 1992. Winderosion. Handb. Bodenschutzes Kap 2, 200–215.

Hoffmann, C., Funk, R., 2015. Diurnal changes of PM10-emission from arable soils in NE-Germany. Aeolian Res. 17, 117–127.

Holmén, B.A., James, T.A., Ashbaugh, L.L., Flocchini, R.G., 2001. Lidar-assisted measurement of PM10 emissions from agricultural tilling in California's San Joaquin Valley – Part II: emission factors. Atmos. Environ. 35, 3265–3277. https://doi.org/10.1016/S1352-2310(00)00519-7

Huijbers, P.M.C., Blaak, H., de Jong, M.C.M., Graat, E.A.M., Vandenbroucke-Grauls, C.M.J.E., de Roda Husman, A.M., 2015. Role of the Environment in the Transmission of Antimicrobial Resistance to Humans: A Review. Environ. Sci. Technol. 49, 11993–12004. https://doi.org/10.1021/acs.est.5b02566

Idelevich, E.A., Lanckohr, C., Horn, D., Wieler, L.H., Becker, K., Köck, R., 2016. Antibiotika-resistente Erreger in Deutschland. Bundesgesundheitsblatt-Gesundheitsforschung-Gesundheitsschutz 59, 113–123.

Iturri, L.A., Funk, R., Leue, M., Sommer, M., Buschiazzo, D.E., 2017. Wind sorting affects differently the organo-mineral composition of saltating and particulate materials in contrasting texture agricultural soils. Aeolian Res. 28, 39–49. https://doi.org/10.1016/j.aeolia.2017.07.005

Jahne, M.A., Rogers, S.W., Holsen, T.M., Grimberg, S.J., 2015. Quantitative microbial risk assessment of bioaerosols from a manure application site. Aerobiologia 31, 73–87. https://doi.org/10.1007/s10453-014-9348-0

Kabelitz, T., Ammon, C., Funk, R., Münch, S., Biniasch, O., Nübel, U., Thiel, N., Rösler, U., Siller, P., Amon, B., Aarnink, A.J.A., Amon, T., 2020. Functional relationship of particulate matter (PM) emissions, animal species, and moisture content during manure application. Environ. Int. 143, 105577. https://doi.org/10.1016/j.envint.2020.105577

Kabelitz, T., Biniasch, O., Ammon, C., Nübel, U., Thiel, N., Janke, D., Swaminathan, S., Funk, R., Münch, S., Rösler, U., Siller, P., Amon, B., Aarnink, A.J.A., Amon, T., 2021. Particulate matter emissions during field application of poultry manure - The influence of moisture content and treatment. Sci. Total Environ. 146652. https://doi.org/10.1016/j.scitotenv.2021.146652

Katra, I., 2020. Soil Erosion by Wind and Dust Emission in Semi-Arid Soils Due to Agricultural Activities. Agronomy 10, 89. https://doi.org/10.3390/agronomy10010089

Kola, A., Kohler, C., Pfeifer, Y., Schwab, F., Kühn, K., Schulz, K., Balau, V., Breitbach, K., Bast, A., Witte, W., Gastmeier, P., Steinmetz, I., 2012. High prevalence of extended-spectrum-β-lactamase-producing Enterobacteriaceae in organic and

conventional retail chicken meat, Germany. J. Antimicrob. Chemother. 67, 2631–2634. https://doi.org/10.1093/jac/dks295

Laube, H., Friese, A., Von Salviati, C., Guerra, B., Rösler, U., 2014. Transmission of ESBL/AmpC-producing Escherichia coli from broiler chicken farms to surrounding areas. Vet. Microbiol. 172, 519–527.

Lee, S., Teng, L., DiLorenzo, N., Weppelmann, T.A., Jeong, K.C., 2020. Prevalence and Molecular Characteristics of Extended-Spectrum and AmpC β-Lactamase Producing Escherichia coli in Grazing Beef Cattle. Front. Microbiol. 0. https://doi.org/10.3389/fmicb.2019.03076

Maffia, J., Elio, D., Barbara, A., Paolo, B., 2020. PM emissions from open field crop management: Emission factors, assessment methods and mitigation measures–A review. Atmos. Environ. 117381.

Maki, T., Lee, K.C., Kawai, K., Onishi, K., Hong, C.S., Kurosaki, Y., Shinoda, M., Kai, K., Iwasaka, Y., Archer, S.D.J., Lacap-Bugler, D.C., Hasegawa, H., Pointing, S.B., 2019. Aeolian Dispersal of Bacteria Associated With Desert Dust and Anthropogenic Particles Over Continental and Oceanic Surfaces. J. Geophys. Res. Atmospheres 0. https://doi.org/10.1029/2018JD029597

Münch, S., Papke, N., Thiel, N., Nübel, U., Siller, P., Roesler, U., Biniasch, O., Funk, R., Amon, T., 2020. Effects of farmyard manure application on dust emissions from arable soils. Atmospheric Pollut. Res. 11, 1610–1624. https://doi.org/10.1016/j.apr.2020.06.007

Öttl, D., Funk, R., 2007. PM emission factors for farming activities by means of dispersion modeling. Presented at the International Conference “Particulate Matter in and from Agriculture.

Prospero, J.M., 1999. Long-range transport of mineral dust in the global atmosphere: Impact of African dust on the environment of the southeastern United States. Proc. Natl. Acad. Sci. 96, 3396–3403. https://doi.org/10.1073/pnas.96.7.3396

Riksen, M., Goossens, D., 2004. Off-site effects of wind erosion on agricultural land in northwestern Europe. Wind Eros. Dust Dyn. Obs. Simul. Model. ESW Publ. Dep. Environ. Sci. Eros. Soil Water Conserv. Group Wagening. Univ. Wagening. 103–122.

Seedorf, J., 2004. An emission inventory of livestock-related bioaerosols for Lower Saxony, Germany. Atmos. Environ., Contains Special Issue section on Measuring the composition of Particulate Matter in the EU 38, 6565–6581. https://doi.org/10.1016/j.atmosenv.2004.08.023

Shao, Y., 2008. Physics and Modelling of Wind Erosion. Springer Science & Business Media.

Shao, Y., Wyrwoll, K.-H., Chappell, A., Huang, J., Lin, Z., McTainsh, G.H., Mikami, M., Tanaka, T.Y., Wang, X., Yoon, S., 2011. Dust cycle: An emerging core theme in Earth system science. Aeolian Res. 2, 181–204. https://doi.org/10.1016/j.aeolia.2011.02.001

Sharp, H., Valentin, L., Fischer, J., Guerra, B., Appel, B., Käsbohrer, A., 2014. [Estimation of the transfer of ESBL-producing Escherichia coli to humans in Germany]. Berl. Munch. Tierarztl. Wochenschr. 127, 464–477.

Sharratt, B., Auvermann, B., 2014. Dust pollution from agriculture. Encycl. Agric. Food Syst. 2, 487–504.

Silbergeld, E.K., Graham, J., Price, L.B., 2008. Industrial food animal production, antimicrobial resistance, and human health. Annu. Rev. Public Health 29, 151–169. https://doi.org/10.1146/annurev.publhealth.29.020907.090904

Siller, P., Daehre, K., Rosen, K., Münch, S., Bartel, A., Funk, R., Nübel, U., Amon, T., Roesler, U., 2021. Low airborne tenacity and spread of ESBL-/AmpC-producing Escherichia coli from fertilized soil by wind erosion. Environ. Microbiol. n/a. https://doi.org/10.1111/1462-2920.15437

Siller, P., Daehre, K., Thiel, N., Nübel, U., Roesler, U., 2020. Impact of short-term storage on the quantity of extended-spectrum beta-lactamase–producing Escherichia coli in broiler litter under practical conditions. Poult. Sci. 99, 2125–2135. https://doi.org/10.1016/j.psj.2019.11.043

Skidmore, E.L., 1986. Wind erosion control. Clim. Change 9, 209–218. https://doi.org/10.1007/BF00140537

Steininger, M., Wurbs, D., 2017. Bundesweite Gefährdung der Böden durch Winderosion und Bewertung der Veränderung infolge des Wandels klimatischer Steuergrößen als Grundlage zur Weiterentwicklung der Vorsorge und Gefahrenabwehr im Bodenschutzrecht. Umweltbundesamt Texte | 13/2017, 119.

Steinke, I., Funk, R., Busse, J., Iturri, A., Kirchen, S., Leue, M., Möhler, O., Schwartz, T., Schnaiter, M., Sierau, B., Toprak, E., Ullrich, R., Ulrich, A., Hoose, C., Leisner, T., 2016. Ice nucleation activity of agricultural soil dust aerosols from Mongolia, Argentina, and Germany. J. Geophys. Res. Atmospheres 121, 13,559-13,576. https://doi.org/10.1002/2016JD025160

Sterk, Geert, Goossens, D., 2007. Emissions of soil dust and related problems in Europe: an overview. Presented at the DustConf International Conference, Maastricht, the Netherlands, pp. 23–24.

Sterk, G., Goossens, D., 2007. On-site and off-site impacts of wind erosion in Europe: an overview. Presented at the Proceedings of the International conference on Off-site impacts of soil erosion and sediment transport.

Takai, H., Pedersen, S., Johnsen, J.O., Metz, J.H.M., Groot Koerkamp, P.W.G., Uenk, G.H., Phillips, V.R., Holden, M.R., Sneath, R.W., Short, J.L., White, R.P., Hartung, J., Seedorf, J., Schröder, M., Linkert, K.H., Wathes, C.M., 1998. Concentrations and Emissions of Airborne Dust in Livestock Buildings in Northern Europe. J. Agric. Eng. Res. 70, 59–77. https://doi.org/10.1006/jaer.1997.0280

Tatarko, J., 2001. Soil aggregation and wind erosion: processes and measurements. Ann. Arid Zone 40, 251–264.

Thiel, N., Münch, S., Behrens, W., Junker, V., Faust, M., Biniasch, O., Kabelitz, T., Siller, P., Boedeker, C., Schumann, P., Roesler, U., Amon, T., Schepanski, K., Funk, R., Nübel, U., 2020. Airborne bacterial emission fluxes from manure-fertilized agricultural soil. Microb. Biotechnol. 13, 1631–1647. https://doi.org/10.1111/1751-7915.13632

Tyrrell, C., Burgess, C.M., Brennan, F.P., Walsh, F., 2019. Antibiotic resistance in grass and soil. Biochem. Soc. Trans. 47, 477–486. https://doi.org/10.1042/BST20180552

von Salviati, C., Laube, H., Guerra, B., Roesler, U., Friese, A., 2015. Emission of ESBL/AmpC-producing Escherichia coli from pig fattening farms to surrounding areas. Vet. Microbiol. 175, 77–84. https://doi.org/10.1016/j.vetmic.2014.10.010

WHO, W.H.O., 2015. Antibiotic resistance: multi-country public awareness survey. World Health Organization.

Wiggs, G.F.S., 2006. Wind erosion on agricultural land in Europe: research results for land managers, edited by Andrew Warren. European Commission, Brussels, 2002. ISBN 92 894 3958 0, o + 76pp. Land Degrad. Dev. 17, 109–109. https://doi.org/10.1002/ldr.685

Xie, W.-Y., Shen, Q., Zhao, F.J., 2018. Antibiotics and antibiotic resistance from animal manures to soil: a review. Eur. J. Soil Sci. 69, 181–195. https://doi.org/10.1111/ejss.12494

Zaman, S.B., Hussain, M.A., Nye, R., Mehta, V., Mamun, K.T., Hossain, N., 2017. A Review on Antibiotic Resistance: Alarm Bells are Ringing. Cureus 9. https://doi.org/10.7759/cureus.1403

Zheng, B., Huang, C., Xu, H., Guo, L., Zhang, J., Wang, X., Jiang, X., Yu, X., Jin, L., Li, X., Feng, Y., Xiao, Y., Li, L., 2017. Occurrence and Genomic Characterization of ESBL-Producing, MCR-1-Harboring Escherichia coli in Farming Soil. Front. Microbiol. 0. https://doi.org/10.3389/fmicb.2017.02510

Acknowledgments

I would like to take this opportunity to express my sincere thanks to the following people for their support during my doctoral thesis:

My special thanks go to Dr. Roger Funk for his supervision and support of this thesis. In the form of valuable advices and suggestions, he was helpful to me during my doctoral studies.

I am grateful to Prof. Dr. Michael Sommer who gave me the opportunity to write the PhD thesis at the working group “Landscape Pedology” “Research Area 1” (former Institute of Soil Landscape Research), and for his support and supervision.

I would also like to thank my colleagues from the project SOARiAL and at ZALF, especially those from Research Area 1 for their encouragement and Dr. Carsten Hoffmann for mentoring.

Further, I would like to thank the Examination Committee (Prof. Dr. Michael Sommer, Dr. Roger Funk, Prof. Dr. Ulrich Nübel, Prof. Dr. Gunnar Lischeid, Prof. Dr. Monika Wulf and Prof. Dr. Annegret Thieken) for their support in the organization of the oral examination (Disputation).

Last but not least, I would like to thank my family for their active support during my PhD.

Erklärung

Ich versichere hiermit, dass ich die vorliegende Dissertation selbstständig verfasst und keine anderen als die im Literaturverzeichnis angegebenen Quellen benutzt habe. Ich habe die Regeln der guten wissenschaftlichen Praxis eingehalten.

Alle Stellen, die wörtlich oder sinngemäß aus veröffentlichten oder noch nicht veröffentlichten Quellen entnommen sind, sind als solche kenntlich gemacht.

Die Zeichnungen oder Abbildungen in dieser Dissertation sind von mir selbst erstellt worden oder mit einem entsprechenden Quellennachweis versehen.

Diese Dissertation ist in gleicher oder ähnlicher Form noch bei keiner anderen Prüfungsbehörde eingereicht worden.

Strausberg, den 19.09.2021

Unterschrift